

Benchmark interest rates when the government is risky*

Patrick Augustin,[†] Mikhail Chernov,[‡] Lukas Schmid,[§] and Dongho Song[¶]

Abstract

Since the Global Financial Crisis, interest rate swap rates, which represent future uncollateralized interbank borrowing, have fallen below maturity-matched Treasury rates. This is surprising, because U.S. Treasuries, which are deemed expensive because of superior liquidity and safety, should produce yields that are lower than those of swap rates. We show, by no-arbitrage, that sovereign default risk explains negative swap spreads even without frictions such as balance sheet constraints, convenience yield, and hedging demand. We support this explanation with an equilibrium model that jointly accounts for macroeconomic fundamentals and the term structures of interest and U.S. credit default swap rates.

JEL classification codes: C1, E43, E44, G12, H60

Keywords: sovereign credit risk, negative swap rates, recursive preferences, term structure

*We are grateful to the editor, William Schwert, and an anonymous referee, for invaluable feedback. We also thank Vadim di Pietro, Michael Gallmeyer, Valentin Haddad, Michael Johannes, Arvind Krishnamurthy, Lars Lochstoer, Francis Longstaff, Renate Marold, Guillaume Roussellet, Suresh Sundaresan, and Tony Zhang for comments on earlier drafts, as well as participants in seminars at, and conferences sponsored by the Canadian Derivatives Institute, Duke, McGill, OSU, UCLA, St. Gallen, the Bank for International Settlements, the Bank of Canada, the Federal Reserve Bank of San Francisco Conference on Advances in Financial Research, Finance Down Under 2020 at the University of Melbourne, the HEC-McGill 2019 Summer Finance Workshop, and the ICEF 2019 International Finance Conference. The authors acknowledge financial support from the Canadian Derivatives Institute.

[†]Corresponding author. Desautels Faculty of Management, McGill University, and Canadian Derivatives Institute; 1001 Sherbrooke Street West, Montréal, QC H3A 1G5, Canada; patrick.augustin@mcgill.ca.

[‡]Anderson School of Management, UCLA, NBER, and CEPR; 101 Westwood Plaza, Los Angeles, CA 90095, USA; mikhail.chernov@anderson.ucla.edu.

[§]Fuqua School of Business, Duke University, and CEPR; 100 Fuqua Drive, Durham, NC, 27708, USA; lukas.schmid@duke.edu.

[¶]Carey Business School, Johns Hopkins University; 100 International Drive, Baltimore, MD 21202, USA; dongho.song@jhu.edu.

1. Introduction

The financial crisis of 2008 marked the first of continuing disruptions in financial markets. Three phenomena are particularly significant in the fixed-income markets: (i) long-term swap rates linked to LIBOR fell below maturity matched U.S. Treasury yields (Klingler and Sundaresan, 2019b; Jermann, 2019), (ii) short- to intermediate-term maturity swap rates linked to the Effective Federal Funds Rate (EFFR) also fell below maturity matched U.S. Treasury yields (Klingler and Sundaresan, 2019a), and (iii) premiums on CDS contracts for the U.S. government have risen to at least 100 times their pre-crisis levels (Chernov, Schmid, and Schneider, 2020).

Observations (i) and (ii) appear puzzling from the perspective of the standard asset pricing theory. They imply that swap spreads (i.e., the difference between swap and Treasury rates) linked to LIBOR and EFFR are negative, an irregularity often referred to as the “negative swap spread puzzle.” Although these issues have been the focus of research, they are typically studied in isolation. The third phenomenon is also perceived as puzzling because of the sheer magnitude of U.S. CDS premiums.

In this paper, we argue that these phenomena are interrelated and can be understood together by accounting for a change in the perceived credit quality of the U.S. after the crisis. In contrast, although the factors behind extant explanations of phenomena (i) and (ii) are valid, the factors were also present before the crisis when swap spreads were positive.

The no-arbitrage argument for the relative magnitude of interest rates can account for these puzzles. Consider a strategy that sells short a par Treasury bond borrowed via a reverse repo transaction, together with a position in a swap contract that receives a fixed rate of interest. The total cash flows are equal to the difference between the swap rate and the Treasury yield (a coupon in the case of par), net of the difference between the floating payments in the swap and the reverse repo. Uncollateralized interest rates are expected to be greater than collateralized rates, so the present value of the floating payments (one-period interest rates) is positive. Thus, the difference between the swap rate and the Treasury yield must also be positive. We analyze violations of this condition in three steps.

First, we examine various interest rate spreads. The swap linked to the EFFR is known as the overnight indexed swap (OIS), and that linked to LIBOR as the interest rate swap (IRS). The difference between the OIS and Treasury rates continues to be negative at longer maturities. The difference between the IRS and Treasury rates is negative between maturities of 7 years and up to 30 years. Finally, the spread between the IRS and OIS rates is positive across all maturities for the entire sample, as would have been expected in 2007. Thus, the negative swap spread puzzles must have a common source, which can be derived from the relation between OIS and Treasury rates. We also provide evidence suggesting that OIS swap spreads and CDS premiums exhibit significant co-movement.

Second, we argue that the negative difference between swap and Treasury rates is driven by the credit riskiness of the U.S. government. If the U.S. can default, a credit-risk-free

position can be restored by combining a short Treasury bond and Treasury protection sold via a CDS contract. Thus, the original no-arbitrage argument reviewed above should be modified if a CDS position is introduced, and the difference between the swap rate and the Treasury yield minus the CDS premium should be positive, implying that negative swap spreads can persist even in the absence of arbitrage. The key insight is that Treasury bonds can default, but benchmark indices like LIBOR or EFR cannot because they are not investable, and so swap contracts can be more valuable than Treasuries, thereby lowering swap rates relative to those of bonds.

Third, we propose a realistic quantitative model that can explain negative swap spreads by accounting for the sovereign credit risk of the U.S. government. As [Chernov, Schmid, and Schneider \(2020\)](#) observe, an equilibrium model is required to measure the credit risk premium in the absence of an observed risk-free reference rate, and so we follow their modeling strategy but make two adjustments. A high level of quantitative realism is required, so we specify a more realistic model of the joint behavior of macroeconomic fundamentals. We also simplify the modeling of the default trigger and take an intensity-based rather than a structural approach. The macroeconomic variables that drive the default intensity are selected based on the analysis of [Augustin \(2018\)](#) and [Chernov, Schmid, and Schneider \(2020\)](#).

To provide plausible quantitative guidance on swap spreads, our model must account for other factors beyond sovereign credit risk that may affect differences between interest rates in current markets. We focus on a convenience yield on Treasuries, bank risk (credit and funding liquidity), and the opportunity cost of collateral associated with swap transactions. The first lowers Treasury yields, the second increases swap rates, and the third increases swap rates if the short interest rate and the cost of collateral are positively correlated ([Johannes and Sundaresan, 2007](#)). We evaluate the contributions of these different channels and sovereign credit risk to the overall swap spreads.

We identify the convenience yield and bank risk empirically using observable interest rate spreads and the unobserved collateral factor by matching the one-year IRS and the term structure of the CDS. We are then able to value the OIS and IRS without using the data on their respective rates. This valuation is thus an actual relative value exercise, in which we determine the theoretical value of the swap rates using the market values of other instruments. We estimate our model via Bayesian MCMC methods and thus establish the model-implied time series for the relevant variables in our sample.

We find that our quantitative model provides an accurate account of the dynamics in both OIS and IRS markets. The model generates swap spread series that were positive before the onset of the financial crisis in 2008 and turned negative afterward. We conduct counterfactual experiments to assess how the U.S. credit risk affects the behavior of swap spreads. We find that they are uniformly positive in the absence of this risk, which confirms that the sovereign risk is quantitatively relevant in the pricing of Treasuries and swaps. This relative-value-based view is conceptually different from all other explanations of negative swap spread puzzles, which are based on limits to arbitrage.

We contribute to the literature examining the puzzle that the difference between interest rate swaps denominated in USD and U.S. Treasury rates, a.k.a. swap spreads, turned negative for multiple maturities, effectively suggesting that the U.S. government is riskier than a presumably safe AA-rated bank. Several explanations have been proposed for the apparent pricing anomaly in financial markets, including the demand for duration by underfunded pension plans (Klingler and Sundaresan, 2019b), dealer funding costs (Lou, 2009), or increases in regulatory leverage ratios (Boyarchenko, Gupta, Steele, and Yen, 2018). Klingler and Sundaresan (2019a) consider fading demand for U.S. Treasury bonds to be a significant factor in negative OIS-Treasury spreads. Jermann (2019) proposes a theoretical equilibrium explanation for negative swap spreads by considering regulatory leverage constraints for dealer balance sheets. The main differences between our approach and others are summarized in Table 1.

The explanations based on frictions, although plausible, fail to provide a comprehensive explanation of Treasury spreads that exceed the maturity matched spreads of short-term and long-term funding instruments in interbank markets. The demand for duration by underfunded pension plans is a plausible explanation for 30-year negative swap spreads, but less so for shorter maturities, even if they have been persistently negative for many years. Second, limits-to-arbitrage arguments can account for the persistence of negative swap spreads but do not explain why they turned negative in the first place. Third, focusing on individual segments of the maturity structure or selective instruments ignores the inherent equilibrium relationships that must exist between benchmark interest rates. We propose a model that explains both positive swap spreads before and negative swap spreads after the crisis.

We suggest that negative swap spreads can be obtained without frictions (even though frictions may amplify the phenomenon). We aim to provide a unified explanation of the price dynamics of various fixed income instruments during the financial crisis, by incorporating sovereign default risk into the modeling of benchmark interest rates, thus addressing the challenge faced by the current partial equilibrium pricing models. Dittmar, Hsu, Roussellet, and Simasek (2019) propose that sovereign default risk can explain the pricing anomalies observed among inflation-indexed securities (Fleckenstein, Longstaff, and Lustig, 2013; Hilscher, Raviv, and Reis, 2014).

Our study also contributes to the extensive literature on no-arbitrage affine term structure modeling and credit-sensitive instruments, as summarized by Duffie and Singleton (2003), to the modeling of the term structure of overnight index swaps, interest rate swaps, or LIBOR rates (Duffie and Huang, 1996; Duffie and Singleton, 1997; Collin-Dufresne and Solnik, 2001; Grinblatt, 2001; He, 2001; Liu, Longstaff, and Mandell, 2006; Johannes and Sundaresan, 2007; Feldhutter and Lando, 2008; Filipovic and B.Trolle, 2013; Dubecq, Monfort, Renne, and Roussellet, 2016) and to other empirical examinations (Litzenberger, 1992; Sun, Sundaresan, and Wang, 1993; Gupta and Subrahmanyam, 2000; Wang and Yang, 2018). Our study also relates to investigations into the convenience yield embedded in Treasury bonds (Krishnamurthy, 2002; Longstaff, 2004; Gurkaynak, Sack, and Wright,

2007; Goyenko, Subrahmanyam, and Ukhov, 2011; Krishnamurthy and Vissing-Jorgensen, 2012; Nagel, 2016; Du, Im, and Schreger, 2018).

2. Preliminary evidence

First, we discuss benchmark U.S. interest rates. Second, we present the data. Third, we review the evidence on swap spreads. Finally, we explain the no-arbitrage arguments that relate swap and Treasury rates.

2.1. Benchmark interest rates in the U.S.

Four types of U.S. interest rates and their interactions are considered in our analysis: (i) Treasury yields; (ii) OIS premiums; (iii) IRS premiums; and (iv) CDS premiums. The U.S. Treasury borrows money on behalf of the government by issuing debt securities of different maturities. The effective annual interest that can be earned along the maturity spectrum characterizes the Treasury yield curve. The Treasury yield curve can be characterized using zero coupon, coupon, par, or forward rates. The most convenient method is to use zero-coupon yields that are bootstrapped from coupon bonds (e.g., Gurkaynak et al., 2007, henceforth GSW). The constant maturity Treasury (CMT) yield curve, or par rates, are a common indicator of the U.S. government's borrowing costs, and are also bootstrapped from coupon bonds. CMT_t^n denotes the coupon at time t of a bond maturing in n periods.

Overnight indexed swaps (OIS) are fully collateralized contracts, in which a fixed rate payer exchanges a constant cash flow, i.e., the OIS rate, against a floating payment that is computed as the geometric average of the daily EFFR. The Federal Funds Target Rate is determined by the Federal Open Market Committee so monetary policy can be established. The EFFR is the actual interest rate at which banks lend reserve balances to other banks overnight without collateral. This has been measured as the volume-weighted median of the bilaterally negotiated transactions since March 1, 2016, and before then as the volume-weighted average. OIS contracts with maturities of up to one year have only one settlement (the geometric average is computed over the lifetime of the contract), while cash payments for contracts with maturities of over one year arise quarterly (the geometric average is re-computed every quarter). Hull and White (2013) and Wang and Yang (2018) discuss the institutional details of OIS contracts, and OIS_t^n denotes the rate at time t of a swap maturing in n periods.

The arrangements of interest rate swaps (IRS) are similar to those of OIS but have a different reference floating rate, which is the 3-month London interbank offered rate (LIBOR), which is fixed at the previous settlement date of an IRS. LIBOR is the interest rate at which banks in the Eurodollar area are willing to lend to each other on an uncollateralized basis. See Duffie and Singleton (1997), Collin-Dufresne and Solnik (2001), and Johannes

and Sundaresan (2007) for discussions on the institutional details of LIBOR swap contracts. IRS_t^n denotes the rate at time t of a swap maturing in n periods.

The definitions of LIBOR and EFFR are conceptually similar, as they both relate to uncollateralized interbank lending, so overnight LIBOR can be assumed to be similar to EFFR, but the rates should not be identical. The banks in the LIBOR panel differ from those in the Fed system, and the logistics of lending within the Fed system are different from those in the Eurodollar area. Figure 1 compares the two rates.

The single exception to the identical positions corresponds to the onset of the banking crisis of 2008. The difference between the instruments linked to LIBOR and EFFR is due to the term effect. The floating legs are linked to the 3-month LIBOR and the daily EFFR compounded over 3 months. The presence of bank credit risk means that lending to banks without collateral for 3 months outright (at LIBOR) is more risky than lending overnight (at EFFR) and rolling that over daily for 3 months.

The interest earned on collateralized borrowing through a repurchase agreement contract (henceforth repo) is also a closely related rate, but it is not one that we consider in this paper, as it has its own distinct issues and puzzles, although it does have some relevance to our analysis. General collateral (GC) repo rates appear to be like a natural proxy for the risk-free rate. Duffie and Stein (2015) suggest that GC rates exhibit similar flight-to-quality spikes as Treasury bills and excess volatility due to the very short-term maturity of one day. The GC repo market is also not active at maturities beyond 3 months, so no term structure information is readily available. In addition, the post-2008 quantitative easing program involved the purchase of Treasury bonds and thus affected the supply of collateral in repo transactions, leading to distortions in rates. We limit our consideration of repo rates and use them only qualitatively, without considering the specific values or their dynamics.

We also focus on the premium on credit default swaps (CDS) associated with the U.S. government. CDS are effectively insurance contracts, in which the protection seller must make payments in case of a credit event, which may include a failure to pay, repudiation/moratorium, and restructuring. CDS_t^n denotes the rate at time t of a swap maturing in n periods.

If the U.S. government has no credit risk, these premiums would be expected to be approximately zero, which was the case before October 2007. The subsequent elevation in the CDS premiums is prima facie evidence of U.S. credit risk, as Chernov, Schmid, and Schneider (2020) argue. Whether CDS premiums reflect compensation for credit risk at all is a matter of debate. In our view, both the arguments and the evidence for the U.S. credit risk explanation are persuasive. See Appendix A.

2.2. Data

We source data on LIBOR, IRS, and OIS rates from Bloomberg, and U.S. CDS premiums from Markit. Our sample begins on May 8, 2002, when observations on OIS rates are found

to be frequently available in the data, and ends on September 26, 2018. The 30-year OIS rates are often discarded by researchers because of their low liquidity. In addition, no OIS data are available for maturities beyond 10 years during the crisis. Thus, longer-term OIS rates are available only for part of the sample period. As the swap rates are par rates, we use the constant maturity Treasury (CMT) rates published by the U.S. Federal Reserve Bank as a maturity matched Treasury rate.

We report basic summary statistics for the term structure of all rates in Table 2, summarizing the information for maturities of 3 and 6 months, and for 3, 5, 7, 10, 20, and 30 years. Panels A, B, and C in Table 2 show that on average, CMTs are lowest, with an upward sloping term structure ranging from 1.25% at the short end to 3.95% at the 30-year horizon. The OIS rates, reported in Panel A, are higher and range on average from 1.40% to 2.54% at 5-year maturity. Average OIS rates with maturities above 5 years are not directly comparable to the CMTs, as there are fewer observations. OIS data for 7-year and 10-year maturities start in May 2012 and August 2008, respectively, while those for 20- and 30-year maturities start in September 2011. The LIBOR/swap rates reported in Panel B are the largest, ranging on average from 1.66% to 3.97% at the short and long ends of the maturity spectrum. All interest rates exhibit a decreasing term structure of volatility, as the standard deviation for long-term maturities is lower than that for short-term maturities.

In Panel D, we report statistics for the [Gurkaynak, Sack, and Wright \(2007\)](#) zero coupon Treasury yields, which we use in our estimation. These are available for 1 to 30 years, and are slightly larger than the CMTs, with an average yield of 1.50% to 4.07%.

In Panels E and F of Table 2, we report both USD and EUR denominated CDS premiums on the U.S. Treasury. We use USD denominated contracts in our empirical analysis. EUR contracts cover a longer span of data (from 2007 instead of 2010), so they can give us a qualitative indication of the magnitude of the U.S. credit risk premium during the crisis. The average cost of insurance against a default by the U.S. Treasury ranges from 11 bps to 37 bps for USD contracts, and from 13 bps to 44 bps for EUR denominated contracts. The 5-year contract is the most liquid. At the 99th percentile of the distribution, the 5-year insurance premium reaches 66 bps during the post-2010 period, but at the height of the global financial crisis (GFC), 5-year spreads jumped to a maximum of 95 bps (unreported in the Table).

2.3. Swap spreads

Figure 2 visualizes the evidence on swap spreads, i.e., the difference between OIS or IRS rates and maturity matched Treasury rates. Panel (d) of the figure confirms the negative long-term IRS swap spreads observed in the post-crisis period, as emphasized by [Jermann \(2019\)](#) and [Klingler and Sundaresan \(2019b\)](#). According to [Boyarchenko, Gupta, Steele, and Yen \(2018\)](#) and [Jermann \(2019\)](#), long-term swap spreads remain negative because regulatory caps on leverage ratios make it too costly for investors to arbitrage away the

difference. Panels (a) and (b) of the figure confirm the negative short-term OIS spreads observed in the post-crisis period, as identified by [Klingler and Sundaresan \(2019a\)](#), who associate this inversion with a fading demand for U.S. Treasury notes and a corresponding decline in the convenience yield.

Together, the panels provide additional evidence. The OIS swap spreads continue to be negative at longer maturities, and the liquidity of OIS with maturities of over 5 years declines. Nevertheless, the prices convey qualitative information about the relative magnitudes of OIS and Treasury rates. The difference is too large to be easily explained away by liquidity effects.¹

2.4. U.S. credit risk and negative swap spreads

In this section, we explain our intuition behind the proposed relation between negative swap spreads and U.S. credit risk, and how we rely on the no-arbitrage bound type of argument. Revisiting the case without credit risk can help us to appreciate the impact of credit risk. A negative swap spread suggests that the Treasury is relatively less expensive. An arbitrageur would aim to exploit this by buying the Treasury via a repo transaction and take a position that pays the fixed (and receives the floating) rate in a swap contract. The cash flows corresponding to these positions are displayed in Table 4.

We use notation CMS_0^n for a generic swap rate, either OIS_0^n or IRS_0^n . The contractual floating rate in a swap (a LIBOR rate, or EFR compounded over the period between tenors) is f_t . The 3-month repo rate is r_t . SS_0^n denotes the swap spread and equals $CMS_0^n - CMT_0^n$. The term S_t denotes the difference $f_t - r_t$. For expositional simplicity, we assume that floating and fixed payments are paid each period.

One receives $S_{t-1} - SS_0^n$ at each point t . No-arbitrage implies that $PV(SS_0^n) = PV(S_{t-1})$, where PV denotes the present value computed at time 0 (the swap inception). As the uncollateralized borrowing costs are greater than the collateralized borrowing costs, the present value of the floating payments must be positive, which implies a pure arbitrage opportunity if $SS_0^n < 0$.

If the Treasury is credit-risky, the no-arbitrage argument above no longer holds. On default at a random date τ , the Treasury bond terminates, the future interest payments CMT_0^n are no longer received, and the bond pays $1 - L$ instead of the full face value, which then affects the repayment of the repo loan. The swap contract is unaffected by the Treasury default because it is linked to an index f_t that is not investable. A swap is then more valuable than a credit-risky Treasury bond.

¹In fact, the direction of liquidity effects could be ambiguous, ex ante, as for assets in zero net supply, such as swaps, the liquidity premium is earned by the marginal investor, who is either long or short swaps on average (see, e.g., [Bongaerts et al., 2011](#), [Deuskar et al., 2011](#), and [Brenner et al., 2001](#)).

A position in the bond can be complemented with the purchase of default protection via a CDS contract, thus hedging the credit risk. This affects the cash flows of the overall position (See Table 5). Specifically, in the case of default, the joint bond-CDS position has full recovery of par, which is used to close out the repo loan. In addition, one receives the unwind value of the swap, U_τ . For simplicity, we assume that accruals due upon default are rolled into the unwind value.

On balance, one receives $S_{t-1} - SS_0^n - CDS_0^n$ every period t in which there is no default. If there is a default at time τ , one receives U_τ . No-arbitrage means that the present value of these cash flows must be equal to zero at the swap inception, implying

$$PV_0(SS_0^n) = PV_0(S_{t-1}) - PV_0(CDS_0^n) + PV_0(U_\tau) \geq -PV_0(CDS_0^n) + PV_0(U_\tau).$$

Thus, for sufficiently large CDS premiums and sufficiently small values of $PV(U_\tau)$, the swap spread can be negative, and then the lower bound for the swap spread can be negative, and observing a negative swap spread would not necessarily lead to arbitrage opportunities.

Accounting for the cumulative probability of no default, S_0^n , the no-arbitrage relation can be represented as

$$SS_0^n = -CDS_0^n + PV_0(S_{t-1} + U_\tau)/S_0^n \geq -CDS_0^n + PV_0(U_\tau)/S_0^n. \quad (1)$$

Figure 2 demonstrates the relation between swap spreads and the negative of the CDS premiums. For IRS, $SS_0^n > -CDS_0^n$, suggesting a small value of $PV_0(U_\tau)$, while for OIS, SS_0^n is occasionally less than $-CDS_0^n$, implying a negative value of $PV_0(U_\tau)$.

Figure 2 suggests that CDS premiums co-move with swap spreads in addition to serving as an approximate lower bound for them. Because both swap spreads and CDS premiums are persistent, it is better to study the co-movement of their changes. We can infer the implications of the no-arbitrage relation (1) for changes by differencing the terms featuring in the equality, leading to a prediction for the relation between changes in swap spreads and changes in CDS premiums:

$$\Delta SS = -\Delta CDS + F(U, S, \mathcal{S}),$$

where the last term $F(\cdot)$ represents a function of the differences in present values of the floating spread and unwind values, appropriately scaled by the survival probability.

Motivated by this relation, Table 3 provides additional evidence regarding the relation between changes in OIS spreads and U.S. CDS premiums by regressing the former on the latter at monthly frequency, including a large battery of control variables.² We run panel

²We examine the relation between swap spreads and U.S. credit risk at a monthly frequency because the decision interval in our model is monthly. The results for the weekly frequency, which are stronger, are available upon request.

regressions by pooling all maturities and match the 3-month swap spreads with the 6-month CDS premium because there are no CDS contracts with a lower level of maturity. We add maturity-specific fixed effects to absorb time-invariant cross-maturity differences due to the different possible clienteles.

The finding in column (1) is consistent with a negative relation between OIS swap spreads and CDS premiums. The finding of a coefficient that is -0.07 , rather than the predicted coefficient of -1 , is suggestive of an omitted variable bias driven by a strong association between the omitted term $F(\cdot)$ and ΔCDS . In column (2), we show that the economic magnitude is similar for maturities above 5 years, and in column (3), we pool all maturities together. The estimated coefficient suggests that a 10 bps increase in the CDS premium is associated with a 0.7 bps drop in the OIS swap spread. The larger coefficient (-0.13) reported in column (4) suggests that the sensitivity of the changes in OIS-Treasury to changes in CDS premiums has recently increased.

In columns (5) to (10), we successively introduce lagged swap spreads, quarterly fixed effects to absorb the influence of common macroeconomic and financial factors, and controls.³ Even the conservative specification with the interaction of maturity and quarterly fixed effects in column (7) does not alter the significance or economic magnitude of the regression coefficient. Longer-term OIS contracts were less liquid around the crisis and became successively more liquid, as discounting using OIS rates became more common over time. Thus, the negative relation between swap spreads and CDS premiums is apparent in later years, as demonstrated by the larger magnitude of the regression coefficient in columns (4), (8), and (12), in which we restrict the regression to the time period post-2014. This finding also suggests that our results are not merely driven by the U.S. debt ceiling episodes in August 2011 and October 2013.

3. A realistic model

As established, a negative swap spread can be obtained even in the absence of arbitrage opportunities and may in fact be plausible in the context of current market data. To determine the real situation, we must explicitly model the forces behind the magnitude of swap spreads. In addition, the perceived credit risk of the U.S. government means that we do not get to observe a risk-free rate. Thus, an equilibrium model is required to identify such a rate, and we use a model of a representative agent with recursive preferences.

Another more subtle advantage of using the equilibrium framework concerns the change in how the industry approaches the discounting of cash flows associated with collateralized

³The control variables include the CBOE VIX index, the exchange rate of the USD against a basket of a broad group of major U.S. trading partners, the West Texas Intermediate oil price index, the economic policy uncertainty index, the high-yield and investment-grade bond indices, inflation, the TED spread, the 3-month LIBOR-OIS spread, the 3-month T-bill rate, the U.S. Treasury total cash balances, and CDS depth defined as the number of dealer quotes used to compute the mid-market spread.

swap agreements. Full collateralization at the end of 2007 led market participants to use the OIS rates instead of the LIBOR rates, and by the end of 2008 the whole industry had switched to OIS (e.g., [Cameron, 2013](#), [Spears, 2019](#)). Thus, a no-arbitrage model would need to address the choice of reference interest rate.⁴

Under the null of our model, we obtain an equilibrium pricing kernel that we use to discount cash flows of a given financial instrument. The reference interest rate here is the theoretical real risk-free rate. All other interest rates appear as derived quantities in this framework and are internally consistent.

3.1. Joint dynamics of macroeconomic fundamentals

As the literature on long-run risk suggests, accounting for the variation in conditional expectations and the volatility of consumption growth is essential for the framework to quantitatively be a success. We therefore identify these quantities from a rich model that includes the joint dynamics of consumption growth, inflation, output growth, and government expenditures.

The strengths of this strategy are as follows. First, we can identify risk-free rates (both real and nominal) without relying on asset price data. Second, we can exploit the rich joint interactions between the macro fundamentals to identify conditional moments of consumption growth ([Schorfheide et al., 2018](#), [Zviadadze, 2017](#)). Third, we identify the dynamics of macro variables required in our model, other than consumption: inflation to value nominal assets; output growth and government expenditures to model the default probability of the U.S. government (as in [Chernov et al., 2020](#)); and macroeconomic uncertainty, which is an important driver of sovereign credit risk in developed economies (as in [Augustin, 2018](#)).

Thus, we introduce a vector z_t of macroeconomic fundamentals:

$$z_t = (\Delta c_t, d_t, g_t, \pi_t)^\top,$$

where $\Delta c_t = \log(C_{t+1}/C_t)$ is log consumption growth, d_t is log output growth, g_t is the government expenditure-to-output ratio, and π_t is inflation. The dynamics of state variables in many long-run risk models are specified as a VAR(1) process in observable macro and latent states, e.g., [Bansal and Yaron \(2004\)](#), or [Bansal and Shaliastovich \(2013\)](#). They are similar to VARMA(1,1) models in observable macro states only (they are literally the same in homoscedastic cases).

⁴For example, [Chernov and Creal \(2016\)](#) reflect this change, using OIS rates as a measure of reference rates starting in 2009 and using a weighted average of LIBOR and OIS in 2008, with weights gradually shifting towards OIS by the end of 2008.

Thus, we assume that z_t follows a VARMA(1,1) process with time-varying variance:

$$z_{t+1} = \mu_z + \Phi_z z_t + \Phi_{zv} v_t + \Sigma_z \cdot V_{z,t}^{1/2} \cdot \varepsilon_{z,t+1} + \Theta_z \cdot \Sigma_z \cdot V_{z,t-1}^{1/2} \cdot \varepsilon_{z,t}, \quad (2)$$

where z_{t+1} denotes a $N \times 1$ vector ($N = 4$ in our case), $\varepsilon_{z,t+1} \sim \mathcal{N}(0, I)$, μ_z is an $N \times 1$ vector, Φ_z is an $N \times N$ matrix, and Σ_z is an $N \times N$ matrix, where the diagonal elements of Σ_z are defined as σ_{z_i} , for $i = 1, 2, \dots, N$. Denote the last term in equation (2) as w_{t+1} ,

$$w_{t+1} = \Theta_z \cdot \Sigma_z \cdot V_{z,t}^{1/2} \cdot \varepsilon_{z,t+1},$$

and stack the elements of z_t and w_t into a new vector $y_t = [z_t^\top, w_t^\top]^\top$.

We treat π_t as Granger-caused by the other macro variables, but not vice versa. This is a reduced-form representation of the exogenous and endogenous variables that enables us to be consistent with the setup of [Chernov, Schmid, and Schneider \(2020\)](#) by restricting the off-diagonal elements of the last column of Φ_z and Θ_z to zero.

The vector y_t follows a VAR(1):

$$y_{t+1} = \mu_y + \Phi_y y_t + \Phi_{yv} v_t + \Sigma_y \cdot V_{y,t}^{1/2} \cdot \varepsilon_{y,t+1},$$

where y_{t+1} denotes a $2N \times 1$ vector, $\varepsilon_{y,t+1} \sim \mathcal{N}(0, I)$, μ_y is a $2N \times 1$ vector, Φ_y is a $2N \times 2N$ matrix, and Σ_y is a $2N \times 2N$ matrix, where the diagonal elements of Σ_y are defined as σ_{y_i} , for $i = 1, 2, \dots, 2N$.

We assume that the volatility vector consists of autonomous univariate autoregressive gamma processes characterized by the bivariate vector v_t , such that each element $v_{i,t+1}$ follows an autoregressive gamma process $v_{i,t+1} \sim ARG(\nu_i, \phi_i, c_i)$ ([Gourieroux and Jasiak, 2006](#) and [Le et al., 2010](#)), that is,

$$v_{i,t+1} = \nu_i c_i + \phi_i v_{i,t} + \eta_{i,t+1}, \quad \text{var}_t \eta_{i,t+1} = \nu_i c_i^2 + 2c_i \phi_i v_{i,t}.$$

The unconditional mean is $E v_{i,t} = \nu_i c_i (1 - \phi_i)^{-1}$, and we select $c_i = (1 - \phi_i) \nu_i^{-1}$ to set it to 1 for identification purposes.

We add the volatility vector to the state vector y_t to obtain $x_t = [z_t^\top, w_t^\top, v_t^\top]^\top$. With $K = (2 \times N + 2)$, the $K \times 1$ -dimensional multivariate state vector x_{t+1} follows a VAR(1) process:

$$x_{t+1} = \mu + \Phi x_t + \Sigma \cdot V_t^{1/2} \cdot \varepsilon_{x,t+1},$$

where $\varepsilon_{x,t+1}$ defines a vector of independent shocks, Φ is a $K \times K$ matrix with positive diagonal elements, Σ is a $K \times K$ matrix with strictly positive elements, and V is a $K \times K$ diagonal matrix with elements given by:

$$V_{i,t} = a_i + b_i^\top v_t,$$

where parameter restrictions are required to guarantee the non-negativity of the volatility process.

3.2. The pricing kernel

We assume a representative agent with recursive preferences:

$$\begin{aligned} U_t &= [(1 - \beta)C_t^\rho + \beta\mu_t(U_{t+1})^\rho]^{1/\rho}, \\ \mu_t(U_{t+1}) &= E_t(U_{t+1}^\alpha)^{1/\alpha}, \end{aligned}$$

where $\rho < 1$ captures time preferences (the intertemporal elasticity of substitution is $(1 - \rho)^{-1}$), and $\alpha < 1$ captures the risk aversion (the relative risk aversion is $1 - \alpha$). Aggregate consumption is denoted by C_t . With this utility function, the real pricing kernel is

$$\widehat{M}_{t+1} = \beta(C_{t+1}/C_t)^{\rho-1}(U_{t+1}/\mu_t(U_{t+1}))^{\alpha-\rho}.$$

We can approximate the (log) pricing kernel using the solution method outlined in [Hansen, Heaton, and Li \(2008\)](#) and [Backus, Chernov, and Zin \(2014\)](#). We log-linearize the scaled time aggregator:

$$\log(U_t/C_t) \equiv u_t \approx b_0 + b_1 \log \mu_t(e^{\Delta c_{t+1} + u_{t+1}}),$$

where

$$\begin{aligned} b_1 &= \beta e^{\rho \log \mu} ((1 - \beta) + \beta e^{\rho \log \mu})^{-1} \\ b_0 &= \rho^{-1} \log((1 - \beta) + \beta e^{\rho \log \mu}) - b_1 \log \mu, \end{aligned}$$

with $\log \mu = E(\log \mu_t)$. We guess u_t to be a linear function of the state x_t , substitute this guess into the log-linearized expression for u_t , and use the method of undetermined coefficients to solve for u_t . Then the log pricing kernel is

$$\begin{aligned} \widehat{m}_{t,t+1} &= \log \beta + (\rho - 1) \Delta c_{t+1} + (\alpha - \rho) [\Delta c_{t+1} + u_{t+1} - \log \mu_t (e^{\Delta c_{t+1} + u_{t+1}})] \\ &= \log \beta - (\alpha - \rho) b_0 b_1^{-1} + (\alpha - 1) \Delta c_{t+1} + (\alpha - \rho) [u_{t+1} - b_1^{-1} u_t]. \end{aligned}$$

See [Appendix B](#) for details.

3.3. Equilibrium risk-free rates

The price of a zero-coupon bond paying one unit of consumption n periods ahead from now must satisfy the Euler equation

$$\widehat{P}_t^n = E_t [\widehat{M}_{t,t+n}].$$

We show in C.1 that the term structure of real interest rates is affine in the state vector x_t .

Similarly, the price of an n -period zero-coupon nominal bond is obtained from the nominal stochastic discount factor and must satisfy the Euler equation

$$P_t^n = E_t[M_{t,t+n}],$$

where the nominal (log) stochastic discount factor is defined as $m_{t,t+1} = \widehat{m}_{t,t+1} - \pi_{t+1} = \widehat{m}_{t,t+1} - e_2^\top y_{t+1}$. We show in C.2 that the term structure of nominal interest rates is affine in the state vector x_t .

3.4. The valuation approach for defaultable interest rates

To capture the credit risk of the U.S. government, we use the model of Chernov et al. (2020) as a basis. This model is based on the contingent claims approach (CCA), which delivers a fiscal default via the budget deficit that can no longer be restored by raising taxes or eroding the real value of debt by creating inflation. The model requires a numerical solution even under oversimplified assumptions about the underlying economy. As we are seeking a high degree of realism, we do not model the whole elaborate structure of the default mechanism for tractability, and instead exploit the equivalence between the CCA and compound Poisson approaches (Duffie and Lando, 2001) and model a default hazard rate.

The exogenous variables of Chernov et al. (2020) that drive the U.S. credit risk are the aggregate consumption growth rate, output growth, and the government expenditures-to-output ratio. Augustin (2018) also shows that macroeconomic uncertainty is an important driver of sovereign credit risk in developed economies. Thus, we assume that the government’s default risk is driven by a default intensity h_t defined as

$$h_t = h + h_c \Delta c_t + h_d d_t + h_g g_t + h_{v_1} v_{1,t} + h_{v_2} v_{2,t}. \quad (3)$$

To model default risk, we also need a corresponding loss given the default (LGD), denoted by L , which we assume to be constant. Although it is reasonable to expect that a U.S. default would affect the representative agent’s consumption, we, following Chernov et al. (2020), do not allow for this in our model. That allows us to implement our strategy of using macro data only for identifying the real pricing kernel.

Inflation or the bank credit risk may also be assumed to affect the default probability of the U.S. government. Inflation may be relevant if we believe that the U.S. government may attempt to “inflate away” its nominal debt. The bank credit risk may be important because of the potential link between banks’ solvency and government default (see, e.g., Acharya et al., 2014). For example, if the Fed bails out the banks, it could be forced into insolvency. This could trigger government default because of the fiscal support provided by the Treasury (Reis, 2015).

As discussed earlier in the case of π_t and as we show later in the case of the factor capturing bank risk, the two variables are Granger-caused by macro variables, but not vice versa. Nevertheless, inflation and bank credit risk are related to the default probability of the U.S. government, albeit implicitly.

Given these assumptions, we can follow the approach of [Duffie and Singleton \(1999\)](#), which implies that under the recovery-of-market-value assumption, credit risk can be accounted for by augmenting the (log) discount factor with $L \cdot h_t$:

$$\bar{P}_t^n \approx E_t e^{\sum_{j=1}^n m_{t+j-1,t+j} - L \cdot h_{t+j}}.$$

However, \bar{P}_t^n does not correspond to an observable bond price, because Treasury prices also reflect the convenience yield.

Thus, to progress, we must address the following conceptual challenge. The swap spreads are affected by factors other than the U.S. credit risk, although this is our main focus. First, Treasury bonds are considered to be expensive and include a convenience yield relative to other asset classes (e.g., [Longstaff, 2004](#); [Krishnamurthy and Vissing-Jorgensen, 2012](#); [Nagel, 2016](#); [Du, Im, and Schreger, 2018](#)). Second, the swap rates typically reflect the credit and funding risk of financial intermediaries (e.g., [Feldhutter and Lando, 2008](#)). Third, as pointed out by [Johannes and Sundaresan \(2007\)](#), full collateralization of swaps increases the rates because of an opportunity cost of collateral (if the correlation between the short interest rate and the cost of collateral is positive). Thus, we must model all of these additional drivers of swap spreads.

In addition, no single asset is sensitive to only one of these factors, and so to identify them, we must use several assets simultaneously. Both Treasuries and U.S. CDS provide information about the U.S. credit risk, and while the former also reflects the convenience yield, the latter does not. Similarly, the U.S. CDS reflects the opportunity cost of collateral, which is irrelevant for Treasuries, but also affects swap rates. IRS contracts are also exposed to the opportunity cost of collateral and the credit risk of banks in the Eurodollar area. Thus, combining these assets will help us identify all of the required factors, and we can then use them to evaluate the central object of the negative swap spread puzzle, i.e., the OIS-Treasury spread, as an out-of-sample test of our model.

3.5. Spread factors

Empirically, we identify the safety factor via the difference between the 1-month OIS rate o_t and (risky) Treasury rates \tilde{y}_t^1 , $s_{1,t} = o_t - \tilde{y}_t^1$. As discussed, this factor reflects not only the ease of trading in Treasuries, but also the credit risk of banks in the Federal Reserve system. We identify the bank credit factor via the difference between 1-month LIBOR and OIS rates, $s_{2,t} = \ell_t - o_t$. We refer to s_2 as the LIBOR-OIS spread. The cost of collateral $s_{3,t}$ is treated as latent in the absence of an observable measure. We stack them into a vector $s_t = [s_{1,t}, s_{2,t}, s_{3,t}]^\top$.

The quantitative and conceptual evolution of these spreads provides a great deal of scope for discussion, but we focus on the key takeaways. The difference between LIBOR and EFFR can roughly represent the credit risk of banks in the Eurodollar area, while the difference between EFFR and a Treasury bill rate can represent the convenience yield.

The first distinction is consistent with the view of the LIBOR-OIS spread and its use as an indicator of the health of the banking sector in the wake of the financial crisis of 2008. The use of OIS here is subtle, because it reflects the credit risk of banks in the Federal Reserve system. Thus, the spread $s_{2,t}$, reflects the relative riskiness of the banks in the Eurodollar area. The U.S. LIBOR is used in practice for transactions between banks and other financial institutions, such as mutual funds, while the EFFR is used for transactions between banks in the Fed system.

The second distinction assumes that the EFFR and the Treasury rate represent the same credit quality. Many researchers and practitioners treat the whole OIS curve as risk-free because it is used to discount fully collateralized transactions. Full collateralization largely mitigates the counterparty risk, but not the cash flow risk of the underlying asset, which in this case is the EFFR. The credit risk of the U.S. Treasury is linked to that of the Federal Reserve system because the Treasury fiscally supports the Fed (Reis, 2015), so the Fed will never be insolvent separately from the Treasury. If the EFFR is assumed to be risk-free and the Treasury credit-risky, it would be much easier to explain the negative swap spread. The aforementioned bank risk embedded in the EFFR then suggests that the spread $s_{1,t}$ would reflect that risk, in addition to the convenience yield of Treasuries.

We assume that s_t follows a multivariate Gaussian AR(1) process, and it may also be affected by the dynamics of the macro volatility v_t :

$$s_{t+1} = \mu_s + \Phi_{sv}v_t + \Phi_s s_t + \Sigma_s \varepsilon_{s,t+1}, \quad (4)$$

where the innovations $\varepsilon_{s,t+1} \sim \mathcal{N}(0, \mathbb{I})$. By construction, s_t does not Granger cause the macro variables (z_t, v_t) . The conditional covariance of the one-period pricing kernel and the factor is zero, so there is no one-period risk premium associated with s_t .⁵ Their multi-period counterparts covary, thereby generating risk premiums because of the presence of macro fundamentals in the conditional expectation of s_t . We introduce an extended state vector $\tilde{x}_t^\top = [x_t^\top, s_t^\top]$.

3.6. Valuation of credit sensitive instruments

We successively discuss the valuation of risky Treasury bonds, hypothetical LIBOR bonds, as well as IRS, OIS, and CDS rates.

⁵The impact of macro innovations on s_{t+1} was estimated imprecisely, so we zeroed that out to save on cumbersome notation.

3.7. Risky Treasury bonds

Following [Duffie and Singleton \(1999\)](#), the resulting risky Treasury price is

$$\tilde{P}_t^n \approx E_t e^{\sum_{j=1}^n m_{t+j-1,t+j} - L \cdot h_{t+j} + s_{1,t+j}},$$

and we show in [C.3](#) that the term structure of risky interest rates is affine in the extended state vector \tilde{x}_t .

3.8. Hypothetical LIBOR bonds

We work with hypothetical zero-coupon LIBOR bonds L_t^n discounted at the continuously compounded yield ℓ_t^n (defined at the monthly frequency), such that

$$L_t^n = \exp(-\ell_t^n \cdot n), \quad (5)$$

where $n \leq 12$ corresponds to LIBOR rate maturities of up to 12 months.⁶ Using the approach of [Duffie and Singleton \(1999\)](#), the resulting price is

$$L_t^n \approx E_t e^{\sum_{j=1}^n m_{t+j-1,t+j} - L \cdot h_{t+j} - s_{2,t+j}},$$

and we show in [C.4](#) that the term structure of LIBOR rates is affine in the extended state vector \tilde{x}_t , with rates ℓ_t^n inferred from Equation (5).

3.9. IRS

The fixed rate payer pays the annual interest rate swap premium $IRS_{t,T}$. The floating rate payer pays the LIBOR rate that has been realized at the previous coupon period. We assume monthly time intervals to match the frequency of macroeconomic data. Thus, in the case of a quarterly IRS payment frequency, the floating leg would pay each period the 3-month LIBOR rate realized on the previous coupon period, ℓ_{t-1}^3 . The 1-month LIBOR rate is equal to $\ell_t \equiv \ell_t^1 = \tilde{y}_t^1 + s_{1,t} + s_{2,t}$.

We value the term structure of zero-coupon LIBOR rates in [C.4](#) and can thus directly use the 3-month LIBOR rates for the computation of the LIBOR swap contracts.⁷ We discount

⁶Because actual LIBOR rates $\ell_t^{q,n}$ are periodic and quoted on an annualized basis, we map the data into continuously compounded rates according to the formula $\ell_t^n = n^{-1} \log(1 + \ell_t^{q,n} \cdot n \cdot 30/360)$. The day count convention for LIBOR rates is act/360. We use 30/360 as the daycount convention given that it is numerically close to act/360, and it simplifies the implementation.

⁷For maturities up to one year, zero-coupon rates are equivalent to par rates. For the numerical implementation, we map the continuously compounded LIBOR rates into periodic rates assuming a 30/360 day count convention for simplicity.

all cash flows accounting for the cost of collateral $s_{3,t}$ following [Johannes and Sundaresan \(2007\)](#). Thus, the present value of expected future payments by the fixed leg is given by

$$\omega_t^{fix} = IRS_t^n \sum_{j=1}^{n\Delta-1} E_t [e^{m_{t,t+j\Delta} + s_{3,t+j\Delta}}],$$

where Δ defines the time interval between two successive coupon periods. The present value of expected future payments by the floating leg is given by

$$\omega_t^{float} = \sum_{j=1}^{n\Delta-1} E_t \left[e^{m_{t,t+j\Delta} + s_{3,t+j\Delta}} \left(e^{\Delta \cdot \ell_{t+(j-1)\Delta}^3} - 1 \right) \right].$$

where Δ defines the time interval between two successive coupon periods.

A LIBOR swap contract is priced fairly if both the fixed and the floating legs have the same value. The condition yields the formula for the IRS spread IRS_t^n :

$$IRS_t^n = \frac{\sum_{j=1}^{n\Delta-1} E_t \left[e^{m_{t,t+j\Delta} + s_{3,t+j\Delta}} \left(e^{\Delta \cdot \ell_{t+(j-1)\Delta}^3} - 1 \right) \right]}{\sum_{j=1}^{n\Delta-1} E_t [e^{m_{t,t+j\Delta} + s_{3,t+j\Delta}}]}. \quad (6)$$

See [Appendix C.5](#) for the derivation.

3.10. OIS

The fixed rate payer pays the annual OIS premium OIS_t^n , and the floating rate payer pays the geometric mean of daily overnight rates. As in our model a monthly minimal time interval is assumed, there is no distinction between $o_t \equiv OIS_t^1$ and EFRR compounded over a month. Thus, the quarterly payment frequency corresponds to the floating leg paying the geometric average of three 1-month OIS rates.

As for IRS premiums, we discount all cash flows accounting for the cost of collateral $s_{3,t+1}$. The present value of expected future payments by the fixed leg is given by

$$\pi_t^{fix} = OIS_t^n \sum_{j=1}^{n\Delta-1} E_t [e^{m_{t,t+j\Delta} + s_{3,t+j\Delta}}],$$

where Δ defines the time interval between two successive coupon periods. The present value of expected future payments by the floating leg is given by

$$\pi_t^{float} = \sum_{j=1}^{n\Delta-1} E_t \left[e^{m_{t,t+j\Delta} + s_{3,t+j\Delta}} \left[\exp \left(\sum_{i=1}^{\Delta} o_{t+j\Delta-i} \right) - 1 \right] \right].$$

OIS swaps with maturity of less than one year are subject to only one payment settlement, while those with maturities equal to or greater than one year are subject to quarterly payments.

An OIS contract is priced fairly if both the fixed and the floating legs have the same value. This condition yields the formula for the OIS spread OIS_t^n :

$$OIS_t^n = \frac{\sum_{j=1}^{n\Delta^{-1}} E_t \left[e^{m_{t,t+j\Delta} + s_{3,t+j\Delta}} \left[\exp \left(\sum_{i=1}^{\Delta} o_{t+j\Delta-i} \right) - 1 \right] \right]}{\sum_{j=1}^{n\Delta^{-1}} E_t [e^{m_{t,t+j\Delta} + s_{3,t+j\Delta}}]}. \quad (7)$$

See Appendix C.6 for the derivation.

3.11. CDS

To value CDS contracts, we must model both the premium leg that pays the annual CDS premium CDS_t^n and the protection leg that pays the loss given default L . We note the distinction between CDS contracts, which contractually recover a fraction of face value, and risky Treasuries, which are usually modeled as recovering a fraction of market value. Duffie and Singleton (1999) find little difference across different modeling assumptions of recovery in the term structure of defaultable interest rates (see Figure 2 on p. 703).

A CDS contract with time to maturity n pays the annual premium until an earlier default or the contract's termination date. As for other swap contracts, we account for the cost of collateral. Accordingly, the present value of the premium payments of a USD-denominated CDS contract is equal to

$$\pi_t^{pb} = CDS_t^n \sum_{j=1}^{n\Delta^{-1}} E_t [e^{m_{t,t+j\Delta} + s_{3,t+j\Delta}} I(\tau > t + j\Delta)],$$

where Δ defines the time interval between two successive coupon periods, and $I(\cdot)$ is an indicator function that is equal to one if the condition inside the brackets is met, and zero otherwise. For simplicity, we omit accrual payments in the notation, but account for them in the formal implementation of the model. The present value of expected future payments by the protection seller is given by

$$\pi_t^{ps} = L \cdot E_t [e^{m_{t,\tau} + s_{3,\tau}} I(\tau \leq n)].$$

A CDS contract is priced fairly if both the premium and the protection legs have the same value. This condition yields the formula for the CDS premium CDS_t^n :

$$CDS_t^n = L \cdot \frac{E_t [e^{m_{t,\tau} + s_{3,\tau}} I(\tau \leq n)]}{\sum_{j=1}^{n\Delta^{-1}} E_t [e^{m_{t,t+j\Delta} + s_{3,t+j\Delta}} I(\tau > t + j\Delta)]}. \quad (8)$$

See Appendix C.7 for the derivation of the CDS premiums.

4. Results

We first present the estimation approach, describe the model’s state variables, and discuss the model fit. Next, we characterize the U.S. “credit spread”. Last, we illustrate the model-implied results for swap spreads and quantify the importance of credit risk for observed prices.

4.1. Estimation

We use macroeconomic fundamentals and financial asset data to estimate the model via Bayesian MCMC with diffuse priors. The outputs of the procedure are the state variables and parameter estimates. Posterior estimates are provided in Table 6 and Table 7.

We conduct a two-stage estimation, which is the key feature of our approach. In the first stage, we estimate the macro dynamics described by the autonomous VARMA for z_t . In the second stage, we use asset market data for the identification of the financial factors s_t conditional on the estimated z_t .

The advantages of this are first that as the available data on CDS and interest rate swap premiums provide a much shorter time interval, starting in 2002 (USD-denominated U.S. CDS start even later, in 2010), the first stage enables us to use a longer history of macroeconomic fundamentals to investigate z_t . Second, we can identify the dynamics of the macroeconomic factors and thus of the pricing kernel, without relying on asset market data. We therefore avoid the “dark matter” critique of Dou et al. (2017).

We next provide a brief outline of our two-stage estimation procedure, and give the details in Appendix D. In the first stage, we use consumption growth, output growth, log government expenditure-to-output ratio, and inflation from 1982 to 2018. Apart from the monthly inflation data, the other macro variables are quarterly.⁸ The decision interval is one month in our model, so we estimate the monthly counterparts of the respective quarterly series. We adjust the state-space representation to address the mixed frequency of the observables. Posterior estimates from the first stage estimation are provided in Table 6.

The estimated AR matrix Φ_z and MA matrix Θ_z imply that consumption and output growth rates do not affect inflation and government expenditure. Output growth rates affect all macro fundamentals (consumption is affected indirectly via output and the MA term).

⁸Our choice of quarterly consumption growth avoids modeling measurement errors in monthly consumption growth (see Schorfheide et al., 2018 for a detailed discussion). This significantly reduces the dimension of the state vector leading to a much more tractable estimation problem.

The two variance factors only affect the conditional mean of inflation. The other elements of the matrix Φ_{zv} are set to zero because they were poorly identified in our sample.

After filtering out the estimates for z_t and v_t at the monthly frequency, we use data on the term structure of Treasury GSW zero-coupon rates (maturity of 1, 3, 5, 7, 10, 20, and 30 years), the term structure of CDS premiums (maturity of 1, 3, 5, 7, 10, 20, and 30 years), and the empirical measures of $s_{1,t}$ and $s_{2,t}$ to investigate the joint dynamics of s_t . We do not use the IRS and OIS data in the estimation, so we can evaluate the implied swap spreads as an out-of-sample test of our model. The one-year IRS is the only exception to this strategy because it can help identify the latent cost of collateral, s_3 .⁹ We use the bootstrap particle filter to estimate $s_{3,t}$.

To estimate the dynamics of the financial variables in the second stage, we condition on the filtered macroeconomic fundamentals from the corresponding period. These fundamentals visibly shift in level in the later part of our sample, so we re-estimate the constant term μ_z to accommodate possible structural breaks in the level of macroeconomic fundamentals z_t . Similarly, we impose a one-time structural break in the default intensity h_t by assuming that it switched from zero to a positive value in December 2007 to reflect the previous near-zero U.S. CDS premiums. Posterior estimates from the second stage estimation are provided in Table 7.

Apart from the variance factors, the macro variables do not affect the financial variables (the matrix Φ_{sy} was poorly identified). The variances have a significant impact on the convenience yield s_1 , perhaps reflecting the flight-to-safety effect, and the cost of collateral s_3 , reflecting lenders' collateral demand. Apart from output growth, all of the macro variables play an important role in the default intensity. Output growth affects forecasts of future h_t via its impact on consumption growth (matrix Φ_z).

In most no-arbitrage modeling of credit-sensitive assets, the LGD is not estimated separately from the default intensity because of a joint identification problem. We separate the two solely to simplify the interpretation of the magnitude of the default rate. Thus, following Chernov et al. (2020), we calibrate the LGD to a specific value of $L = 0.3$.

The estimated risk aversion is $1 - \alpha \approx 5$. This value is clearly insufficient to match the equity premium, which is natural in a bond pricing model. The elasticity of intertemporal substitution $(1 - \rho)^{-1} \approx 1.33$ is in line with standard calibrations in the long-run risk literature.

4.2. Factors

Figures 3 and 4 illustrate the factors we use in our model. The first figure shows the macro variables z_t . The downward trend in inflation throughout the sample can be

⁹Using the one-year IRS data for estimation is innocuous because it is the shortest maturity and does not exhibit any puzzles.

attributed to the extensive moderation in the early part of our sample period, but it is somewhat puzzling in the post-crisis sample, when monetary policy was particularly accommodating. However, our series are consistent with the observation that inflation is low in spite of expansionary monetary policies conducted by central banks around the globe, which has been referred to as the “missing inflation puzzle” (Arias et al., 2016).

We also note a gradual elevation in government expenditures (as a fraction of output) throughout the sample, consistent with the stabilization policies put in place after the onset of the financial crisis. Log consumption and output growth are standard series. In particular, the latter part of the sample period exhibits lower consumption growth volatility, consistent with the period of extensive moderation, except for a bump in anticipation of potential turmoil in 2008.

The second figure shows the observable finance variables, s_1 and s_2 , together with the latent finance variable s_3 . The convenience yield and the LIBOR-OIS factors exhibit familiar patterns with substantial spikes during the period surrounding the financial crisis of 2008, reflecting both a flight to quality and the increasing perceptions of bank risk in the aftermath of Lehman’s collapse. The cost of posting collateral gradually increases during the period of overheating in the credit markets as they headed into the crisis, when investment opportunities were abundant.

Both s_1 and s_3 collapse after the crisis, which is an important pattern, as a decline in both factors diminishes their effects on swap spreads. The credit risk of the U.S. Treasury is thus quantitatively the main force affecting the spreads.

The post-crisis pattern in s_1 and s_3 is natural. The decline in convenience is associated with an increase in the riskiness of Treasuries, and our estimated parameters do imply that both variance factors are associated with an increase in the default intensity and a decline in s_1 . The cost-of-collateral is influenced by the cost of holding cash and lending out Treasuries in rehypothecation, and interest rates have in fact been at historical lows since the financial crisis.

4.3. Fit

Figures 5 - 6 demonstrate the model’s fit to the financial data used in the estimation. Our setup is unusual as our model is a hybrid of an endowment economy and a reduced-form no-arbitrage valuation. Formally, it belongs to the class of affine models, but we impose various additional economic restrictions that are not typically found in a traditional no-arbitrage model. Thus, we do not expect as pristine a fit as a regular affine no-arbitrage model would deliver. Nevertheless, we aim for a high degree of realism, as otherwise, the implications for the IRS-Treasury and OIS-Treasury spreads would not be particularly plausible or relevant.

Figure 5 compares model-implied credit-risky and observed zero-coupon Treasury yields of different maturities up to a 30-year horizon. The model has some difficulty matching the

one-year rate, but it performs well at longer horizons, which is not surprising. Our model does not explicitly account for the prolonged near-zero-bound interest rate experience after the crisis, and the short end of the curve is much more sensitive to it than the long end.

Figure 6 shows the observed and the model-implied U.S. CDS rates. CDS premiums are stripped of the level of benchmark interest rates, so they naturally do not have a first-order sensitivity to the misspecification of the short interest rates. The fit of the model is good throughout all maturities.

4.4. The U.S. “credit spread”

After verifying a reasonable fit of the model, we can explore its implications. Figure 7 displays nominal credit-risk-free interest rates (without convenience yield) against the risky nominal Treasury benchmark. Before the financial crisis, there is, as expected, little difference between the riskless and the risky nominal rates because the U.S. CDS premium was zero before the crisis. They are not identical because of the presence of the convenience yield.

U.S. CDS premiums jumped in the financial crisis and have remained elevated ever since. Figure 6 shows that CDS premiums fluctuated between 20 and 60 bps at different maturities between 2011 and 2018. Accordingly, the ignition of U.S. credit risk is reflected in the difference between risky and riskless nominal Treasury interest rates. The difference between these rates is small at short horizons but becomes progressively more visible at longer horizons. For example, the difference averages around 44 bps (70 bps) at the 5-year (10-year) maturity during the post-crisis period and reaches a maximum level of 74 bps (91 bps).

We focus on the variation in the quantitative magnitude of credit risk and plot the U.S. default intensity in Figure 8(A). The likelihood of a U.S. default spikes at 0.2% during the global financial crisis (GFC) and then flares up again in times of elevated fiscal stress. Over the last decade, the threats of government shutdowns in response to U.S. debt ceiling breaches have become increasingly common. On August 5, 2011, the rating agency Standard & Poor’s downgraded the U.S., lowering its AAA credit rating by one notch to AA+. During the post-GFC period, the average intensity is about 0.05%.

Figure 8(B) quantifies the impact of the credit risk premium on the CDS valuation. Specifically, we characterize the “distress” risk premium associated with unpredictable variation in the arrival rate h_t . We follow Longstaff et al. (2005) and Pan and Singleton (2008) and report the difference between the model-based 5-year CDS premium and a hypothetical premium for the case of a risk-neutral investor (denoted CDS^\dagger). We omit the cost of collateral s_3 to focus on the pure effect of the credit risk premium.

The difference between CDS and CDS^\dagger is stable throughout the sample, averaging 14 bps. The relative difference when measuring the fraction of the CDS premium due to the

distress risk ranges between 20 and 80 percent. In contrast to the difference in levels, the relative measure trend is upwards throughout the sample. While CDS premiums decline in the post-GFC period, the relative contribution of the risk premium increases.

In Figure 9, we conduct an exercise to better gauge the impact of modeling the default risk of the U.S. Treasury. We compare the sensitivity to all state variables of the “U.S. credit spread” illustrated in Figure 7. We measure the sensitivities as factor loadings appearing in the theoretical linear relation between the credit spread and the state variables. To enable a quantitative interpretation of the results, we multiply these loadings by unconditional standard deviations of the respective state variables. Thus, the reported numbers represent a monthly change in the credit spread (expressed in decimals) in response to a one standard deviation change in any given state variable.

Our discussion focuses on the four quantitatively most important variables. Higher government expenditures elevate the risky yield relative to the nominal yield and this effect is particularly pronounced at the short end of the term structure, which is intuitive, as the government can balance its budget in the long run either by raising taxes or by issuing more debt in expectation. Either measure is likely to be accompanied by poorer default prospects, either directly or through the negative effects of elevated taxes on growth projections, as Chernov et al. (2020) find. Quantitatively, a one-standard-deviation increase in the government expenditure-to-output ratio increases the credit spread by approximately 20 bps for the 5-year maturity.

Higher macroeconomic uncertainty also leads to greater risky yields, as the representative agent in our model dislikes the economic uncertainty that accompanies a higher likelihood of extreme events. Inflation variance has a greater impact at the short end of the yield curve, as inflation surprises are more relevant for this maturity segment. Consumption variance has a greater impact at the long end of the curve, which is reminiscent of the long-run risk in volatility that has an impact due to the combination of recursive preferences with a preference for early resolution of uncertainty.

The convenience yield affects the risky Treasury directly. A higher convenience yield implies a lower yield. This effect is particularly pronounced for short-term bills, possibly due to the importance of Treasuries in short-horizon repo transactions, and it affects the credit spread by as much as 45 bps in response to a single standard deviation move. At longer maturities, the effect stabilizes at around 10 bps.

Bank risk and the cost of collateral have indirect effects via their interactions with the macroeconomic fundamentals and all spread factors. The LIBOR-OIS spread captures bank risk. Bank risk interacts positively with U.S. credit risk, and so the effect on the credit spread is positive. The cost of collateral is indirectly reflected through a negative impact on the credit spread.

4.5. Swap spreads

Figure 10 displays our headline result: the model-implied OIS-Treasury spread. Importantly, OIS information was not used in the model estimation. The model captures both the positive spread before the crisis when the U.S. credit risk was next to nil, and the negative spread in the post-crisis period. The results are quantitatively realistic for all maturities.

In Figure 11, we also plot the model-implied IRS-Treasury spread. Recall that we only use the 1-year maturity in our estimation. We qualitatively fit the evolution of the swap spreads well for OIS-Treasury spreads. We match positive swaps spreads before the crisis, and negative ones thereafter.

In our analysis in section 2.4, we offer qualitative arguments and suggestive evidence linking U.S. credit risk to swap spreads. Our quantitative model allows for a rich set of different effects beyond the sovereign risk channel, including the convenience yield, bank risk, cost of collateral, and time-varying risk premiums. Thus, a natural question is whether the quantitative effect due to a U.S. credit risk premium is large enough to support our qualitative analysis.

In our counterfactual analysis, we can use our model to evaluate the contribution of U.S. credit risk to the spreads. Figure 12 reports the results of a decomposition of the OIS-Treasury spread into the respective contributions coming from default and non-default risk. We can then gauge the contribution of the default risk premium to the negative swap spreads in our model. We plot the decomposition for maturities of 1, 3, 5, 10, 20, and 30 years. We provide a similar decomposition for IRS-Treasury spreads in Figure 13.

The quantitative implication is clear. The model-implied OIS-Treasury spreads are uniformly positive when we only account for liquidity and bank frictions. The few negative swap spread realizations are quantitatively very small. Accounting for the U.S. credit risk premium, however, shifts the OIS-Treasury spread significantly downwards. The downward shift is increasing in maturity, which clearly illustrates the critical role of U.S. credit risk in matching negative OIS-Treasury spreads in an equilibrium model that explains multiple benchmark rates jointly, even if we account for realistic liquidity and bank frictions.

In Table 8, we report model-implied regressions of changes in swap spreads on changes in CDS premiums, similar to those reported in Table 3. We do not control for common time fixed effects in these regressions because by construction, our model is driven by a limited number of state variables that drive the common variation across swap spreads. The relation between swap spreads and U.S. credit risk in the model reflects the salient features of the data well. The relation is weakly significant for short-term maturities (column 1), highly significant for maturities above 7 years (column 2), and becomes stronger over time (columns 3 and 4). The economic magnitudes are also similar to those in the data, slightly weaker at short-term maturities, and stronger at longer maturities. For example, according to the results in column (5), a 10-bps increase in CDS premiums lowers swap spreads by

0.4 bps, with an R^2 of 16%. The most comparable regression in Table 3 is that in column (5), which indicates a 0.7-bps change for a 10-bps change in CDS premiums, with an R^2 of 2%. A regression at the weekly frequency (unreported results) yields an R^2 of 5% with a regression coefficient of 2.1 bps. Post 2014, the coefficient in the data is negative at 0.13, while it is negative at 0.11 in the model.

Thus, our model suggests that quantitatively, sovereign credit risk is a relevant factor that is required to account for the negative swap-Treasury spread. The sovereign risk channel operates through the U.S. credit risk premium, which can be large, even if the physical default probability is small. Such a risk premium channel complements other explanations based on frictions. We reach this conclusion based on a realistic model of benchmark interest rates, in which frictions are identified via observable quantities (convenience yield and LIBOR-OIS spread) and a latent factor (cost of collateral); time-varying risk premia are established by the preferences of a representative risk averse agent and observed macroeconomic fundamentals.

5. Conclusion

The puzzling behavior of benchmark interest rates has been a challenge for researchers since the financial crisis. Most prominently, short-term and long-term overnight bank borrowing costs, reflected in overnight indexed and interest rate swap contracts, have been lower than maturity matched Treasury rates. The main explanations of these negative swap spread puzzles are based on frictions, such as the demand for duration, caps on leverage, or fading convenience yields for U.S. Treasuries.

We demonstrate that accounting for high-quality sovereign credit risk is important in our understanding of post-crisis pricing phenomena. A low probability of U.S. Treasury default reduces the no-arbitrage bounds of swap spreads to negative levels. Accounting for a U.S. credit risk premium in Treasuries is thus essential for jointly explaining the dynamics of the term structures of multiple benchmark interest rates. Even if the probability of a U.S. credit event is small, the risk premium associated with it may be large.

References

- Acharya, V. V., Drechsler, I., Schnabl, P., 2014. A pyrrhic victory? - bank bailouts and sovereign credit risk. *The Journal of Finance* 69, 2689–2739.
- Arias, J., Erceg, C., Trabandt, M., 2016. The macroeconomic risks of undesirably low inflation. *European Economic Review* 88, 88–107.
- Arora, N., Gandhi, P., Longstaff, F. A., 2012. Counterparty credit risk and the credit default swap market. *Journal of Financial Economics* 103, 280–293.
- Augustin, P., 2014. Sovereign credit default swap premia. *Journal of Investment Management* 12, 65–102.
- Augustin, P., 2018. The term structure of cds spreads and sovereign credit risk. *Journal of Monetary Economics* 96, 53–76.
- Augustin, P., Sokolovski, V., Subrahmanyam, M. G., Tomio, D., 2018. How sovereign is sovereign credit risk? global prices, local quantities. Working Paper New York University, Stern School of Business .
- Backus, D., Chernov, M., Zin, S., 2014. Sources of entropy in representative agent models. *Journal of Finance* 69, 51–99.
- Bansal, R., Shaliastovich, I., 2013. A long-run risks explanation of predictability puzzles in bond and currency markets. *Review of Financial Studies* 26, 1–33.
- Bansal, R., Yaron, A., 2004. Risks for the long run: A potential resolution of asset pricing puzzles. *The Journal of Finance* 59, 1481–1509.
- Bongaerts, D., De Jong, F., Driessen, J., J., 2011. Derivative pricing with liquidity risk: Theory and evidence from the credit default swap market. *Journal of Finance* 66, 203–240.
- Boyarchenko, N., Gupta, P., Steele, N., Yen, J., 2018. Negative swap spreads. Federal Reserve Bank of New York Economic Policy Review 24.
- Brenner, M., Eldor, R., Hauser, S., 2001. The price of options illiquidity. *Journal of Finance* 56, 789–805.
- Cameron, M., 2013. Goldman and the ois gold rush. *Risk Magazine* June, 15–19.
- Chernov, M., Creal, D. D., 2016. The ppp view of multihorizon currency returns. Working paper .
- Chernov, M., Gorbenko, A. S., Makarov, I., 2013. Cds auctions. *Review of Financial Studies* 26, 768–805.
- Chernov, M., Schmid, L., Schneider, A., 2020. A macrofinance view of us sovereign cds premiums. *Journal of Finance* Forthcoming.

- Collin-Dufresne, P., Solnik, B., 2001. On the term structure of default premia in the swap and libor markets. *The Journal of Finance* 56, 1095–1115.
- Deuskar, P., Gupta, A., Subrahmanyam, M. G., 2011. Liquidity effect in otc options markets: Premium or discount? *Journal of Financial Markets* 14, 127–160.
- Dittmar, R., Hsu, A. C., Roussellet, G., Simasek, P., 2019. Default risk and the pricing of u.s. sovereign bonds. Working Paper .
- Dou, W., Chen, H., Kogan, L., 2017. Measuring the “dark matter” in asset pricing models. Working Paper MIT .
- Du, W., Gordy, M. B., Gadgil, S., Vega, C., 2016. Counterparty risk and counterparty choice in the credit default swap market. Working Paper Federal Reserve Board .
- Du, W., Im, J., Schreger, J., 2018. The u.s. treasury premium. *Journal of International Economics* 112, 167–181.
- Dubecq, S., Monfort, A., Renne, J.-P., Roussellet, G., 2016. Credit and liquidity in interbank rates: A quadratic approach. *Journal of Banking and Finance* 68, 29–46.
- Duffie, D., Huang, M., 1996. Swap rates and credit quality. *Journal of Finance* 51, 921–949.
- Duffie, D., Lando, D., 2001. Term structures of credit spreads with incomplete accounting information. *Econometrica* 69, 633–664.
- Duffie, D., Singleton, K. J., 1997. An econometric model of the term structure of interest-rate swap yields. *The Journal of Finance* 52, 1287–1321.
- Duffie, D., Singleton, K. J., 1999. Modeling term structures of defaultable bonds. *Review of Financial Studies* 12, 687–720.
- Duffie, D., Singleton, K. J., 2003. *Credit Risk: Pricing, Measurement and Management*. Princeton University Press.
- Duffie, D., Stein, J., 2015. *Journal of economic perspectives* 29, 191–212.
- Edwards, S., 2018. *American Default*. Princeton University Press.
- English, W. B., 1996. Understanding the costs of sovereign default: American state debts in the 1840’s. *American Economic Review* 86, 259–275.
- Feldhutter, P., Lando, D., 2008. Decomposing swap spreads. *Journal of Financial Economics* 88, 375–405.
- Filipovic, D., B.Trolle, A., 2013. The term structure of interbank risk. *Journal of Financial Economics* 109, 707–733.
- Fleckenstein, M., Longstaff, F. A., Lustig, H., 2013. Deflation risk. NBER Working Paper No. 19238 .

- Gomes, J. F., Kilic, M., Plante, S., 2019. Leverage risk and investment: The case of gold clauses in the 1930s. SSRN Working Paper 3342943 .
- Gourieroux, C., Jasiak, J., 2006. Autoregressive gamma processes. *Journal of Forecasting* 25, 129–152.
- Goyenko, R., Subrahmanyam, A., Ukhov, A., 2011. The term structure of bond market liquidity and its implications for expected bond returns. *Journal of Financial and Quantitative Analysis* 46, 111–139.
- Grinblatt, M., 2001. An analytic solution for interest rate swap spreads. *International Review of Finance* 2, 113–149.
- Gupta, A., Subrahmanyam, M. G., 2000. An empirical examination of the convexity bias in the pricing of interest rate swaps. *Journal of Financial Economics* 55, 239–279.
- Gurkaynak, R. S., Sack, B., Wright, J. H., 2007. The u.s. treasury yield curve: 1961 to the present. *Journal of Monetary Economics* 54, 2291–2304.
- Hansen, L. P., Heaton, J. C., Li, N., 2008. Consumption strikes back? measuring long-run risk. *The Journal of Political Economy* 116, pp. 260–302.
- He, H., 2001. Modeling term structures of swap spreads. Working Paper .
- Hilscher, J., Raviv, A., Reis, R., 2014. Inflating away the public debt? an empirical assessment. NBER Working Paper No. 20339 .
- Hull, J., White, A., 2013. Libor vs. ois: The derivatives discounting dilemma. *Journal Of Investment Management* 11, 14–27.
- Jermann, U. J., 2019. Negative swap spreads and limited arbitrage. *Review of Financial Studies* 33, 212–238.
- Johannes, M., Sundareshan, S. M., 2007. The impact of collateralization on swap rates. *The Journal of Finance* 62, 383–410.
- Klingler, S., Sundareshan, S., 2019a. How safe are safe havens? Working Paper Columbia University .
- Klingler, S., Sundareshan, S. M., 2019b. An explanation of negative swap spreads: Demand for duration from underfunded pension plans. *The Journal of Finance* 74, 675–710.
- Krishnamurthy, A., 2002. The bond/old-bond spread. *Journal of Financial Economics* 66, 463–506.
- Krishnamurthy, A., Vissing-Jorgensen, A., 2012. The aggregate demand for treasury debt. *Journal of Political Economy* 120, 233–267.
- Lando, D., Klingler, S., 2018. Safe-haven cds premia. *Review of Financial Studies* 31, 1856–1895.

- Le, A., Singleton, K. J., Dai, Q., 2010. Discrete-time affine term structure models with generalized market prices of risk. *Review of Financial Studies* 23, 2184–2227.
- Litzenberger, R., 1992. Swaps: Plain and fanciful. *Journal of Finance* 47, 831–850.
- Liu, J., Longstaff, F., Mandell, R. E., 2006. The market price of risk in interest rate swaps: The roles of default and liquidity risks. *The Journal of Business* 79, 2337–2360.
- Longstaff, F. A., 2004. The flight-to-liquidity premium in U.S. treasury bond prices. *Journal of Business* 77, 511–526.
- Longstaff, F. A., Mithal, S., Neis, E., 2005. Corporate yield spreads: Default risk or liquidity? new evidence from the credit default swap market. *Journal of Finance* 60, 2213–2253.
- Lou, W., 2009. On asymmetric funding of swaps and derivatives—a funding cost explanation of negative swap spreads. SSRN Working Paper 1610338 .
- Nagel, S., 2016. The liquidity premium of near-money assets. *Quarterly Journal of Economics* 131, 1927–1971.
- Pan, J., Singleton, K. J., 2008. Default and recovery implicit in the term structure of sovereign cds spreads. *Journal of Finance* 63, 2345–2384.
- Reinhart, C. M., Rogoff, K. S., 2008. This time is different: A panoramic view of eight centuries of financial crises. NBER Working Papers 13882, National Bureau of Economic Research, Inc.
- Reis, R., 2015. Different types of central bank insolvency and the central role of seignorage. *Journal of Monetary Economics* 73, 20–25.
- Schorfheide, F., Song, D., Yaron, A., 2018. Identifying long-run risks: A bayesian mixed-frequency approach. *Econometrica* 86, 617–654.
- Spears, T., 2019. Discounting collateral: quants, derivatives and the reconstruction of the ‘risk-free rate’ after the financial crisis. *Economy and Society*, forthcoming 48, 342–370.
- Sun, T.-S., Sundaresan, S., Wang, C., 1993. Interest rate swaps: An empirical investigation. *Journal of Financial Economics* 34, 77–99.
- Wang, Z., Yang, W., 2018. Ois risk premiums. Working Paper .
- Zivney, T. L., Marcus, R. D., 1989. The day the united states defaulted on treasury bills. *The Financial Review* 24, 475–489.
- Zviadadze, I., 2017. Term-structure of consumption risk premia in the cross-section of currency returns. *The Journal of Finance* 72, 1529–1566.

Fig. 1. USD overnight LIBOR and EFFR

In this figure we report the time series of the difference between the overnight London Interbank Offered Rate (LIBOR) and the Effective Federal Funds Rate (EFFR). LIBOR is the average interest rate at which leading banks borrow funds of a sizeable amount from other banks in the Eurodollar area. The EFFR is calculated as a volume-weighted median of overnight federal funds transactions provided by domestic banks, U.S. branches, and agencies of foreign banks, as reported in the reporting form FR 2420. The data frequency is weekly and based on Wednesday rates. All spreads are expressed in percentages. The sample period is 8 May 2002 to 26 September 2018. Source: Federal Reserve Bank of St. Louis. The y -axis is in annualized percentage terms.

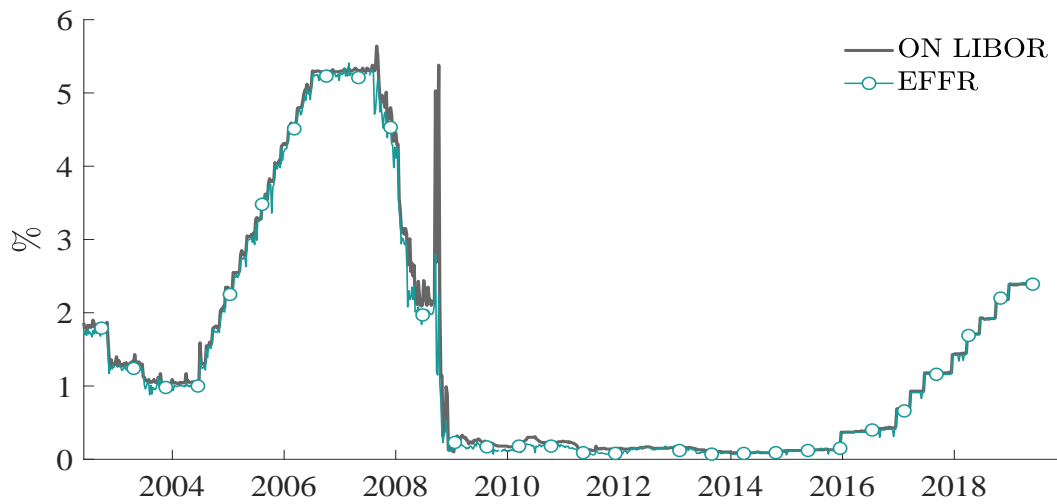


Fig. 2. IRS-Treasury and OIS-Treasury spreads

In these figures we report the time series of the USD denominated IRS-Treasury and OIS-Treasury swap spreads, defined as the difference between the interest rate swap (IRS) rate or the overnight indexed swap (OIS) rate and the maturity matched constant maturity Treasury (CMT) rate. Spreads for the 6-month maturity are based on LIBOR. Spreads for maturities of 5 years and higher are based on IRS rates. We overlay the (negative of the) USD maturity-matched U.S. CDS premium, i.e., the CDS premium multiplied by (-1). The data frequency is weekly and based on Wednesday rates. All spreads are expressed in percentages. The sample period is 8 May 2002 to 26 September 2018. Source: Bloomberg (OIS, IRS, LIBOR), FRED (CMT), Markit (CDS).

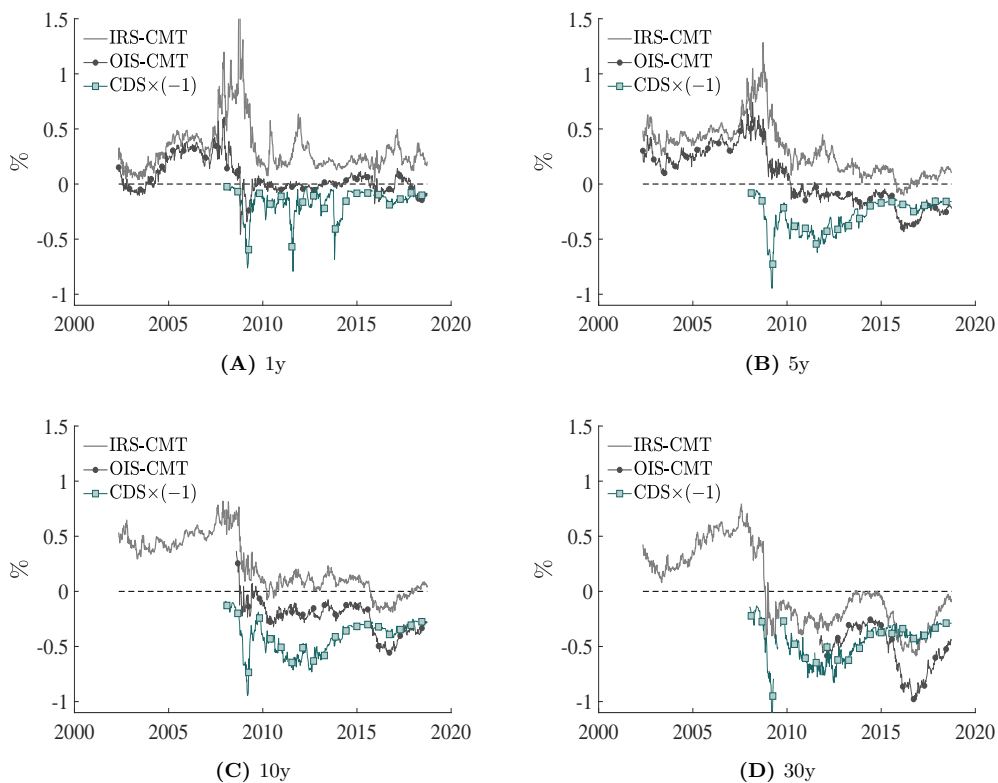


Fig. 3. Macro factors

In these figures we plot the dynamics of the macroeconomic state variables in our model: log consumption growth (z_1), output growth (z_2), government expenditures-to-output ratio (z_3), and inflation (z_4), and consumption volatility (v_1) and inflation volatility (v_2). All variables are annualized and represented in percentage terms, except for the government expenditures-to-output ratio, which is represented in logs. The sample period is 1982 to 2018. The data frequency is quarterly for z_1 , z_2 , and z_3 , and monthly for z_4 . Source: Federal Reserve Bank of St. Louis H.15 Report.

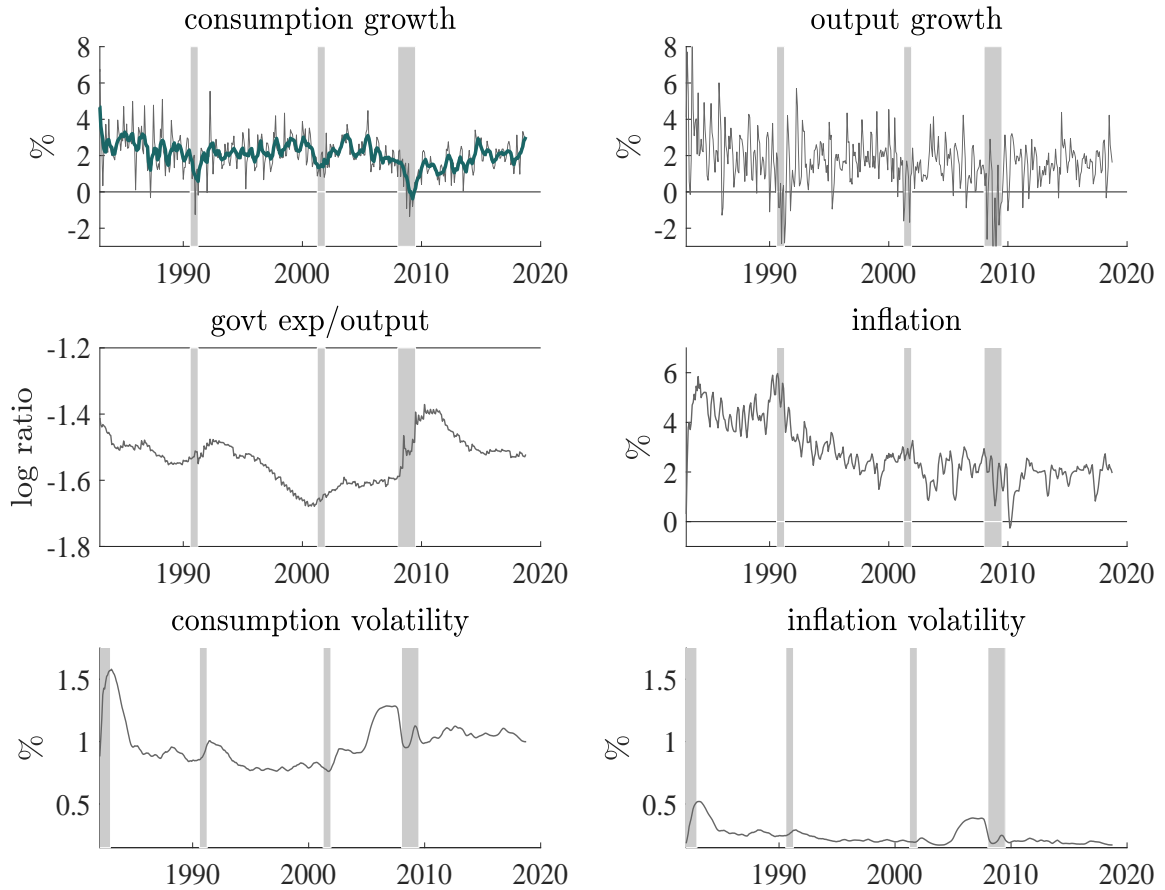


Fig. 4. Finance factors

We plot the spread factors: s_1 is the convenience yield, defined as the 1-month OIS-Treasury spread; s_2 captures the interbank credit and funding liquidity risk, defined as the 1-month LIBOR-OIS spread; s_3 is latent and captures the opportunity cost of collateral. The sample period is May 2002 to September 2018. All variables are plotted at a monthly frequency, and are expressed in percentages. Source: Bloomberg (OIS, LIBOR), FRED (CMT).

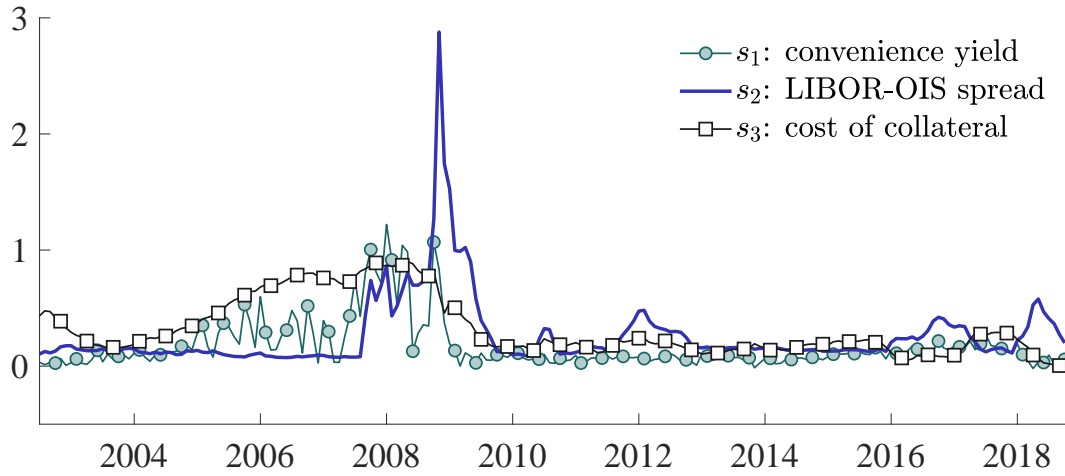


Fig. 5. Model-implied risky zero-coupon yields and nominal Treasury yields

In these figures we plot the model-implied risky zero-coupon bond yields (green line with bullets) together with their 90% confidence bands, and compare them with the observed nominal zero-coupon Treasury yields (solid black line) from Gurkaynak et al. (2007). We plot observed and model-implied yields for maturities of 1y, 3y, 5y, 10y, 20y, and 30y. All variables are plotted at a monthly frequency and are expressed in annualized percentage terms. The sample period is May 2002 to September 2018.

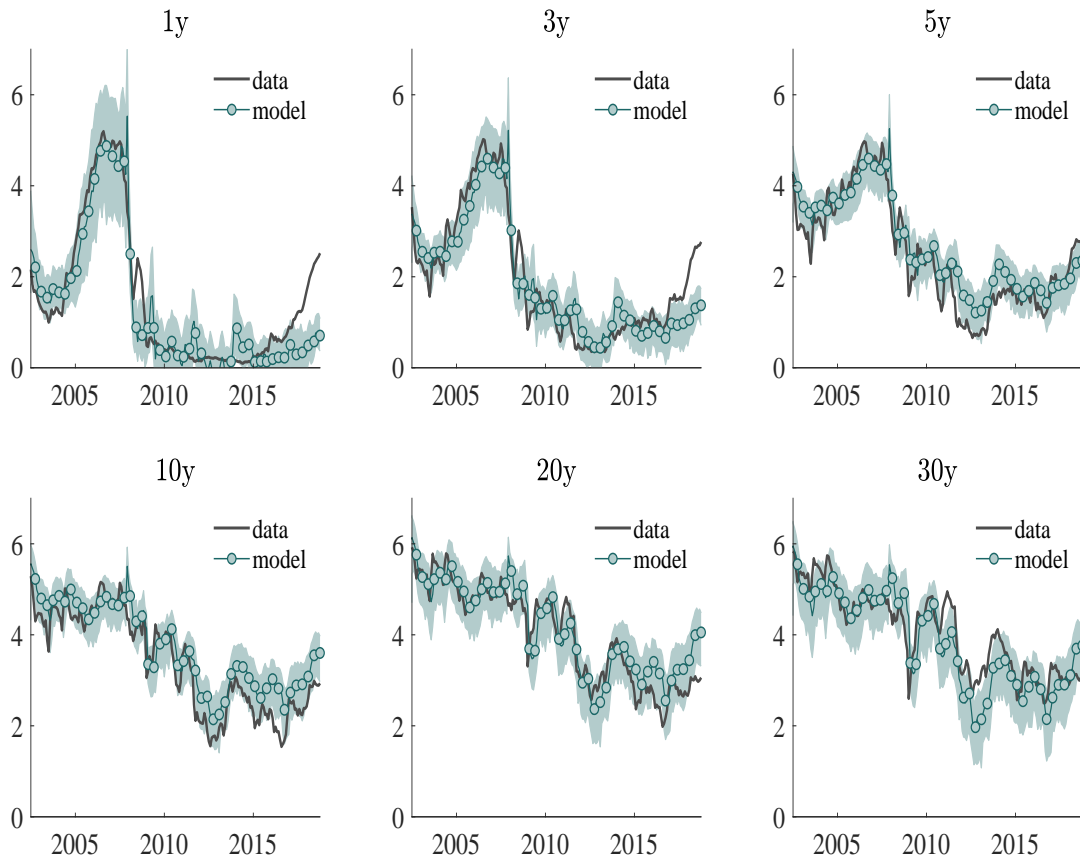


Fig. 6. Model-implied and actual CDS premiums

In these figures we plot the model-implied (green line with bullets), their 90% confidence bands, and observed (solid black line) CDS premiums. We plot observed and model-implied CDS premiums for maturities of 1y, 3y, 5y, and 10y. All variables are plotted at a monthly frequency and are expressed in annualized percentage terms. The sample period is May 2002 to September 2018. Source: Markit.

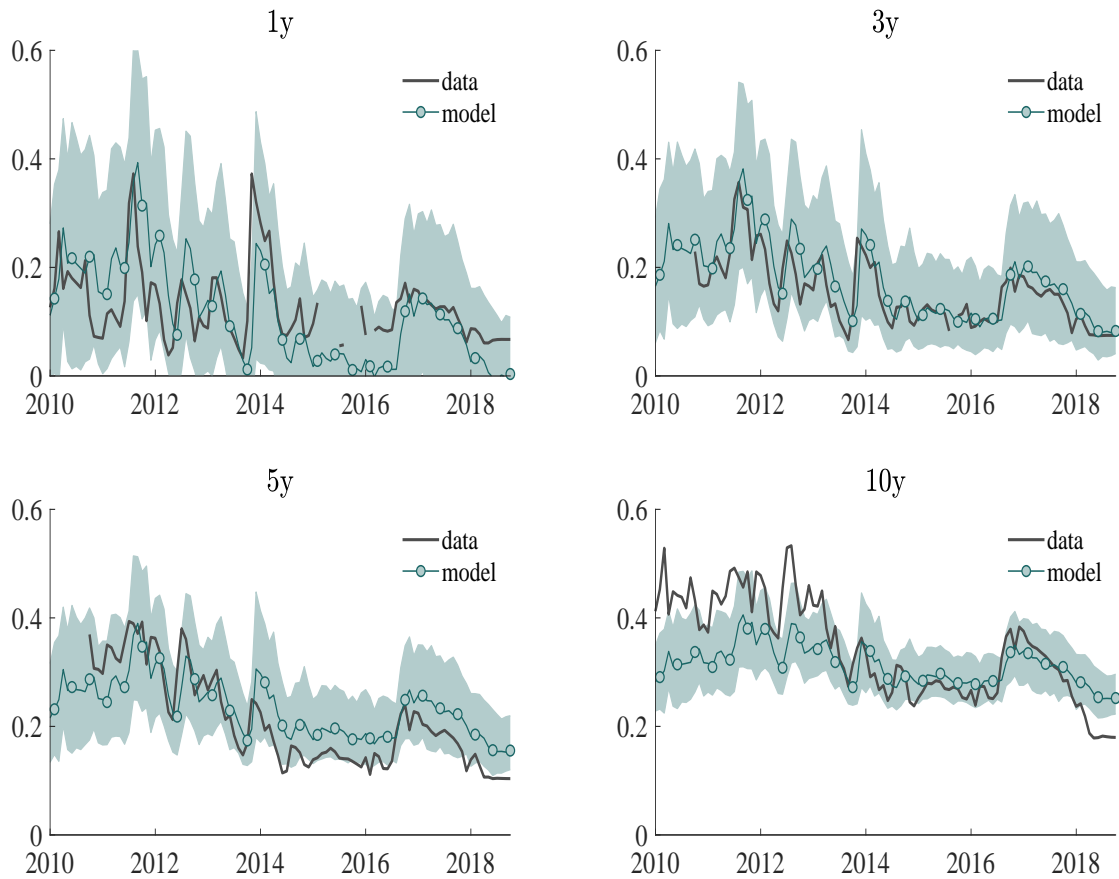


Fig. 7. Model-implied zero-coupon yields

In these figures we plot the model-implied zero-coupon yields for nominal bonds (gray line with bullets), risky Treasury bonds (solid black line), and the “credit/safety” spread (green line with squares). We plot model-implied zero-coupon yields for maturities of 1y, 3y, 5y, and 10y. All variables are plotted at a monthly frequency and are expressed in annualized percentage terms. The sample period is May 2002 to September 2018. Source: Authors’ computations.

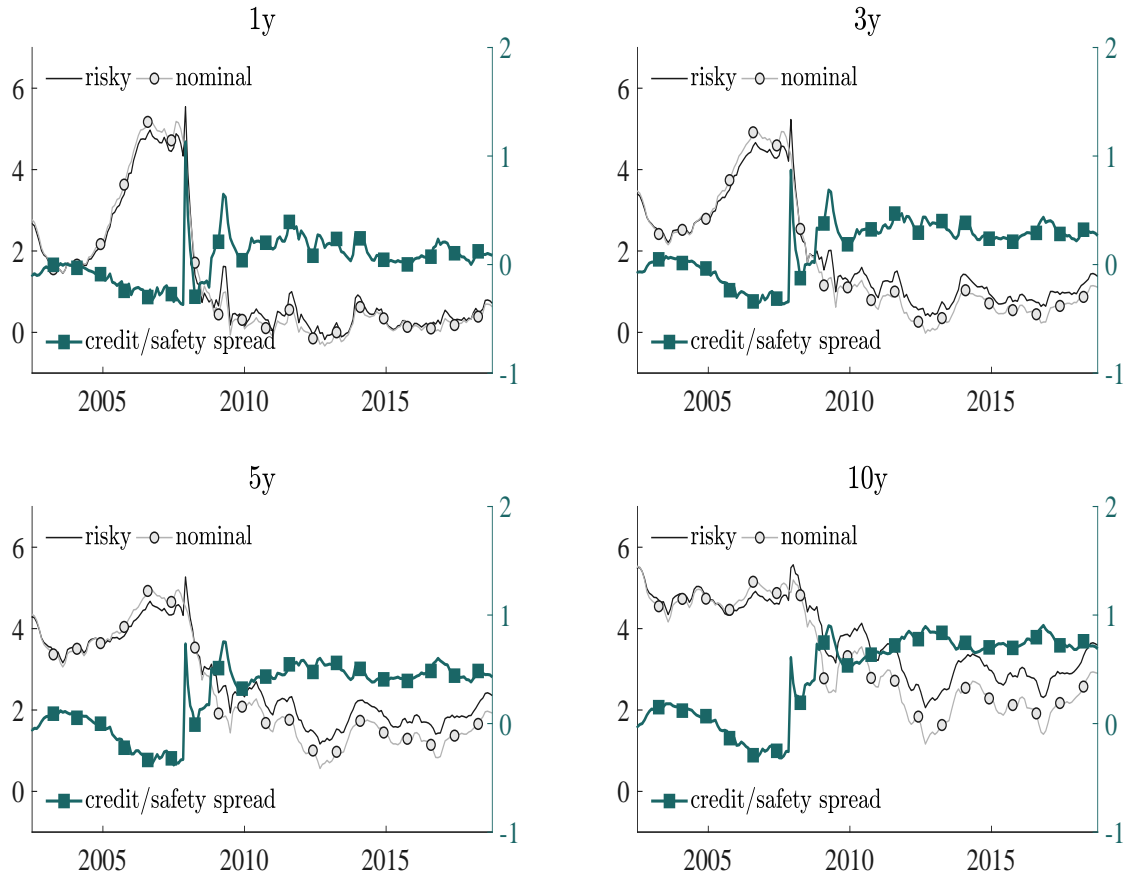
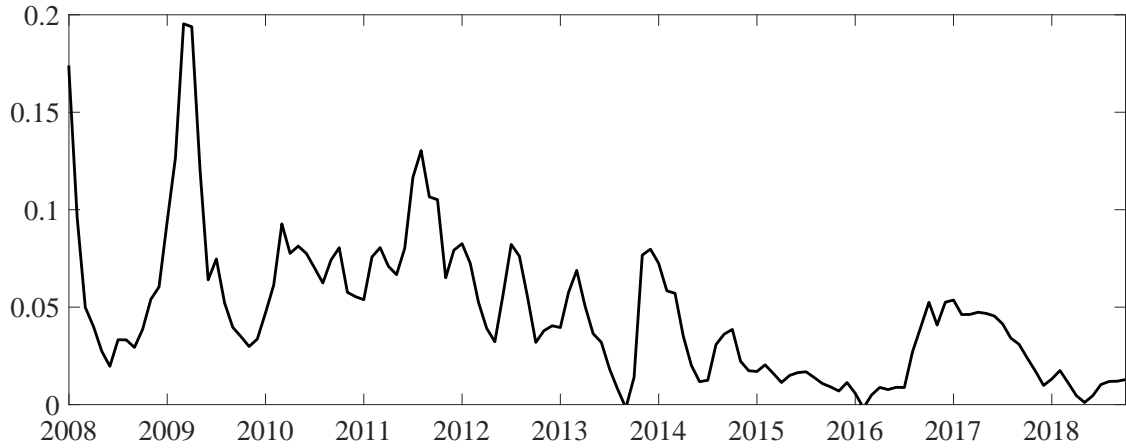


Fig. 8. Default intensity and credit risk premium

In Panel (A), we plot the model-implied physical default intensity for U.S. credit risk from January 2008 to September 2018. In Panel (B), we plot the model implied CDS premiums for maturity 5 years under the risk-neutral CDS and physical CDS^\dagger measures from January 2008 to September 2018. The y -axis is expressed in annualized percentage terms. Source: Authors' computations.

(A) Default intensity



(B) Model-implied CDS premiums under the risk-neutral and physical measures

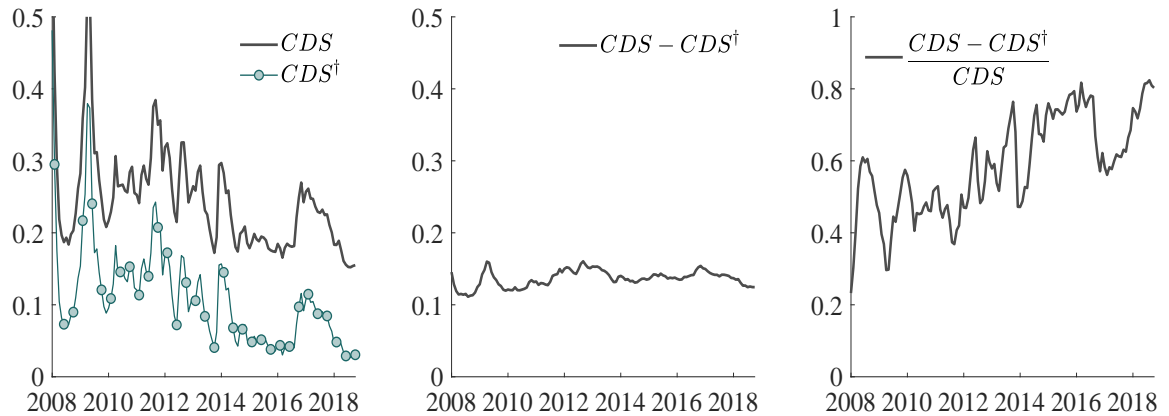


Fig. 9. Credit/safety spread loadings: Risky - nominal rate

In these figures we examine the sensitivity of model-implied risky zero-coupon Treasury yields (which incorporate the convenience yield) to all state variables over and above the sensitivity of model-implied nominal Treasury yields (which exclude the convenience yield). Specifically, we plot the difference of the sensitivity loadings with respect to the state variables as a function of the maturity horizon, up to 20 years. The state variables are log consumption growth (z_1), inflation (z_2), output growth (z_3), government expenditures-to-output ratio (z_4), the convenience yield (s_1), the LIBOR-OIS spread (s_2), the opportunity cost of collateral (s_3), consumption volatility (v_1), and inflation volatility (v_2). Source: Authors' computations.

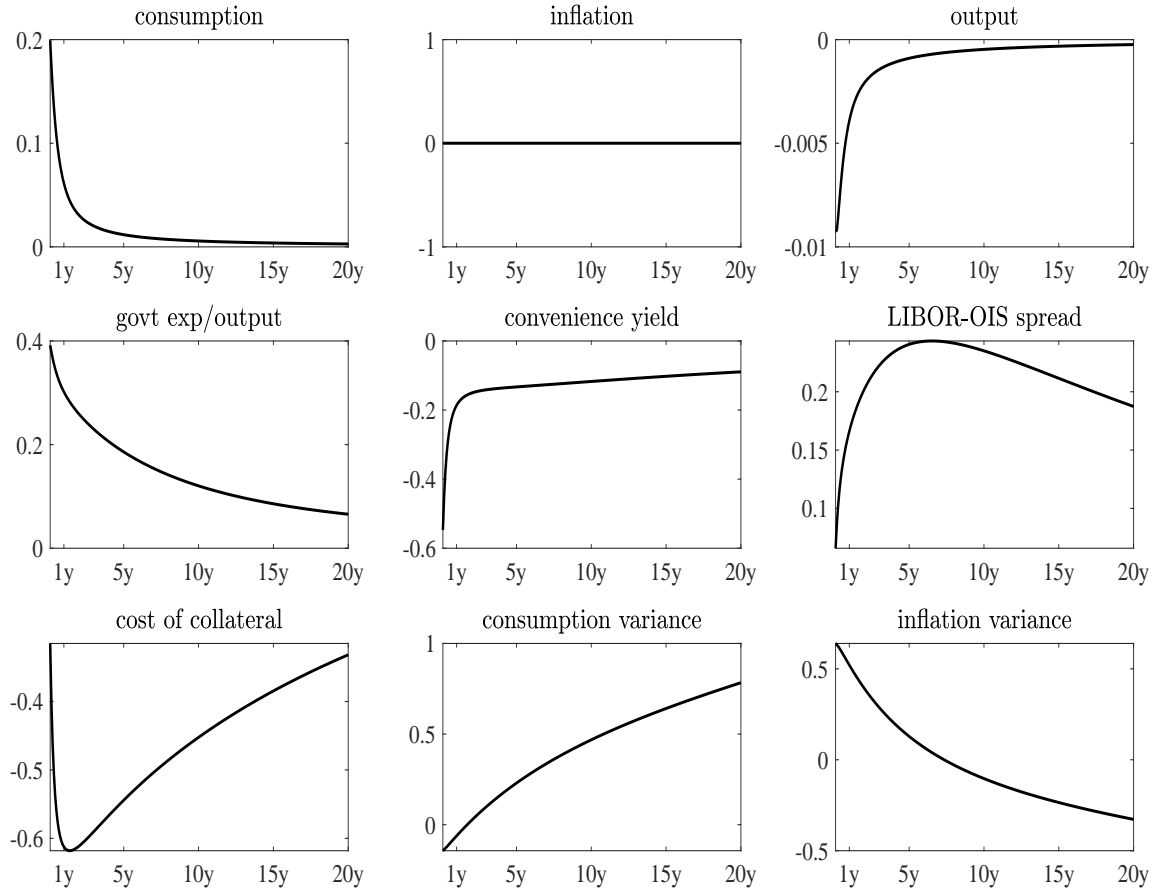


Fig. 10. Model-implied spread between OIS and CMT

In these figures we examine the sensitivity of model-implied risky zero-coupon Treasury yields (which incorporate the convenience yield) to all state variables over and above the sensitivity of model-implied nominal Treasury yields (which exclude the convenience yield). Specifically, we plot the difference of the sensitivity loadings with respect to the state variables as a function of the maturity horizon, up to 20 years. The state variables are log consumption growth (z_1), inflation (z_2), output growth (z_3), government expenditures-to-output ratio (z_4), the convenience yield (s_1), the LIBOR-OIS spread (s_2), the opportunity cost of collateral (s_3), consumption volatility (v_1), and inflation volatility (v_2). Source: Authors' computations.

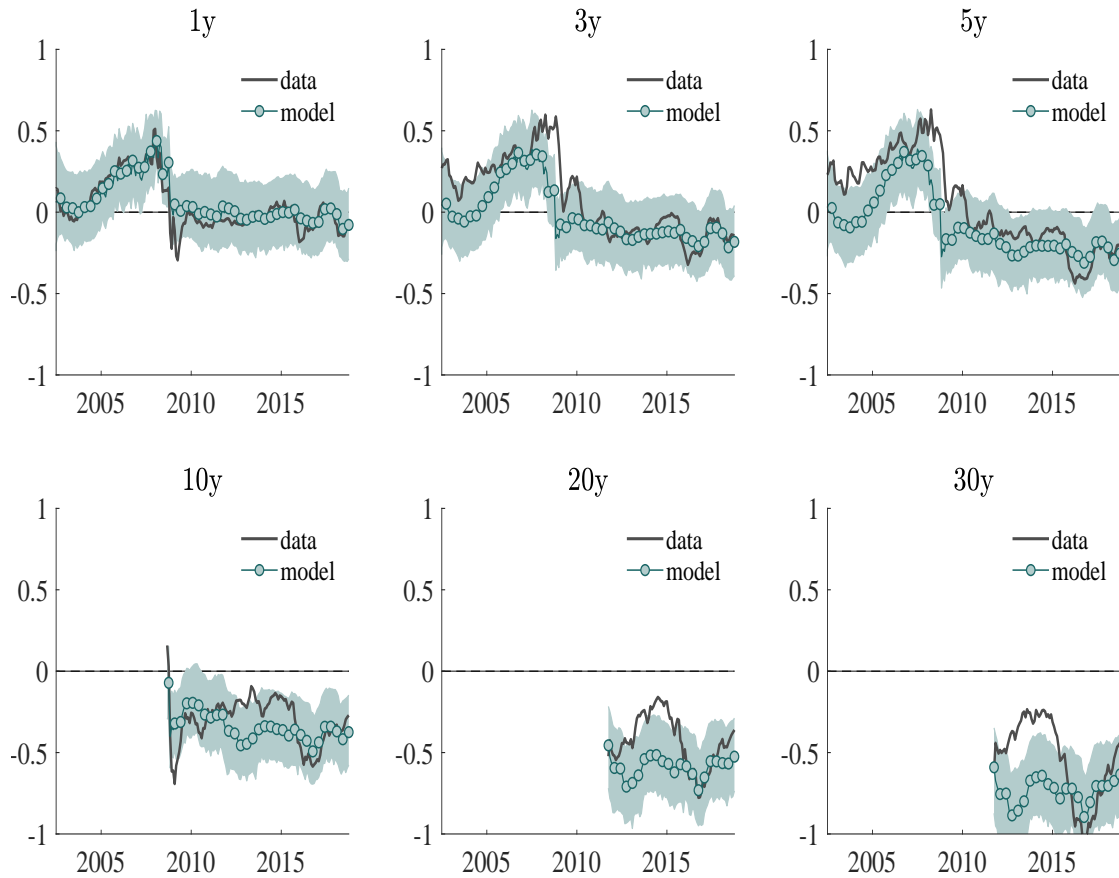


Fig. 11. Model-implied spread between IRS and CMT

In these figures we plot the model-implied (green line with bullets), their 90% confidence bands, and observed (solid black line) IRS-Treasury spreads, where we use the constant maturity Treasury par rates. We plot observed and model-implied IRS-CMT spreads for maturities of 1y, 3y, 5y, 10y, 20y, and 30y. All variables are plotted at a monthly frequency and are expressed in annualized percentage terms. The sample period is May 2002 to September 2018. Source: Bloomberg (IRS) and FRED (CMT).

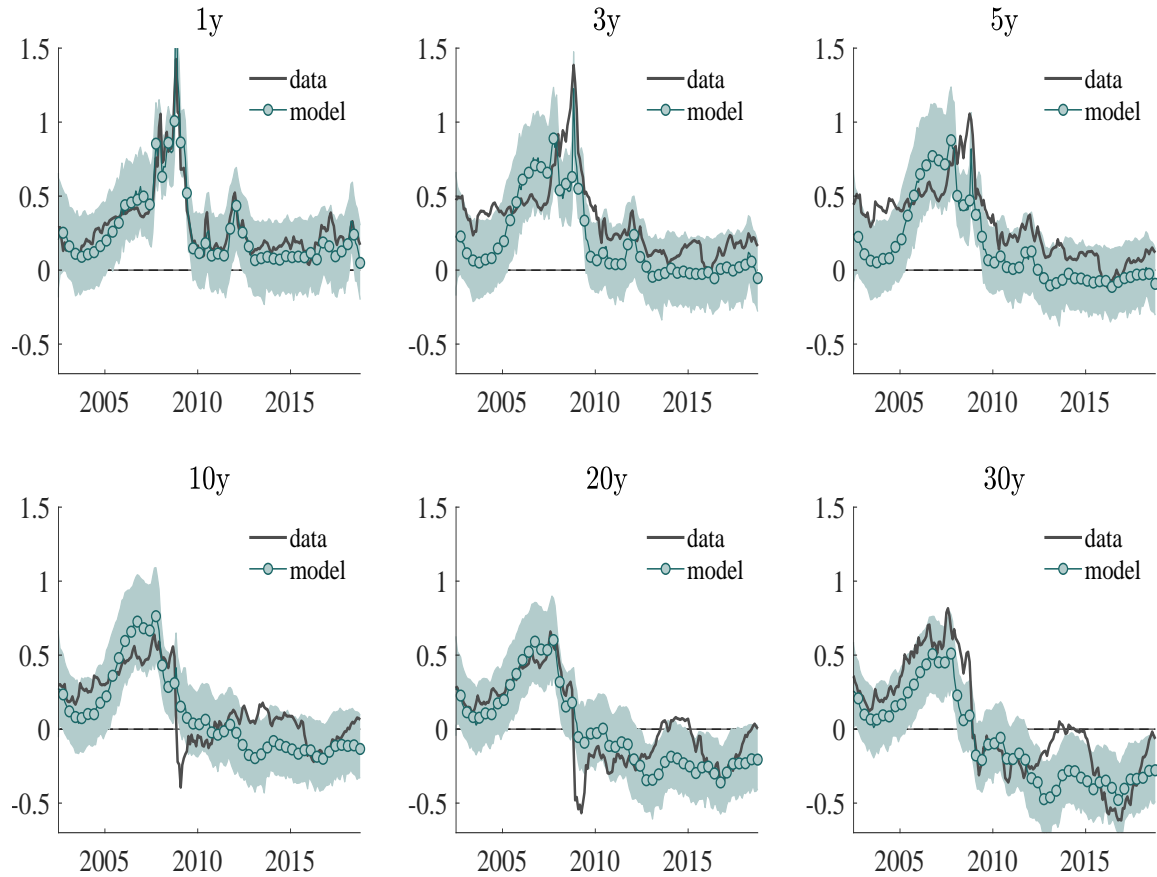


Fig. 12. Model-implied spread between OIS and CMT: Counterfactual

In these figures we compare the fitted OIS-CMT spreads (black line) with their counterfactual values when U.S. credit risk is shut down (gray boxes). All rates are expressed on a par basis. We plot the OIS-CMT spreads for maturities of 1y, 3y, 5y, 10y, 20y, and 30y. All variables are plotted at a monthly frequency and are expressed in annualized percentage terms. The sample period is May 2002 to September 2018. Source: Authors' computations.

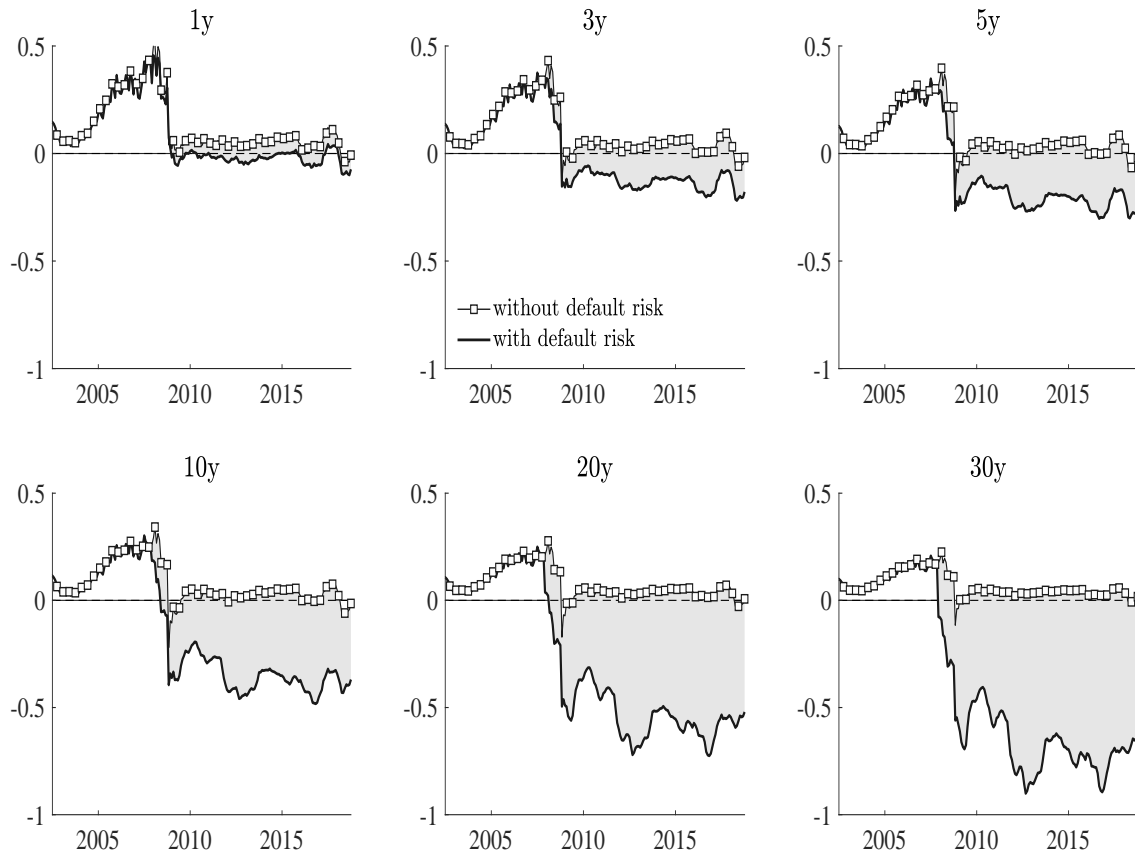


Fig. 13. Model-implied spread between IRS and CMT: Counterfactual

In these figures, we compare the fitted IRS-CMT spreads (black line) with their counterfactual values when U.S. credit risk is shut down (gray boxes). All rates are expressed on a par basis. We plot the IRS-CMT spreads for maturities of 1y, 3y, 5y, 10y, 20y, and 30y. All variables are plotted at a monthly frequency and are expressed in annualized percentage terms. The sample period is May 2002 to September 2018. Source: Authors' computations.

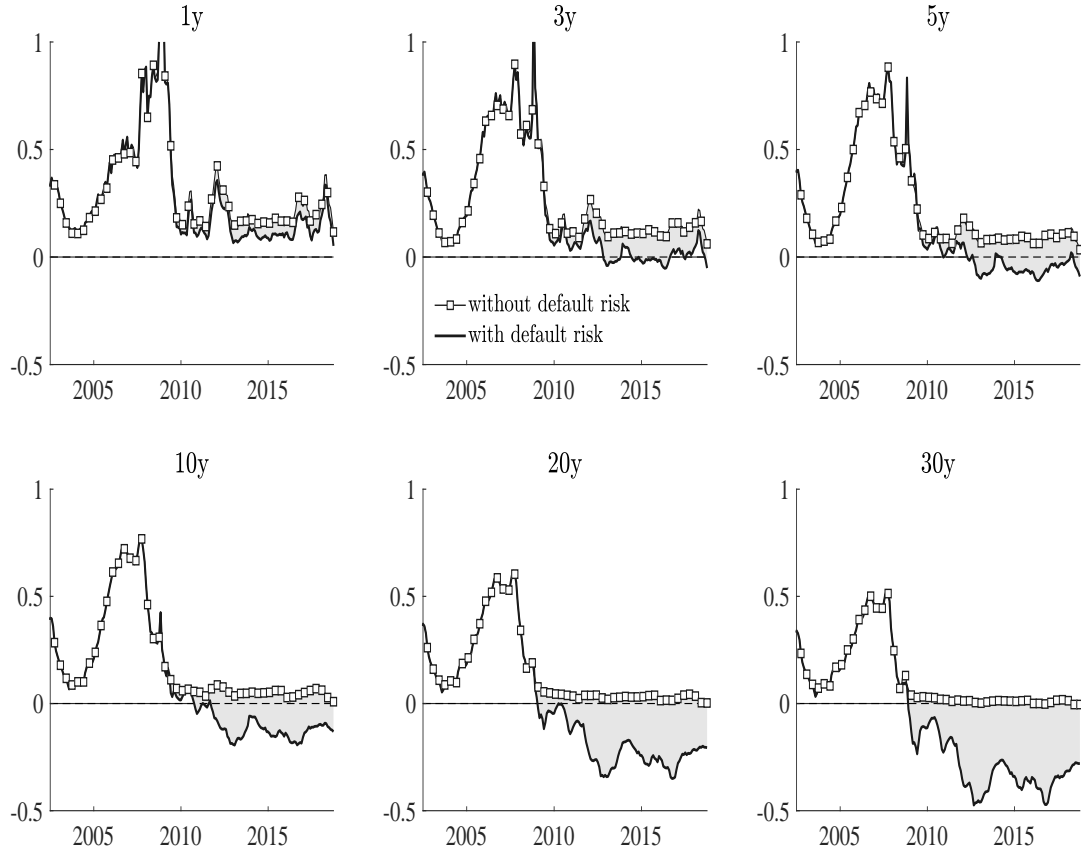


Table 1. Literature on negative IRS-Treasury and OIS-Treasury spreads

This table summarizes the main studies explaining negative OIS-Treasury or IRS-Treasury swap spreads. We describe the focus of the paper (IRS-Treasury or OIS-Treasury), the type of study (empirical or theoretical), and the main explanation proposed by each study.

Study	Focus		Type		Explanations				
	IRS-Treasury	OIS-Treasury	Empirics	Theory	Funding costs	Hedging demand	Leverage ratios	Convenience yield	Sovereign risk
Lou (2009)	✓		✓		✓				
Klingler and Sundaresan (2019b)	✓		✓	✓		✓			
Boyarchenko et al. (2018)	✓		✓				✓		
Klingler and Sundaresan (2019a)		✓	✓					✓	
Jermann (2019)	✓			✓		✓			
The present study	✓	✓	✓	✓					✓

Table 2. Descriptive statistics of USD interest and CDS rates.

In this table, we report the summary statistics (mean, sd, p1, p50, p99) and the number of observations (Obs.) for the term structure of various U.S. interest and credit default swap (CDS) rates with maturities ranging between 3 months and 30 years. We use weekly observations based on Wednesday rates. Statistics are reported for USD denominated overnight index swap (OIS) rates (Panel A), USD denominated interest rate swap (IRS) rates, where maturities below one year correspond to London interbank offered (LIBOR) rates (Panel B), USD denominated constant maturity Treasury yields (Panel C), USD denominated zero coupon Treasury (ZCT) yields from Gurkaynak et al. (2007) (Panel D), USD denominated CDS spreads (Panel E), and EUR denominated CDS spreads (Panel F). All rates are expressed in percentage terms. The sample period is May 8, 2002 through September 26, 2018. Source: Bloomberg (OIS, IRS), Gurkaynak et al. (2007) (ZCT), Federal Reserve Bank of St. Louis (CMT, LIBOR), Markit (CDS).

Maturity	3m	6m	1y	3y	5y	7y	10y	20y	30y	3m	6m	1y	3y	5y	7y	10y	20y	30y	
Panel A: USD OIS Rates																			
Mean	1.40	1.44	1.54	2.07	2.54	1.67	2.31	2.39	2.48	1.66	1.83	1.81	2.33	2.79	3.13	3.46	3.89	3.97	
SD	1.66	1.67	1.67	1.53	1.43	0.49	0.71	0.49	0.51	1.67	1.62	1.64	1.48	1.37	1.30	1.25	1.22	1.21	
P1	0.08	0.09	0.09	0.22	0.53	0.82	1.00	1.24	1.30	0.23	0.32	0.26	0.46	0.79	1.19	1.42	1.70	1.78	
P50	0.68	0.73	0.88	1.57	2.24	1.76	2.22	2.33	2.44	1.12	1.24	1.26	1.87	2.54	2.91	3.23	3.80	3.93	
P99	5.32	5.37	5.41	5.39	5.45	2.68	4.04	3.45	3.59	5.50	5.52	5.51	5.48	5.55	5.61	5.70	5.91	5.94	
Obs.	856	856	856	856	856	333	530	366	366	853	853	856	856	856	856	856	856	856	
Panel B: USD LIBOR/IRS Rates																			
Mean	1.25	1.37	1.49	1.99	2.48	2.87	3.23	3.81	3.95	-	-	1.50	1.73	1.99	2.50	2.93	4.04	4.07	
SD	1.56	1.60	1.55	1.37	1.22	1.11	1.04	1.06	0.93	-	-	1.53	1.44	1.34	1.19	1.12	1.06	0.91	
P1	0.01	0.04	0.10	0.32	0.64	1.04	1.54	1.90	2.29	-	-	0.11	0.22	0.34	0.67	1.07	2.05	2.49	
P50	0.52	0.66	0.89	1.52	2.23	2.79	3.12	3.96	4.13	-	-	0.90	1.22	1.53	2.23	2.83	4.36	4.18	
P99	5.12	5.17	5.09	5.02	5.03	5.06	5.14	5.55	5.58	-	-	5.04	5.00	4.95	4.95	5.03	5.86	5.82	
Obs.	856	856	856	856	856	856	856	856	856	-	-	856	856	856	856	856	856	856	
Panel C: Constant Maturity Treasury Rates																			
Mean	1.25	1.37	1.49	1.99	2.48	2.87	3.23	3.81	3.95	-	-	1.50	1.73	1.99	2.50	2.93	4.04	4.07	
SD	1.56	1.60	1.55	1.37	1.22	1.11	1.04	1.06	0.93	-	-	1.53	1.44	1.34	1.19	1.12	1.06	0.91	
P1	0.01	0.04	0.10	0.32	0.64	1.04	1.54	1.90	2.29	-	-	0.11	0.22	0.34	0.67	1.07	2.05	2.49	
P50	0.52	0.66	0.89	1.52	2.23	2.79	3.12	3.96	4.13	-	-	0.90	1.22	1.53	2.23	2.83	4.36	4.18	
P99	5.12	5.17	5.09	5.02	5.03	5.06	5.14	5.55	5.58	-	-	5.04	5.00	4.95	4.95	5.03	5.86	5.82	
Obs.	856	856	856	856	856	856	856	856	856	-	-	856	856	856	856	856	856	856	
Panel D: Zero-coupon Rates																			
Mean	1.25	1.37	1.49	1.99	2.48	2.87	3.23	3.81	3.95	-	-	1.50	1.73	1.99	2.50	2.93	4.04	4.07	
SD	1.56	1.60	1.55	1.37	1.22	1.11	1.04	1.06	0.93	-	-	1.53	1.44	1.34	1.19	1.12	1.06	0.91	
P1	0.01	0.04	0.10	0.32	0.64	1.04	1.54	1.90	2.29	-	-	0.11	0.22	0.34	0.67	1.07	2.05	2.49	
P50	0.52	0.66	0.89	1.52	2.23	2.79	3.12	3.96	4.13	-	-	0.90	1.22	1.53	2.23	2.83	4.36	4.18	
P99	5.12	5.17	5.09	5.02	5.03	5.06	5.14	5.55	5.58	-	-	5.04	5.00	4.95	4.95	5.03	5.86	5.82	
Obs.	856	856	856	856	856	856	856	856	856	-	-	856	856	856	856	856	856	856	
Panel E: USD CDS Premiums																			
Mean	-	0.11	0.13	0.14	0.18	0.24	0.27	0.36	0.37	-	0.13	0.14	0.16	0.22	0.29	0.32	0.43	0.44	
SD	-	0.08	0.11	0.12	0.16	0.16	0.18	0.15	0.16	-	0.10	0.12	0.14	0.18	0.18	0.21	0.18	0.19	
P1	-	0.01	0.01	0.01	0.01	0.02	0.02	0.03	0.03	-	0.01	0.01	0.01	0.01	0.02	0.02	0.03	0.03	
P50	-	0.09	0.10	0.13	0.15	0.24	0.28	0.37	0.38	-	0.11	0.12	0.14	0.19	0.27	0.33	0.41	0.42	
P99	-	0.38	0.61	0.67	0.66	0.72	0.74	0.80	0.85	-	0.50	0.63	0.64	0.66	0.72	0.74	0.80	0.85	
Obs.	-	502	538	681	747	677	721	527	513	-	575	608	720	755	685	729	557	572	
Panel F: EUR CDS Premiums																			

Table 3. Link between OIS-Treasury spreads and CDS premiums.

In this table, we report the results from a regression of monthly changes in OIS-Treasury spreads (ΔSS) on monthly changes of the maturity-matched U.S. CDS premium (USD, CR restructuring clause). The 3-month OIS-Treasury spread is matched with the 6-month CDS premium. Maturities for OIS-Treasury spreads are 3/6 months, and 1/2/3/5/7/10/20/30 years to maturity. The sample period is January 2010 to September 2018. All specifications include maturity and/or week fixed effects. In row *Mat.*, we indicate maturity restrictions; in row *YEAR*, we indicate sample period restrictions. Standard errors are heteroscedasticity-robust (*RO*), clustered by time (*CL*) or adjusted for cross-sectional dependence and serial dependence up to 3 weeks using Driscoll-Kraay standard errors. We report the within R^2 of the regression. Control variables include the CBOE VIX index, the exchange rate of the USD against a basket of a broad group of major U.S. trading partners, the West Texas Intermediate oil price index, the economic policy uncertainty index, the high-yield and investment-grade bond indices, inflation, the TED spread, the 3-month LIBOR-OIS spread, the 3-month T-bill rate, the U.S. Treasury total cash balances, and CDS depth defined as the number of dealer quotes used to compute the mid-market spread. ***, **, and * denote significance at the 1%, 5%, and 10%, respectively. CDS data is from Markit; OIS data is from Bloomberg; constant-maturity Treasury rates are from the Federal Reserve Bank of St. Louis H.15 report.

VARIABLES	(1) ΔSS	(2) ΔSS	(3) ΔSS	(4) ΔSS	(5) ΔSS	(6) ΔSS	(7) ΔSS	(8) ΔSS	(9) ΔSS	(10) ΔSS	(11) ΔSS	(12) ΔSS
ΔCDS	-0.07*** (0.02)	-0.08** (0.04)	-0.07*** (0.02)	-0.13* (0.08)	-0.07*** (0.02)	-0.08*** (0.02)	-0.06*** (0.02)	-0.13* (0.08)	-0.07*** (0.02)	-0.07*** (0.02)	-0.07*** (0.02)	-0.23*** (0.08)
ΔSS_{t-1}					-0.09** (0.04)	-0.27*** (0.04)	-0.44*** (0.05)	-0.09* (0.05)	-0.16*** (0.04)	-0.16*** (0.05)	-0.16*** (0.05)	-0.13** (0.06)
ΔVIX									0.00 (0.00)	0.00 (0.00)	0.00 (0.00)	-0.00 (0.00)
ΔFX									0.00** (0.00)	0.00 (0.00)	0.00 (0.00)	0.00 (0.00)
ΔWTI									-0.00 (0.00)	-0.00 (0.00)	-0.00 (0.00)	-0.00 (0.00)
ΔEPU									-0.00 (0.00)	-0.00 (0.00)	-0.00 (0.00)	0.00 (0.00)
ΔIG									-0.06*** (0.02)	-0.06** (0.03)	-0.06** (0.03)	-0.06 (0.04)
ΔHY									-0.01 (0.01)	-0.01 (0.02)	-0.01 (0.02)	-0.02 (0.02)
$\Delta \Pi$									-0.06*** (0.01)	-0.06*** (0.02)	-0.06** (0.02)	-0.02 (0.05)
ΔTED									0.41*** (0.06)	0.41*** (0.10)	0.41*** (0.09)	0.54*** (0.08)
$\Delta LIBOR - OIS_{3m}$									-0.36*** (0.06)	-0.36*** (0.10)	-0.36*** (0.09)	-0.59*** (0.09)
$\Delta TB3$									0.09 (0.06)	0.09 (0.10)	0.09 (0.08)	0.17** (0.07)
ΔCB									0.00 (0.00)	0.00 (0.00)	0.00 (0.00)	0.00 (0.00)
ΔLIQ									0.00** (0.00)	0.00 (0.00)	0.00 (0.00)	0.01*** (0.01)
OBS.	591	347	938	411	935	935	923	411	935	935	935	411
MATURITY FE	YES	YES	YES	YES	YES	YES	NO	YES	YES	YES	YES	YES
QUARTER FE	NO	NO	NO	NO	NO	YES	NO	NO	YES	YES	YES	YES
MATURITY-QUARTER FE	NO	NO	NO	NO	NO	NO	YES	NO	NO	NO	NO	NO
CLUSTER TIME	NO	NO	NO	NO	NO	NO	NO	NO	NO	YES	NO	NO
SE	RO	RO	RO	RO	RO	RO	RO	RO	RO	RO	CL	RO
MAT	<=5	>=7	ALL	ALL	ALL	ALL	ALL	ALL	ALL	ALL	ALL	ALL
YEAR	>2009	>2009	>2009	>2014	>2009	>2009	>2009	>2014	>2009	>2009	>2009	>2014
CONTROLS	NO	NO	NO	NO	NO	NO	NO	NO	YES	YES	YES	YES
WITHIN R ²	0.02	0.01	0.01	0.01	0.02	0.09	0.20	0.02	0.24	0.24	0.34	0.32

Table 4. Cash flows from swap-spread trading strategy: Assuming Treasury cannot default.

This table illustrates the cash flows generated by a stylized form of a swap-spread trading strategy. CMS and CMT denote the fixed swap and Treasury coupon rates. f_t denotes the EFFR rate compounded from the beginning of month t to the end of month $t + 2$, or LIBOR at time t , and r_t denotes the three-month repo rate determined at time t . For expositional simplicity, this table assumes that floating and fixed payments are paid each period. SS denotes the swap spread and equals $CMS - CMT$. The term S_t denotes the difference $f_t - r_t$.

Strategy	Cash flows at time		
	0	t	T
Long Treasury bond	-1	CMT	$CMT + 1$
Repo financing cash flows	1	$-r_{t-1}$	$-r_{T-1} - 1$
Pay fixed on swap	-	$-CMS$	$-CMS$
Receive floating on swap	-	f_{t-1}	f_{T-1}
Total	0	$S_{t-1} - SS$	$S_{T-1} - SS$

Table 5. Cash flows from swap-spread trading strategy: Assuming Treasury can default.

This table illustrates the cash flows generated by a stylized form of a swap-spread trading strategy. CMS and CMT denote the fixed swap and Treasury coupon rates. f_t denotes the EFFR rate compounded from the beginning of month t to the end of month $t + 2$, or LIBOR at time t , and r_t denotes the three-month repo rate determined at time t . For expositional simplicity, this table assumes that floating and fixed payments are paid each period. SS denotes the swap spread and equals $CMS - CMT$. The term S_t denotes the difference $f_t - r_t$. Upon random default τ before maturity T , the bond is worth $1 - L$, but the CDS hedge pays L and terminates. The swap contract is unwound at the current market value of U_τ .

Strategy	Cash flows at time			
	0	t	τ	T
Long Treasury bond	-1	CMT	-	$CMT + 1$
Repo financing cash flows	1	$-r_{t-1}$	-	$-r_{T-1} - 1$
Pay fixed on swap	-	$-CMS$	-	$-CMS$
Receive floating on swap	-	f_{t-1}	-	f_{T-1}
Pay CDS premia	-	$-CDS$	-	$-CDS$
Sell Treasury bond at default	-	-	$1 - L$	-
Receive CDS payoff at default	-	-	L	-
Payoff repo loan at default	-	-	-1	-
Unwind swap at default	-	-	U_τ	-
Total	0	$S_{t-1} - SS - CDS$	U_τ	$S_{T-1} - SS - CDS$

Table 6. Parameter estimates: Macroeconomic factors.

We provide the estimates for the dynamics of the macroeconomic fundamentals z_t . We set Σ_z to be an identity matrix for identification reasons.

$$\begin{aligned}
 z_{t+1} &= (\Delta c_{t+1}, d_{t+1}, g_{t+1}, \pi_{t+1})^\top \\
 z_{t+1} &= \mu_z + \Phi_z z_t + \Phi_{zv} v_t + \Sigma_z V_{z,t}^{1/2} \varepsilon_{z,t+1} + \Theta_z \Sigma_z V_{z,t-1}^{1/2} \varepsilon_{z,t} \\
 &= \begin{bmatrix} 0.0000 \\ [-0.0003, 0.0004] \\ -0.0019 \\ [-0.0032, -0.0011] \\ 0.0181 \\ [0.0134, 0.0197] \\ -0.0007 \\ [-0.0009, -0.0003] \end{bmatrix} + \begin{bmatrix} 0.78 & -0.05 & -0.03 & 0 \\ [0.69, 0.84] & [-0.07, -0.04] & [-0.04, 0.01] & \\ 0.39 & 0.21 & 0.17 & 0 \\ [0.29, 0.43] & [0.16, 0.28] & [0.14, 0.24] & \\ 0.00 & -0.00 & 0.98 & 0 \\ [-0.02, 0.01] & [-0.01, 0.00] & [0.97, 0.99] & \\ 0.00 & 0.01 & -0.12 & 0.71 \\ [-0.07, 0.04] & [-0.00, 0.04] & [-0.15, -0.08] & [0.62, 0.76] \end{bmatrix} z_t \\
 &+ 10^{-4} \begin{bmatrix} 0 & 0 \\ 0 & 0 \\ 0 & 0 \\ 5.45 & -4.95 \\ [2.92, 6.92] & [-6.21, -1.14] \end{bmatrix} v_t + 10^{-3} \text{Diag} \begin{bmatrix} 2.84 & + & 2.80 & v_{1,t} & + & 5.30 & v_{2,t} \\ [2.58, 3.66] & & [1.24, 3.40] & & & [3.01, 7.08] \\ 2.38 & + & 0.11 & v_{1,t} & + & 1.39 & v_{2,t} \\ [1.53, 2.64] & & [0.07, 0.14] & & & [1.00, 1.97] \\ 0.13 & + & 1.79 & v_{1,t} & + & 4.92 & v_{2,t} \\ [0.10, 0.25] & & [1.38, 2.34] & & & [3.12, 6.19] \\ 0.12 & + & 0.40 & v_{1,t} & + & 0.10 & v_{2,t} \\ [0.09, 0.22] & & [0.32, 0.44] & & & [0.05, 0.90] \end{bmatrix}^{1/2} \varepsilon_{z,t+1} \\
 &+ \begin{bmatrix} -1.23 & 0.68 & -0.80 & 0 \\ [-1.44, -0.94] & [0.62, 0.75] & [-0.92, -0.75] & \\ 0.44 & 0.75 & -0.06 & 0 \\ [0.36, 0.62] & [0.43, 1.07] & [-0.17, 0.00] & \\ -0.01 & -0.01 & -0.68 & 0 \\ [-0.09, 0.00] & [-0.03, 0.04] & [-0.73, -0.54] & \\ 0.05 & 0.01 & 0.17 & -0.06 \\ [-0.02, 0.10] & [-0.01, 0.03] & [0.11, 0.21] & [-0.09, -0.02] \end{bmatrix} V_{z,t-1}^{1/2} \varepsilon_{z,t} \\
 v_{1,t+1} &\sim \text{ARG}(\nu_1, \phi_1, \frac{1-\phi_1}{\nu_1}) = \text{ARG}(\underset{[1.04, 5.99]}{2.43}, \underset{[0.951, 0.992]}{0.908}, 0.0377) \\
 v_{2,t+1} &\sim \text{ARG}(\nu_2, \phi_2, \frac{1-\phi_2}{\nu_2}) = \text{ARG}(\underset{[0.75, 5.43]}{2.43}, \underset{[0.985, 0.999]}{0.998}, 0.0008)
 \end{aligned}$$

Table 7. Parameter estimates: Finance factors, default intensity, preferences.

We provide the estimates for the dynamics of the financial variables s_t and the default intensity h_t . We set μ_s, Φ_{sy} to zero for parsimony. Risk aversion is $1 - \alpha$ and intertemporal elasticity of substitution is $(1 - \rho)^{-1}$. We calibrate the value of L .

$$\begin{aligned}
 s_{t+1} &= \mu_s + \Phi_{sv}v_t + \Phi_s s_t + \Sigma_s \varepsilon_{s,t+1} \\
 &= 10^{-4} \begin{bmatrix} -0.20 & -0.04 \\ [-0.33, 0.09] & [-0.08, 0.06] \\ -0.00 & 0.00 \\ [-0.00, 0.00] & [0.00, 0.00] \\ 0.20 & -0.17 \\ [0.13, 0.28] & [-0.23, -0.08] \end{bmatrix} v_t + \begin{bmatrix} 0.61 & -0.05 & 0.19 \\ [0.43, 0.68] & [-0.08, 0.04] & [0.04, 0.22] \\ -0.20 & 0.94 & 0.09 \\ [-0.31, 0.03] & [0.74, 0.98] & [-0.10, 0.23] \\ 0.04 & -0.02 & 0.97 \\ [0.03, 0.19] & [-0.04, 0.10] & [0.89, 0.99] \end{bmatrix} s_t \\
 &\quad + 10^{-4} \begin{bmatrix} 0.17 & 0 & 0 \\ [0.12, 0.24] & & \\ 0 & 3.17 & 0 \\ & [2.32, 4.11] & \\ 0 & 0 & 0.36 \\ & & [0.13, 0.73] \end{bmatrix} \varepsilon_{s,t+1} \\
 h_t &= h + h_c \Delta c_t + h_d d_t + h_g g_t + h_{v_1} v_{1,t} + h_{v_2} v_{2,t} \\
 &= \frac{0.0009}{[0.0003, 0.0011]} + \frac{0.13}{[0.01, 0.15]} \Delta c_t + \frac{0.00}{[-0.01, 0.02]} d_t + \frac{0.88}{[0.47, 1.11]} g_t + \frac{0.0024}{[0.0015, 0.0033]} v_{1,t} + \frac{0.0001}{[0.0000, 0.0003]} v_{2,t} \\
 U_t &= [(1 - \beta)C_t^\rho + \beta \mu_t (U_{t+1})^\rho]^{1/\rho}, \quad \mu(U_{t+1}) = E_t(U_{t+1}^\alpha)^{1/\alpha} \\
 \beta &= \frac{0.9984}{[0.9981, 0.9990]}, \quad \alpha = \frac{-3.91}{[-4.90, -2.12]}, \quad \rho = \frac{0.25}{[0.22, 0.45]} \\
 L &= 0.3
 \end{aligned}$$

Table 8. Model-implied link between OIS-Treasury spreads and CDS premiums.

In this table, we report the model-implied results from a regression of monthly changes in OIS-Treasury spreads (ΔSS) on monthly changes of the maturity-matched U.S. CDS premiums denominated in USD. Maturities for OIS-Treasury spreads are 1, 3, 5, 7, 10, 20, and 30 years to maturity. The sample period is January 2010 to September 2018. As in the data, results are based on an unbalanced sample. All specifications include maturity fixed effects. In row *Mat.*, we indicate maturity restrictions; in row *YEAR*, we indicate sample period restrictions. Standard errors are heteroscedasticity-robust. We report the within R^2 of the regression. ***, **, and * denote significance at the 1%, 5%, and 10%, respectively. Source: Authors' computations.

VARIABLES	(1) ΔSS	(2) ΔSS	(3) ΔSS	(4) ΔSS	(5) ΔSS	(8) ΔSS
ΔCDS	-0.02* (0.01)	-0.37*** (0.07)	-0.06*** (0.01)	-0.16*** (0.06)	-0.04*** (0.01)	-0.11* (0.06)
ΔSS_{t-1}					0.36*** (0.04)	0.40*** (0.06)
OBS.	591	347	938	411	935	411
MATURITY FE	YES	YES	YES	YES	YES	YES
MAT	≤ 5	≥ 7	ALL	ALL	ALL	ALL
YEAR	> 2009	> 2009	> 2009	> 2014	> 2009	> 2014
WITHIN R^2	0.00	0.09	0.01	0.01	0.16	0.16

Appendix A. U.S. CDS premiums and credit risk

In this appendix, we discuss the relevance of alternative explanations for the magnitude of U.S. CDS premiums as a measure of U.S. default risk. We review the available theory and evidence on the credit risk of the U.S. and other safe-haven countries.

The main debate is whether U.S. CDS premiums reflect credit risk. [Chernov, Schmid, and Schneider \(2020\)](#) attribute most of the U.S. CDS premium to the risk of fiscal default. They develop a model with a [Bansal and Yaron \(2004\)](#) pricing kernel, an intertemporal government budget constraint, and a decline in government revenues when taxes are too high, also known as the Laffer curve. A sequence of bad shocks to the expected consumption growth leads to an increase in debt, and the latter can be sustained by increasing taxes, which has its limit due to the Laffer effect. Reaching this limit leads to a credit event.

In contrast, [Lando and Klingler \(2018\)](#) attribute about 50% of the CDS premium of safe-haven countries to regulatory frictions, as the uncollateralized risk exposures toward sovereign counterparties demand capital charges, which can be offset by purchasing CDS protection on these counterparties. Through this channel, demand for regulatory capital relief may artificially inflate CDS premiums. An important observation is that the argument of regulatory frictions in CDS premiums critically depends on the presence of default risk, without which there is no need for regulatory capital relief in the first place.

CDS premiums can reflect compensation for risks that are unrelated to default risk. For example, CDS contracts may command a liquidity premium because they are less actively traded than US Treasuries. [Augustin \(2014\)](#), [Chernov et al. \(2020\)](#), and [Augustin et al. \(2018\)](#) review a number of measures used to gauge the liquidity of the U.S. CDS market. For example, [Augustin et al. \(2018\)](#) report that the average gross (net) notional amount of U.S. CDS contracts outstanding is about \$18.72 billion (\$3.24 billion), which places it among the 20 most active sovereign CDS contracts. [Chernov et al. \(2020\)](#) compare the magnitude of the U.S. CDS market size to that of the most liquid Italian contract. The average ratio of weekly net notional amounts outstanding between U.S. and Italian CDS is 18%, and ranges between 6.5% in 2008 to 33% in late 2011. According to the Bank for International Settlements, the overall sovereign CDS market was \$1.458 trillion in 2018, which corresponds to about 17% of the overall market. More generally, for sovereign CDS contracts, liquidity is also more evenly spread out across the term structure compared to corporate CDS contracts, for which the liquidity is primarily concentrated in the 5-year maturity ([Pan and Singleton, 2008](#)). Based on these observations, we can reasonably assume that U.S. CDS premiums are not entirely attributable to a liquidity premium.

Another potential friction in CDS markets is associated with legal uncertainty. The Credit Determination Committee (DC), a panel of 15 industry participants, decides on the realization of a credit event that triggers the payout from CDS contracts. Many cases in the past, such as the defaults by Windstream, Codere, Hovnanian, or Thomas Cook, have demonstrated that there is much leeway in deciding whether a credit event has occurred or not. At present, there is a poor understanding of the incentives of the DC and how the legal uncertainty introduced by their deliberations feeds into the pricing of CDS premiums. Similarly, there is a risk of uncertain recovery that is determined by a bond auction with a cheapest-to-deliver option ([Chernov et al., 2013](#)).

Counterparty risk is an additional friction that could distort the U.S. CDS premium downwards as a measure of U.S. default risk. Given that swap contracts are fully collateralized, there is little reason to believe that this should be quantitatively important. Indeed, [Arora, Gandhi, and Longstaff \(2012\)](#), who study the impact of counterparty risk on corporate CDS valuation, conclude that the credit risk of the counterparty would need to increase by six percentage points to decrease the CDS premium by one basis point. Similar conclusions of vanishingly small effects from counterparty risk are derived by [Du, Gordy, Gadgil, and Vega \(2016\)](#).

From an empirical perspective, the U.S. has defaulted before, both on external and domestic debt ([Zivney and Marcus, 1989](#); [English, 1996](#); [Reinhart and Rogoff, 2008](#)). One such example is the abrogation of the gold clause by the U.S. Congress in 1933, which led to a significant depreciation of the U.S. dollar in relation to gold, and effectively reduced the debt burden of USD denominated debt contracts by more than half ([Edwards, 2018](#); [Gomes et al., 2019](#)). Abandoning the gold clause, which indexed the repayment of USD

denominated debt to the price of gold, led to many lawsuits against U.S. Congress, and even several members of Congress compared the situation to a repudiation of debt contracts. The Supreme Court’s 1935 5-to-4 decision to uphold the abrogation of the gold clause sealed the verdict on an event that represented a de facto U.S. default.

Such past experiences are relevant to today’s increasing debt levels of the U.S. government. According to the U.S. Treasury, the total federal public debt almost quadrupled over the last 20 years, ballooning from \$5.526 trillion in the third quarter of 1998 to \$21.516 trillion in the third quarter of 2018.¹ This recent figure corresponds to about 104% of the gross domestic product (GDP). In their 2019 long-term budget outlook, the Congressional budget office foresees large budget deficits in the years to come, with a central estimate of federal debt to GDP of 144% by 2049. This is a magnitude consistent with the default trigger computations in [Chernov, Schmid, and Schneider \(2020\)](#). Since 2002, the U.S. has consistently reported a deficit, with the most recent estimates for 2018 being around negative 3.8 percent.

Similarly, Standard & Poor’s stripped the U.S. of the highest AAA credit rating in 2011, suggesting the presence of credit risk. In modern times, we have also experienced effective defaults by high-quality sovereigns despite relatively low CDS premiums. Ireland, which still enjoyed a AAA credit rating going into the global financial crisis, saw its CDS premiums rise from about 2 bps in 2007 to north of 400 bps when it was bailed out by the Eurozone countries in 2010 (see discussions around Figure 1 in [Acharya et al., 2014](#)). Similarly, Spain received a AAA credit rating in 2003 when its CDS premiums fluctuated at around 3 to 4 bps. However, it was at the cusp of junk status in 2012 when it received financial support from the Eurozone, and CDS premiums reached levels close to 600 bps.

Appendix B. Derivation of the real pricing kernel

Since utility is defined by a constant elasticity of substitution recursion and the certainty equivalent is homogeneous of degree one, we can scale utility and take logs:

$$\log(U_t/C_t) \equiv u_t = \rho^{-1} \log \left[(1 - \beta) + \beta \mu_t \left(e^{\Delta c_{t+1} + u_{t+1}} \right)^\rho \right].$$

Taking a first-order Taylor approximation of u_t around the point $E[\log \mu_t] = \log \mu$, we obtain the log-linearized form

$$\begin{aligned} u_t &\approx \rho^{-1} \log \left[(1 - \beta) + \beta e^{\rho \log \mu} \right] + \rho^{-1} \frac{\beta e^{\rho \log \mu} \rho}{[(1 - \beta) + \beta e^{\rho \log \mu}]} \left[\log \mu_t \left(e^{\Delta c_{t+1} + u_{t+1}} \right) - \log \mu \right] \\ &\approx b_0 + b_1 \log \mu_t \left(e^{\Delta c_{t+1} + u_{t+1}} \right), \end{aligned}$$

where

$$\begin{aligned} b_1 &= \beta e^{\rho \log \mu} \left((1 - \beta) + \beta e^{\rho \log \mu} \right)^{-1} \\ b_0 &= \rho^{-1} \log \left[(1 - \beta) + \beta e^{\rho \log \mu} \right] - b_1 \log \mu. \end{aligned}$$

The state vector $x_t = (\Delta c_t, \pi_t, d_t, g_t, w_{c,t}, w_{\pi,t}, w_{y,t}, w_{g,t}, v_{1,t}, v_{2,t})$ describes the economy, where $\Delta c_t = \log(C_{t+1}/C_t)$ is log consumption growth, π_t is inflation, d_t is log output growth, g_t is the government expenditure to output ratio, $w_t = [w_{c,t}, w_{\pi,t}, w_{d,t}, w_{g,t}]^\top$ is the vector of moving average components, and $v_t = [v_{1,t}, v_{2,t}]^\top$ is a vector of common stochastic variance processes.

¹These estimates are from the U.S. Department of the Treasury and retrieved from FRED, the Federal Reserve Bank of St. Louis. We focus on total public debt (GFDEBTN), total public debt as percent of gross domestic product (GFDEGDQ188S), and the federal surplus or deficit as percent of gross domestic product (FYFSGDA188S).

Guess that the log scaled utility is affine in the state vector x_t

$$\begin{aligned} u_t &= \log u + P_x^\top x_t = \log u + P_y^\top y_t + p_v^\top v_t \\ &= \log u + p_c \Delta c_t + p_\pi \pi_t + p_d d_t + p_g g_t + p_{v1} v_{1,t} + p_{v2} v_{2,t}, \end{aligned}$$

which implies that $P_x = [P_y^\top, p_v^\top]^\top = [p_c, p_\pi, p_d, p_g, 0, 0, 0, 0, p_{v1}, p_{v2}]^\top$.

Next compute $\log(e^{\Delta c_{t+1} + u_{t+1}})$ and $\log \mu_t(e^{\Delta c_{t+1} + u_{t+1}})$, plug terms into the log-linearized scaled utility u_t and verify. Given the initial guess, this results in a system of seven equations, which can be solved using the method of undetermined coefficients for the constant and the loadings of the log scaled utility on x_t . For the derivations, define the coordinate vectors e_i ($i = 1, 2, \dots, 8$) and e_{v_i} ($i = 1, 2$) with all elements equal to zero except element i , which is equal to one.

Step 1: Compute $\log(e^{\Delta c_{t+1} + u_{t+1}})$:

$$\begin{aligned} \log(e^{\Delta c_{t+1} + u_{t+1}}) &= \Delta c_{t+1} + u_{t+1} = e_1^\top y_{t+1} + \log u + P_y^\top y_{t+1} + p_v^\top v_{t+1} \\ &= \log u + (P_y + e_1)^\top \mu_y + (P_y + e_1)^\top \Phi_y y_t + (P_y + e_1)^\top \Phi_{yv} v_t \\ &\quad + (P_y + e_1)^\top \Sigma_y V_{y,t}^{1/2} \varepsilon_{y,t+1} + p_v^\top v_{t+1}. \end{aligned}$$

Step 2: Compute $\log \mu_t(e^{\Delta c_{t+1} + u_{t+1}})$:

$$\begin{aligned} \log \mu_t(e^{\Delta c_{t+1} + u_{t+1}}) &= \log \left[E_t \left(e^{\Delta c_{t+1} + u_{t+1}} \right)^\alpha \right]^{1/\alpha} = \alpha^{-1} \log \left[E_t \left(e^{\alpha(\Delta c_{t+1} + u_{t+1})} \right) \right] \\ &= \log u + (P_y + e_1)^\top \mu_y + (P_y + e_1)^\top \Phi_y y_t + (P_y + e_1)^\top \Phi_{yv} v_t \\ &\quad + \frac{\alpha}{2} (P_y + e_1)^\top \Omega_{y,t} (P_y + e_1) + \sum_{j=1}^2 \frac{-v_{v_j}}{\alpha} \log(1 - \alpha p_{v_j} c_{v_j}) + \frac{p_{v_j} \phi_{v_j}}{1 - \alpha p_{v_j} c_{v_j}} v_{j,t}, \end{aligned}$$

where $\Omega_{y,t} = \Sigma_y V_{y,t} \Sigma_y^\top$.

Step 3: Plug into u_t and verify:

$$\begin{aligned} u_t &\approx b_0 + b_1 \log \mu_t(e^{\Delta c_{t+1} + u_{t+1}}) \\ &= b_0 + b_1 \left[\log u + (P_y + e_1)^\top \mu_y - \sum_{j=1}^2 \frac{v_{v_j}}{\alpha} \log(1 - \alpha p_{v_j} c_{v_j}) \right] + b_1 \left[(P_y + e_1)^\top \Phi_y y_t \right] \\ &\quad + b_1 \left[(P_y + e_1)^\top \Phi_{yv} v_t + \frac{\alpha}{2} (P_y + e_1)^\top \Omega_{y,t} (P_y + e_1) + \sum_{j=1}^2 \frac{p_{v_j} \phi_{v_j}}{1 - \alpha p_{v_j} c_{v_j}} v_{j,t} \right]. \end{aligned}$$

Given the initial guess, this results in a system of seven equations:

$$\begin{aligned}
\log u &= b_0 + b_1 \left[\log u + (P_y + e_1)^\top \mu_y + \frac{\alpha}{2} (P_y + e_1)^\top \Sigma_y \left[\mathbf{I} \odot \left(\mathbf{1}^\top \otimes \mathbf{A} \right) \right] \Sigma_y^\top (P_y + e_1) \right. \\
&\quad \left. - \sum_{j=1}^2 \frac{v_{v_j}}{\alpha} \log (1 - \alpha p_{v_j} c_{v_j}) \right] \\
p_c &= b_1 (P_y + e_1)^\top \Phi_y e_1 \\
p_\pi &= u_1 (P_y + e_1)^\top \Phi_y e_2 \\
p_d &= b_1 (P_y + e_1)^\top \Phi_y e_3 \\
p_g &= b_1 (P_y + e_1)^\top \Phi_y e_4 \\
p_{v_1} &= b_1 \left[(P_y + e_1)^\top \Phi_{y v} e_{v_1} + \frac{\alpha}{2} (P_y + e_1)^\top \Sigma_y \left[\mathbf{I} \odot \left(\mathbf{1}^\top \otimes \mathbf{B}_1 \right) \right] \Sigma_y^\top (P_y + e_1) + \frac{p_{v_1} \phi_{v_1}}{1 - \alpha p_{v_1} c_{v_1}} \right] \\
p_{v_2} &= b_1 \left[(P_y + e_1)^\top \Phi_{y v} e_{v_2} + \frac{\alpha}{2} (P_y + e_1)^\top \Sigma_y \left[\mathbf{I} \odot \left(\mathbf{1}^\top \otimes \mathbf{B}_2 \right) \right] \Sigma_y^\top (P_y + e_1) + \frac{p_{v_2} \phi_{v_2}}{1 - \alpha p_{v_2} c_{v_2}} \right],
\end{aligned}$$

where \otimes defines the Kronecker product, \odot the Hadamar product, \mathbf{I} is the identity matrix, and $\mathbf{1}$ is a column vector of ones, and where we have defined the column vectors \mathbf{A} , \mathbf{B}_1 , \mathbf{B}_2 as follows:

$$\begin{aligned}
\mathbf{A} &= [a_c, a_\pi, a_d, a_g, 0, 0, 0, 0]^\top \\
\mathbf{B}_1 &= [b_{c v_1}, b_{\pi v_1}, b_{d v_1}, b_{g v_1}, 0, 0, 0, 0]^\top \\
\mathbf{B}_2 &= [b_{c v_2}, b_{\pi v_2}, b_{d v_2}, b_{g v_2}, 0, 0, 0, 0]^\top.
\end{aligned} \tag{B.1}$$

Since, the equations for p_c , p_π , p_d , and p_g are linear, their solutions are given by

$$\begin{aligned}
p_c &= -e_1^\top (b_1^2 [\Phi_z - \mathbf{I}]^{-1} \phi_c) \\
p_\pi &= -e_2^\top (b_1^2 [\Phi_z - \mathbf{I}]^{-1} \phi_c) \\
p_y &= -e_3^\top (b_1^2 [\Phi_z - \mathbf{I}]^{-1} \phi_c) \\
p_g &= -e_4^\top (b_1^2 [\Phi_z - \mathbf{I}]^{-1} \phi_c).
\end{aligned}$$

The equations for p_v are quadratic and have two roots. We choose the root such that $\lim_{c_j \rightarrow 0} c_j p_{v_j} = 0$ as $c_j \rightarrow 0$. We have that for $j = 1, 2$:

$$\begin{aligned}
&\underbrace{\left[b_1 \left(\phi_{v_j} - \alpha c_{v_j} \left[(P_y + e_1)^\top \Phi_{y v} e_{v_j} + \frac{\alpha}{2} (P_y + e_1)^\top \Sigma_y \left[\mathbf{I} \odot \left(\mathbf{1}^\top \otimes \mathbf{B}_j \right) \right] \Sigma_y^\top (P_y + e_1) \right] \right) - 1 \right]}_{B_j^*} p_{v_j} \\
&+ \underbrace{\alpha c_{v_j} p_{v_j}^2}_{A_j^*} + \underbrace{b_1 \left[(P_y + e_1)^\top \Phi_{y v} e_{v_j} + \frac{\alpha}{2} (P_y + e_1)^\top \Sigma_y \left[\mathbf{I} \odot \left(\mathbf{1}^\top \otimes \mathbf{B}_j \right) \right] \Sigma_y^\top (P_y + e_1) \right]}_{C_j^*} = 0,
\end{aligned}$$

where the roots to the quadratic equation are determined by:

$$p_{v_j} = \frac{-B_j^* + / - \sqrt{(B_j^*)^2 - 4A_j^*C_j^*}}{2A_j^*}.$$

Finally, we have that

$$\begin{aligned} \log u &= (1 - b_1)^{-1} \left[b_0 + b_1 \left((P_y + e_1)^\top \mu_y + \frac{\alpha}{2} (P_y + e_1)^\top \Sigma_y \left[\mathbf{I} \odot \left(\mathbf{1}^\top \otimes \mathbf{A} \right) \right] \Sigma_y^\top (P_y + e_1) \right. \right. \\ &\quad \left. \left. - \sum_{j=1}^2 \frac{v_{v_j}}{\alpha} \log (1 - \alpha p_{v_j} c_{v_j}) \right) \right]. \end{aligned}$$

Plugging terms into the expression for the marginal rate of substitution, we obtain the final solution to the real pricing kernel

$$\begin{aligned} \widehat{m}_{t,t+1} &= \bar{m} + (\rho - 1) e_1^\top \Phi_y y_t + (\rho - 1) e_1^\top \Phi_{yv} v_t \\ &\quad - \sum_{j=1}^2 \left[\frac{(\alpha - \rho) p_{v_j} \phi_{v_j}}{1 - \alpha p_{v_j} c_{v_j}} + \frac{\alpha}{2} (\alpha - \rho) (P_y + e_1)^\top \Sigma_y \left[\mathbf{I} \odot \left(\mathbf{1}^\top \otimes \mathbf{B}_j \right) \right] \Sigma_y^\top (P_y + e_1) \right] v_{j,t} \\ &\quad + [(\rho - 1) e_1 + (\alpha - \rho) (P_y + e_1)]^\top \Sigma_y V_{y,t}^{1/2} \varepsilon_{y,t+1} + (\alpha - \rho) p_v^\top v_{t+1}, \end{aligned} \quad (\text{B.2})$$

where

$$\begin{aligned} \bar{m} &= \log \beta + (\rho - 1) e_1^\top \mu_y + (\alpha - \rho) \sum_{j=1}^2 \frac{v_{v_j}}{\alpha} \log (1 - \alpha p_{v_j} c_{v_j}) \\ &\quad - \frac{\alpha}{2} (\alpha - \rho) (P_y + e_1)^\top \Sigma_y \left[\mathbf{I} \odot \left(\mathbf{1}^\top \otimes \mathbf{A} \right) \right] \Sigma_y^\top (P_y + e_1). \end{aligned} \quad (\text{B.3})$$

The numerical solution to the mean log certainty equivalent $E[\log \mu_t] = \log \mu$ depends on the approximated constants from the log-linearization of the scaled log utility b_0 and b_1 , which themselves depend on the mean log certainty equivalent $\log \mu$. Model consistency thus requires to solve a fixed-point equation for the mean log certainty equivalent. More specifically, using a convergence criterion of $10e^{-12}$, we solve for the fixed-point equation $\log \mu = f(\log \mu)$.

Appendix C. Valuation

C.1. Term structure of real interest rates

The price of an n -period real zero-coupon bond must satisfy the Euler equation $\widehat{P}_t^n = E_t \left[\widehat{M}_{t,t+n} \right]$. To derive closed-form solutions for the term structure of real interest rates, we conjecture that log zero-coupon bond prices \widehat{p}_t are affine in the state vector x_t

$$\widehat{p}_t^n = \log \widehat{P}_t^n = -\widehat{A}_n - \widehat{B}_{y,n}^\top y_t - \widehat{B}_{v,n}^\top v_t,$$

where the coefficients of the vectors $\widehat{B}_{y,n}$ and $\widehat{B}_{v,n}$ measure the sensitivity of real bond prices to the risk factors and where n refers to the maturity of the bond. Since the real pricing kernel is an affine function of the state vector, log bond prices are fully characterized by the cumulant-generating function of X_t . The law of iterated expectations implies that \widehat{P}_t^n satisfies the recursion

$$\widehat{P}_t^n = E_t \left[\widehat{M}_{t,t+1} \widehat{P}_{t+1}^{n-1} \right].$$

It can be shown that for all n , the scalar \widehat{A}_n and the components of the column vectors $\widehat{B}_{y_j,n}$ for $j = 1, 2, \dots, 8$ and $\widehat{B}_{v_j,n}$ for $j = 1, 2$, are given by

$$\widehat{A}_n = \widehat{A}_{n-1} - \bar{m} + \widehat{B}_{y,n-1}^\top \mu_y + \sum_{j=1}^2 v_{v_j} \log \left(1 - \left[(\alpha - \rho) p_{v_j} - \widehat{B}_{v_j,n-1} \right] c_{v_j} \right)$$

$$\begin{aligned}
& - \frac{1}{2} \left[(\rho - 1) e_1 + (\alpha - \rho) (P_y + e_1) - \widehat{B}_{y,n-1} \right]^\top \Sigma_y \left[\mathbf{I} \odot \left(\mathbf{1}^\top \otimes \mathbf{A} \right) \right] \Sigma_y^\top \\
& \times \left[(\rho - 1) e_1 + (\alpha - \rho) (P_y + e_1) - \widehat{B}_{y,n-1} \right] \\
\widehat{B}_{y_j,n} & = \left[\widehat{B}_{y,n-1} - (\rho - 1) e_1 \right]^\top \Phi_y e_j \\
\widehat{B}_{v_j,n} & = \left[\widehat{B}_{y,n-1} - (\rho - 1) e_1 \right]^\top \Phi_{yv} e_{v_j} \\
& + \frac{(\alpha - \rho) p_{v_j} \phi_{v_j}}{1 - \alpha p_{v_j} c_{v_j}} + \frac{\alpha}{2} (\alpha - \rho) (P_y + e_1)^\top \Sigma_y \left[\mathbf{I} \odot \left(\mathbf{1}^\top \otimes \mathbf{B}_j \right) \right] \Sigma_y^\top (P_y + e_1) \\
& - \frac{1}{2} \left[(\rho - 1) e_1 + (\alpha - \rho) (P_y + e_1) - \widehat{B}_{y,n-1} \right]^\top \Sigma_y \left[\mathbf{I} \odot \left(\mathbf{1}^\top \otimes \mathbf{B}_j \right) \right] \\
& \times \Sigma_y^\top \left[(\rho - 1) e_1 + (\alpha - \rho) (P_y + e_1) - \widehat{B}_{y,n-1} \right] - \frac{\left[(\alpha - \rho) p_{v_j} - \widehat{B}_{v_j,n-1} \right] \phi_{v_j}}{1 - \left[(\alpha - \rho) p_{v_j} - \widehat{B}_{v_j,n-1} \right] c_{v_j}},
\end{aligned}$$

with initial conditions $\widehat{A}_0 = 0$, $\widehat{B}_{y,0} = \mathbf{0}$, and $\widehat{B}_{v,0} = \mathbf{0}$, and where \otimes defines the Kronecker product, \odot the Hadamar product, \mathbf{I} is the identity matrix, $\mathbf{1}$ is a column vector of ones, e_i ($i = 1, 2, \dots, 8$) and e_{v_i} ($i = 1, 2$) are coordinate vectors with all elements equal to zero except element $i = 1$, the column vectors \mathbf{A} , and \mathbf{B}_j for $j = 1, 2$ are defined in Equation (B.1), and \bar{m} is defined in Equation (B.3).

It follows naturally that the term structure of real interest rates is given by:

$$\widehat{y}_t^n = n^{-1} \left(\widehat{A}_n + \widehat{B}_{y,n}^\top y_t + \widehat{B}_{v,n}^\top v_t \right).$$

C.2. Term structure of nominal interest rates

The price of an n -period nominal zero-coupon bond must satisfy the Euler equation $P_t^n = E_t [M_{t,t+n}]$, where $M_{t,t+1}$ defines the nominal stochastic discount factor defined in logs as

$$m_{t,t+1} = \widehat{m}_{t,t+1} - \pi_{t+1} = \widehat{m}_{t,t+1} - e_2^\top y_{t+1},$$

with the real pricing kernel $\widehat{m}_{t,t+1}$ defined in Equation (B.2). To derive closed-form solutions for the term structure of nominal interest rates, we conjecture that log zero-coupon bond prices p_t are affine in the state vector x_t

$$p_t^n = \log P_t^n = -A_n - B_{y,n}^\top y_t - B_{v,n}^\top v_t,$$

where the coefficients of the vectors $B_{y,n}$ and $B_{v,n}$ measure the sensitivity of nominal bond prices to the risk factors and where n refers to the maturity of the bond. Since the nominal pricing kernel is an affine function of the state vector, log bond prices are fully characterized by the cumulant-generating function of x_t . The law of iterated expectations implies that P_t^n satisfies the recursion

$$P_t^n = E_t [M_{t,t+1} P_{t+1}^{n-1}].$$

It can be shown that for all n , the scalar A_n and the components of the column vectors $B_{y_j,n}$ for $j = 1, 2, \dots, 8$ and $B_{v_j,n}$ for $j = 1, 2$, are given by

$$\begin{aligned}
A_n & = A_{n-1} - \bar{m} + [e_2 + B_{y,n-1}]^\top \mu_y + \sum_{j=1}^2 v_{v_j} \log \left(1 - [(\alpha - \rho) p_{v_j} - B_{v_j,n-1}] c_{v_j} \right) \\
& - \frac{1}{2} \left[(\rho - 1) e_1 + (\alpha - \rho) (P_y + e_1) - e_2 - B_{y,n-1} \right]^\top \Sigma_y \left[\mathbf{I} \odot \left(\mathbf{1}^\top \otimes \mathbf{A} \right) \right] \\
& \times \Sigma_y^\top \left[(\rho - 1) e_1 + (\alpha - \rho) (P_y + e_1) - e_2 - B_{y,n-1} \right] \\
B_{y_j,n} & = [B_{y,n-1} + e_2 - (\rho - 1) e_1]^\top \Phi_y e_j \\
B_{v_j,n} & = [B_{y,n-1} + e_2 - (\rho - 1) e_1]^\top \Phi_{yv} e_{v_j}
\end{aligned}$$

$$\begin{aligned}
& + \frac{(\alpha - \rho) p_{v_j} \phi_{v_j}}{1 - \alpha p_{v_j} c_{v_j}} + \frac{\alpha}{2} (\alpha - \rho) (P_y + e_1)^\top \Sigma_y \left[\mathbf{I} \odot \left(\mathbf{1}^\top \otimes \mathbf{B}_j \right) \right] \Sigma_y^\top (P_y + e_1) \\
& - \frac{1}{2} [(\rho - 1) e_1 + (\alpha - \rho) (P_y + e_1) - e_2 - B_{y,n-1}]^\top \Sigma_y \left[\mathbf{I} \odot \left(\mathbf{1}^\top \otimes \mathbf{B}_j \right) \right] \\
& \times \Sigma_y^\top [(\rho - 1) e_1 + (\alpha - \rho) (P_y + e_1) - e_2 - B_{y,n-1}] - \frac{[(\alpha - \rho) p_{v_j} - B_{v_j,n-1}] \phi_{v_j}}{1 - [(\alpha - \rho) p_{v_j} - B_{v_j,n-1}] c_{v_j}},
\end{aligned}$$

with initial conditions $A_0 = 0$, $B_{y,0} = \mathbf{0}$, and $B_{v,0} = \mathbf{0}$, and where \otimes defines the Kronecker product, \odot the Hadamar product, \mathbf{I} is the identity matrix, $\mathbf{1}$ is a column vector of ones, e_i ($i = 1, 2, \dots, 8$) and e_{v_i} ($i = 1, 2$) are coordinate vectors with all elements equal to zero except element $i = 1$, the column vectors \mathbf{A} and \mathbf{B}_j for $j = 1, 2$ are defined in Equation (B.1), and \bar{m} is defined in Equation (B.3).

It follows naturally that the term structure of nominal interest rates is given by:

$$y_t^n = n^{-1} \left(A_n + B_{y,n}^\top y_t + B_{v,n}^\top v_t \right).$$

C.3. Term structure of risky treasury yields

U.S. default risk is driven by a default intensity h_t defined as

$$h_t = h + h_c \Delta c_t + h_d d_t + h_g g_t + h_{v_1} v_{1,t} + h_{v_2} v_{2,t} = h + h_z^\top z_t + h_v^\top v_t, \quad (\text{C.1})$$

such that $h_z = [h_c, h_\pi, h_d, h_g]^\top$ and $h_v = [h_{v_1}, h_{v_2}]^\top$. We adopt the convention that $h_y = [h_z, 0, 0, 0, 0]^\top$, and $h_{\bar{y}} = [h_y, 0, 0, 0]^\top$. We connect the default intensity to \mathcal{H}_t , the conditional default probability of a given reference entity at day t via $\mathcal{H}_t \equiv \text{Prob}(\tau = t \mid \tau \geq t; \mathcal{F}_t) = 1 - e^{-h_t}$, where \mathcal{F}_t denotes all the available information available at time t , with the exception of credit events. This implies that the probability of survival (no credit event) until time t is:

$$S_t \equiv \text{Prob}(\tau > t \mid \mathcal{F}_t) = S_0 \prod_{j=1}^t (1 - \mathcal{H}_j), \quad t \geq 1. \quad (\text{C.2})$$

To price risky zero coupon Treasury bonds, we take into account the convenience yield $s_{1,t}$ with dynamics defined in Equation (4), and loss given default L . Using the law of iterated expectations, it is possible to show that risky bond prices follow the recursion

$$\begin{aligned}
\tilde{P}_t^n & = E_t \left(M_{t,t+1} e^{s_{1,t+1}} [\mathcal{I}(\tau > t+1) + (1-L) \cdot \mathcal{I}(t < \tau \leq t+1)] \cdot \tilde{P}_{t+1}^{n-1} \right) \\
& = E_t \left(M_{t,t+1} e^{s_{1,t+1}} [1 - L \mathcal{H}_{t+1}] \cdot \tilde{P}_{t+1}^{n-1} \right) \\
& \approx E_t e^{\sum_{j=1}^n m_{t+j-1,t+j} - L \cdot h_{t+j} + s_{1,t+j}},
\end{aligned}$$

where we follow [Duffie and Singleton \(1999\)](#) by applying a first order Taylor approximation of $\log(1 - L \mathcal{H}_t)$ around 0 such that $\log(1 - L \mathcal{H}_t) \approx -L \cdot h_t$. Since all elements of the bond pricing equation are affine functions of the extended state vector, log bond prices are fully characterized by the cumulant-generating function of \tilde{x}_t . The law of iterated expectations implies that \tilde{P}_t^n satisfies the recursion

$$\tilde{P}_t^n = E_t \left[M_{t,t+1} e^{-L \cdot h_{t+1} + s_{1,t+1}} \tilde{P}_{t+1}^{n-1} \right].$$

To derive closed-form solutions for the term structure of risky Treasury rates, we conjecture that log prices of risky zero-coupon bonds \tilde{p}_t are affine in the extended state vector $\tilde{x}_t = [y_t^\top, s^\top, v_t^\top]^\top = [\tilde{y}_t^\top, v_t^\top]^\top$:

$$\tilde{p}_t = \log \tilde{P}_t^n = -\tilde{A}_n - \tilde{B}_{\bar{y},n}^\top \tilde{y}_t - \tilde{B}_{v,n}^\top v_t.$$

where the coefficients of the vectors $\tilde{B}_{\bar{y},n}$ and $\tilde{B}_{v,n}$ measure the sensitivity of risky bond prices to the risk factors and where n refers to the maturity of the bond. It can be shown that for all n , the scalar \tilde{A}_n and

the components of the column vectors $\tilde{B}_{\tilde{y}_j, n}$ for $j = 1, 2, \dots, 11$ and $\tilde{B}_{v_j, n}$ for $j = 1, 2$, are given by

$$\begin{aligned}
\tilde{A}_n &= \tilde{A}_{n-1} + L \cdot h - \tilde{m} + \left[\tilde{e}_2 + L \cdot h_{\tilde{y}} - \tilde{e}_9 + \tilde{B}_{\tilde{y}, n-1} \right]^\top \tilde{\mu}_y \\
&+ \sum_{j=1}^2 v_{v_j} \log \left(1 - \left[(\alpha - \rho) p_{v_j} - L \cdot h_{v_j} - \tilde{B}_{v_j, n-1} \right. \right. \\
&\quad \left. \left. + \left(\tilde{B}_{s_1, n-1} + 1 \right) v_{s_1 v_j} + \tilde{B}_{s_2, n-1} v_{s_2 v_j} + \tilde{B}_{s_3, n-1} v_{s_3 v_j} \right] c_{v_j} \right) \\
&- \frac{1}{2} \left[(\rho - 1) \tilde{e}_1 + (\alpha - \rho) (P_{\tilde{y}} + \tilde{e}_1) - \left(\tilde{e}_2 + L \cdot h_{\tilde{y}} - \tilde{e}_9 + \tilde{B}_{\tilde{y}, n-1} \right) \right]^\top \tilde{\Sigma}_y \left[\tilde{\mathbf{I}} \odot \left(\tilde{\mathbf{I}}^\top \otimes \tilde{\mathbf{A}} \right) \right] \\
&\times \tilde{\Sigma}_y^\top \left[(\rho - 1) \tilde{e}_1 + (\alpha - \rho) (P_{\tilde{y}} + \tilde{e}_1) - \left(\tilde{e}_2 + L \cdot h_{\tilde{y}} - \tilde{e}_9 + \tilde{B}_{\tilde{y}, n-1} \right) \right] \\
&- \sum_{j=1}^2 \left(\left(\tilde{B}_{s_1, n-1} + 1 \right) v_{s_1 v_j} + \tilde{B}_{s_2, n-1} v_{s_2 v_j} + \tilde{B}_{s_3, n-1} v_{s_3 v_j} \right) v_{v_j} c_{v_j} \\
\tilde{B}_{\tilde{y}_j, n} &= \left[\left(\tilde{e}_2 + L \cdot h_{\tilde{y}} - \tilde{e}_9 + \tilde{B}_{\tilde{y}, n-1} \right) - (\rho - 1) \tilde{e}_1 \right]^\top \tilde{\Phi}_y \tilde{e}_j \\
&+ \frac{(\alpha - \rho) p_{v_j} \phi_{v_j}}{1 - \alpha p_{v_j} c_{v_j}} + \frac{\alpha}{2} (\alpha - \rho) (P_{\tilde{y}} + \tilde{e}_1)^\top \tilde{\Sigma}_y \left[\tilde{\mathbf{I}} \odot \left(\tilde{\mathbf{I}}^\top \otimes \tilde{\mathbf{B}}_j \right) \right] \tilde{\Sigma}_y^\top (P_{\tilde{y}} + \tilde{e}_1) \\
&- \frac{1}{2} \left[(\rho - 1) \tilde{e}_1 + (\alpha - \rho) (P_{\tilde{y}} + \tilde{e}_1) - \left(\tilde{e}_2 + L \cdot h_{\tilde{y}} - \tilde{e}_9 + \tilde{B}_{\tilde{y}, n-1} \right) \right]^\top \tilde{\Sigma}_y \left[\tilde{\mathbf{I}} \odot \left(\tilde{\mathbf{I}}^\top \otimes \tilde{\mathbf{B}}_j \right) \right] \\
&\times \tilde{\Sigma}_y^\top \left[(\rho - 1) \tilde{e}_1 + (\alpha - \rho) (P_{\tilde{y}} + \tilde{e}_1) - \left(\tilde{e}_2 + L \cdot h_{\tilde{y}} - \tilde{e}_9 + \tilde{B}_{\tilde{y}, n-1} \right) \right] \\
&- \frac{\left[(\alpha - \rho) p_{v_j} - L \cdot h_{v_j} - \tilde{B}_{v_j, n-1} + \left(\tilde{B}_{s_1, n-1} + 1 \right) v_{s_1 v_j} + \tilde{B}_{s_2, n-1} v_{s_2 v_j} + \tilde{B}_{s_3, n-1} v_{s_3 v_j} \right] \phi_{v_j}}{1 - \left[(\alpha - \rho) p_{v_j} - L \cdot h_{v_j} - \tilde{B}_{v_j, n-1} + \left(\tilde{B}_{s_1, n-1} + 1 \right) v_{s_1 v_j} + \tilde{B}_{s_2, n-1} v_{s_2 v_j} + \tilde{B}_{s_3, n-1} v_{s_3 v_j} \right] c_{v_j}} \\
&+ \left(\left(\tilde{B}_{s_1, n-1} + 1 \right) v_{s_1 v_j} + \tilde{B}_{s_2, n-1} v_{s_2 v_j} + \tilde{B}_{s_3, n-1} v_{s_3 v_j} \right) \phi_{v_j},
\end{aligned}$$

with initial conditions $\tilde{A}_0 = 0$, $\tilde{B}_{\tilde{y}, 0} = \mathbf{0}$, and $\tilde{B}_{v, 0} = \mathbf{0}$, and where \otimes defines the Kronecker product, \odot the Hadamar product, $\tilde{\mathbf{I}}$ is the identity matrix, $\tilde{\mathbf{1}}$ is a column vector of ones, \tilde{e}_i ($i = 1, 2, \dots, 11$) and e_{v_i} ($i = 1, 2$) are coordinate vectors with all elements equal to zero except element $i = 1$, \tilde{m} is defined in Equation (B.3), and the column vectors $\tilde{\mathbf{A}}$ and $\tilde{\mathbf{B}}_j$ for $j = 1, 2$ are given by

$$\begin{aligned}
\tilde{\mathbf{A}} &= [a_c, a_\pi, a_d, a_g, 0, 0, 0, 0, 1, 1, 1]^\top \\
\tilde{\mathbf{B}}_j &= [b_{cv_j}, b_{\pi v_j}, b_{dv_j}, b_{gv_j}, 0, 0, 0, 0, 0, 0]^\top.
\end{aligned} \tag{C.3}$$

It follows naturally that the term structure of risky interest rates is given by:

$$\tilde{y}_t^n = n^{-1} \left(\tilde{A}_n + \tilde{B}_{\tilde{y}, n}^\top \tilde{y}_t + \tilde{B}_{v, n}^\top v_t \right).$$

C.4. Term structure of LIBOR rates

We work with hypothetical zero-coupon LIBOR bonds L_t^n discounted at the continuously compounded yield ℓ_t^n (defined at the monthly frequency), such that $L_t^n = \exp(-\ell_t^n \cdot n)$, where $n \leq 12$ corresponds to LIBOR rate maturities of up to 12 months. To price LIBOR bonds, we take into account the convenience yield $s_{1,t}$ and bank risk $s_{2,t}$, with dynamics defined in Equation (4), and loss given default L . The LIBOR rate is defined as $\ell_t = \tilde{y}_t^1 + s_{1,t} + s_{2,t}$. Using the law of iterated expectations, it is possible to show that LIBOR bond prices follow the recursion

$$L_t^n \approx E_t e^{\sum_{j=1}^n m_{t+j-1, t+j} - L \cdot h_{t+j} - s_{2, t+j}}.$$

Following the logic developed for risky Treasury bonds in appendix C.3, it is straightforward to show that the log price of a risky n -period zero coupon LIBOR bond is affine in the extended state space \tilde{x}_t :

$$\log L_t^n = -\bar{A}_n - \bar{B}_{\tilde{y},n}^\top \tilde{y}_t - \bar{B}_{v,n}^\top v_t. \quad (\text{C.4})$$

where the constant \bar{A}_n and the coefficients of the column vectors $\bar{B}_{\tilde{y},n}$ and $\bar{B}_{v,n}$ measure the sensitivity of LIBOR bond prices to the risk factors and where n refers to the maturity of the bond. It can be shown that for all n , the scalar \bar{A}_n and the components of the column vectors $\bar{B}_{\tilde{y},n}$ for $j = 1, 2, \dots, 11$ and $\bar{B}_{v_j,n}$ for $j = 1, 2$, are given by

$$\begin{aligned} \bar{A}_n &= \bar{A}_{n-1} + L \cdot h - \bar{m} + (\tilde{e}_2 + L \cdot h_{\tilde{y}} + \tilde{e}_{10} + \bar{B}_{\tilde{y},n-1})^\top \tilde{\mu}_y \\ &+ \sum_{j=1}^2 v_{v_j} \log \left(1 - [(\alpha - \rho) p_{v_j} - L \cdot h_{v_j} - \bar{B}_{v_j,n-1} \right. \\ &\quad \left. + \bar{B}_{s_1,n-1} v_{s_1 v_j} + (\bar{B}_{s_2,n-1} - 1) v_{s_2 v_j} + \bar{B}_{s_3,n-1} v_{s_3 v_j}] c_{v_j} \right) \\ &- \frac{1}{2} [(\rho - 1) \tilde{e}_1 + (\alpha - \rho) (P_{\tilde{y}} + \tilde{e}_1) - (\tilde{e}_2 + L \cdot h_{\tilde{y}} + \tilde{e}_{10} + \bar{B}_{\tilde{y},n-1})]^\top \tilde{\Sigma}_y [\tilde{\mathbf{I}} \odot (\tilde{\mathbf{I}}^\top \otimes \tilde{\mathbf{A}})] \\ &\times \tilde{\Sigma}_y^\top [(\rho - 1) \tilde{e}_1 + (\alpha - \rho) (P_{\tilde{y}} + \tilde{e}_1) - (\tilde{e}_2 + L \cdot h_{\tilde{y}} + \tilde{e}_{10} + \bar{B}_{\tilde{y},n-1})] \\ &+ \sum_{j=1}^2 \bar{B}_{s_1,n-1} v_{s_1 v_j} + ((\bar{B}_{s_2,n-1} - 1) v_{s_2 v_j} + \bar{B}_{s_3,n-1} v_{s_3 v_j}) v_{v_j} c_{v_j} \\ \bar{B}_{\tilde{y}_j,n} &= [(\tilde{e}_2 + L \cdot h_{\tilde{y}} + \tilde{e}_{10} + \bar{B}_{\tilde{y},n-1}) - (\rho - 1) \tilde{e}_1]^\top \tilde{\Phi}_y \tilde{e}_j \\ &+ \frac{(\alpha - \rho) p_{v_j} \phi_{v_j}}{1 - \alpha p_{v_j} c_{v_j}} + \frac{\alpha}{2} (\alpha - \rho) (P_{\tilde{y}} + \tilde{e}_1)^\top \tilde{\Sigma}_y [\tilde{\mathbf{I}} \odot (\tilde{\mathbf{I}}^\top \otimes \tilde{\mathbf{B}}_j)] \tilde{\Sigma}_y^\top (P_{\tilde{y}} + \tilde{e}_1) \\ &- \frac{1}{2} [(\rho - 1) \tilde{e}_1 + (\alpha - \rho) (P_{\tilde{y}} + \tilde{e}_1) - (\tilde{e}_2 + L \cdot h_{\tilde{y}} + \tilde{e}_{10} + \bar{B}_{\tilde{y},n-1})]^\top \tilde{\Sigma}_y [\tilde{\mathbf{I}} \odot (\tilde{\mathbf{I}}^\top \otimes \tilde{\mathbf{B}}_j)] \\ &\times \tilde{\Sigma}_y^\top [(\rho - 1) \tilde{e}_1 + (\alpha - \rho) (P_{\tilde{y}} + \tilde{e}_1) - (\tilde{e}_2 + L \cdot h_{\tilde{y}} + \tilde{e}_{10} + \bar{B}_{\tilde{y},n-1})] \\ &- \frac{[(\alpha - \rho) p_{v_j} - L \cdot h_{v_j} - \bar{B}_{v_j,n-1} + \bar{B}_{s_1,n-1} v_{s_1 v_j} + (\bar{B}_{s_2,n-1} - 1) v_{s_2 v_j} + \bar{B}_{s_3,n-1} v_{s_3 v_j}] \phi_{v_j}}{1 - [(\alpha - \rho) p_{v_j} - L \cdot h_{v_j} - \bar{B}_{v_j,n-1} + \bar{B}_{s_1,n-1} v_{s_1 v_j} + (\bar{B}_{s_2,n-1} - 1) v_{s_2 v_j} + \bar{B}_{s_3,n-1} v_{s_3 v_j}] c_{v_j}} \\ &+ (\bar{B}_{s_1,n-1} v_{s_1 v_j} + (\bar{B}_{s_2,n-1} - 1) v_{s_2 v_j} + \bar{B}_{s_3,n-1} v_{s_3 v_j}) \phi_{v_j} \end{aligned}$$

with initial conditions $\bar{A}_0 = 0$, $\bar{B}_{\tilde{y},0} = \mathbf{0}$, and $\bar{B}_{v,0} = \mathbf{0}$, and where \otimes defines the Kronecker product, \odot the Hadamar product, $\tilde{\mathbf{I}}$ is the identity matrix, $\tilde{\mathbf{1}}$ is a column vector of ones, \tilde{e}_i ($i = 1, 2, \dots, 11$) and e_{v_i} ($i = 1, 2$) are coordinate vectors with all elements equal to zero except element $i = 1$, \bar{m} is defined in Equation (B.3), and the column vectors $\tilde{\mathbf{A}}$ and $\tilde{\mathbf{B}}_j$ are defined in Equation (C.3). It follows naturally that the term structure of risky LIBOR rates is given by:

$$\ell_t^n = n^{-1} \left(\bar{A}_n + \bar{B}_{\tilde{y},n}^\top \tilde{y}_t + \bar{B}_{v,n}^\top v_t \right).$$

C.5. Term structure of IRS rates

To price IRS rates, we take into account the convenience yield $s_{1,t}$, bank risk $s_{2,t}$, and cost of collateral $s_{3,t}$, with dynamics defined in Equation (4). The formula for an n -period IRS rate is given by

$$IRS_t^n = \left(\sum_{j=1}^{n/\Delta} (\tilde{\Psi}_{j,t}^\ell - \Psi_{j,t}^\ell) \right) \left(\sum_{j=1}^{n/\Delta} \Psi_{j,t}^\ell \right)^{-1},$$

where the one-month LIBOR rate is defined as $\ell_t = \tilde{y}_t^1 + s_{1,t} + s_{2,t}$, Δ defines the time interval between two successive coupon periods, and where the expressions for $\tilde{\Psi}^\ell$ and Ψ^ℓ are defined as

$$\tilde{\Psi}_{n,t}^\ell = E_t \left[e^{m_t, t+n\Delta + s_{3,t+n\Delta}} e^{\Delta \cdot \ell_{t+(n-1)\Delta}^3} \right] \quad \text{and} \quad \Psi_{n,t}^\ell = E_t \left[e^{m_t, t+n + s_{3,t+n}} \right].$$

To derive closed-form solutions for the term structure of IRS rates, we conjecture that the expressions for $\tilde{\Psi}^\ell$ and Ψ^ℓ are exponentially affine in the extended state vector $\tilde{x}_t = [y_t^\top, s^\top, v_t^\top]^\top = [\tilde{y}_t^\top, v_t^\top]^\top$:

$$\tilde{\Psi}_{n,t}^\ell = e^{\tilde{A}_n^\ell + \tilde{B}_{\tilde{y},n}^{\ell\top} \tilde{y}_t + \tilde{B}_{v,n}^{\ell\top} v_t} \quad \text{and} \quad \Psi_{n,t}^\ell = e^{A_n^\ell + B_{\tilde{y},n}^{\ell\top} \tilde{y}_t + B_{v,n}^{\ell\top} v_t}.$$

It can be shown that for all n , the scalars \tilde{A}_n^ℓ and A_n^ℓ , and the components of the column vectors $\tilde{B}_{\tilde{y},n}^\ell$ and $B_{\tilde{y},n}^\ell$ for $j = 1, 2, \dots, 11$, and $\tilde{B}_{v_j,n}^\ell$ $B_{v_j,n}^\ell$ for $j = 1, 2$, follow the same recursion and are given by

$$\begin{aligned} A_n^\ell &= A_{n-1}^\ell + \bar{m} - \left[\tilde{e}_2 - B_{\tilde{y},n-1}^\ell - \tilde{e}_{11} \right]^\top \tilde{\mu}_{\tilde{y}} - \sum_{j=1}^2 v_{v_j} \log \left(1 - \left[(\alpha - \rho) p_{v_j} + B_{v_j,n-1}^\ell \right. \right. \\ &\quad \left. \left. + B_{s_1,n-1}^\ell v_{s_1 v_j} + B_{s_2,n-1}^\ell v_{s_2 v_j} + \left(B_{s_3,n-1}^\ell + 1 \right) v_{s_3 v_j} \right] c_{v_j} \right) \\ &\quad + \frac{1}{2} \left[(\rho - 1) \tilde{e}_1 + (\alpha - \rho) (P_{\tilde{y}} + \tilde{e}_1) - \left[\tilde{e}_2 - B_{\tilde{y},n-1}^\ell - \tilde{e}_{11} \right] \right]^\top \tilde{\Sigma}_{\tilde{y}} \left[\tilde{\mathbf{I}} \odot \left(\tilde{\mathbf{I}}^\top \otimes \tilde{\mathbf{A}} \right) \right] \\ &\quad \times \tilde{\Sigma}_{\tilde{y}}^\top \left[(\rho - 1) \tilde{e}_1 + (\alpha - \rho) (P_{\tilde{y}} + \tilde{e}_1) - \left[\tilde{e}_2 - B_{\tilde{y},n-1}^\ell - \tilde{e}_{11} \right] \right] \\ &\quad - \sum_{j=1}^2 \left(B_{s_1,n-1}^\ell v_{s_1 v_j} + B_{s_2,n-1}^\ell v_{s_2 v_j} + \left(B_{s_3,n-1}^\ell + 1 \right) v_{s_3 v_j} \right) v_{v_j} c_{v_j} \\ B_{\tilde{y}_j,n}^\ell &= \left[(\rho - 1) \tilde{e}_1 - \left[\tilde{e}_2 - B_{\tilde{y},n-1}^\ell - \tilde{e}_{11} \right] \right]^\top \tilde{\Phi}_{\tilde{y}} \tilde{e}_j \\ B_{v_j,n}^\ell &= \left[(\rho - 1) \tilde{e}_1 - \left[\tilde{e}_2 - B_{\tilde{y},n-1}^\ell - \tilde{e}_{11} \right] \right]^\top \tilde{\Phi}_{\tilde{y}v} e_{v_j} \\ &\quad - \frac{(\alpha - \rho) p_{v_j} \phi_{v_j}}{1 - \alpha p_{v_j} c_{v_j}} - \frac{\alpha}{2} (\alpha - \rho) (P_{\tilde{y}} + \tilde{e}_1)^\top \tilde{\Sigma}_{\tilde{y}} \left[\tilde{\mathbf{I}} \odot \left(\tilde{\mathbf{I}}^\top \otimes \tilde{\mathbf{B}}_j \right) \right] \tilde{\Sigma}_{\tilde{y}}^\top (P_{\tilde{y}} + \tilde{e}_1) \\ &\quad + \frac{1}{2} \left[(\rho - 1) \tilde{e}_1 + (\alpha - \rho) (P_{\tilde{y}} + \tilde{e}_1) - \left[\tilde{e}_2 - B_{\tilde{y},n-1}^\ell - \tilde{e}_{11} \right] \right]^\top \tilde{\Sigma}_{\tilde{y}} \left[\tilde{\mathbf{I}} \odot \left(\tilde{\mathbf{I}}^\top \otimes \tilde{\mathbf{B}}_j \right) \right] \\ &\quad \times \tilde{\Sigma}_{\tilde{y}}^\top \left[(\rho - 1) \tilde{e}_1 + (\alpha - \rho) (P_{\tilde{y}} + \tilde{e}_1) - \left[\tilde{e}_2 - B_{\tilde{y},n-1}^\ell - \tilde{e}_{11} \right] \right] \\ &\quad + \frac{\left[(\alpha - \rho) p_{v_j} + B_{v_j,n-1}^\ell + B_{s_1,n-1}^\ell v_{s_1 v_j} + B_{s_2,n-1}^\ell v_{s_2 v_j} + \left(B_{s_3,n-1}^\ell + 1 \right) v_{s_3 v_j} \right] \phi_{v_j}}{1 - \left[(\alpha - \rho) p_{v_j} + B_{v_j,n-1}^\ell + B_{s_1,n-1}^\ell v_{s_1 v_j} + B_{s_2,n-1}^\ell v_{s_2 v_j} + \left(B_{s_3,n-1}^\ell + 1 \right) v_{s_3 v_j} \right] c_{v_j}} \\ &\quad - \left(B_{s_1,n-1}^\ell v_{s_1 v_j} + B_{s_2,n-1}^\ell v_{s_2 v_j} + \left(B_{s_3,n-1}^\ell + 1 \right) v_{s_3 v_j} \right) \phi_{v_j}, \end{aligned}$$

where \otimes defines the Kronecker product, \odot the Hadamar product, $\tilde{\mathbf{I}}$ is the identity matrix, $\tilde{\mathbf{1}}$ is a column vector of ones, \tilde{e}_i ($i = 1, 2, \dots, 11$) and e_{v_i} ($i = 1, 2$) are coordinate vectors with all elements equal to zero except element $i = 1$, \bar{m} is defined in Equation (B.3), and the column vectors $\tilde{\mathbf{A}}$ and $\tilde{\mathbf{B}}_j$ are defined in Equation (C.3).

While the expressions $\tilde{\Psi}^\ell$ and Ψ^ℓ have the same recursions, they have different starting conditions. For $\Psi_{n,t}^\ell$, the recursion starts at 0, with initial condition given by $A_0^\ell = 0$, and all elements of $B_{\tilde{y},0}^\ell = 0$ and $B_{v,0}^\ell = 0$, except for $B_{s_3,0}^\ell = 1$. For $\tilde{\Psi}_{n,t}^\ell$, the recursion starts at $n = \Delta$ (i.e., $\Delta = 3$ for quarterly coupon payments), with starting condition given by:

$$\tilde{\Psi}_{\Delta,t}^\ell = e^{\Delta \cdot \ell_t^3} E_t \left[e^{m_t, t+\Delta + s_{3,t+\Delta}} \right].$$

Since $\log E_t \left[e^{m_t, t+\Delta + s_{3,t+\Delta}} \right] = A_\Delta^\ell + B_{\tilde{y},\Delta}^{\ell\top} \tilde{y}_t + B_{v,\Delta}^{\ell\top} v_t$, and $\ell_t^3 = \frac{1}{3} (\bar{A}_3 + \bar{B}_{\tilde{y},3}^\top \tilde{y}_t + \bar{B}_{v,3}^\top v_t)$, the initial

condition for $\tilde{\Psi}_{n,t}^\ell$ is given by:

$$\tilde{\Psi}_{\Delta,t}^\ell = e^{\frac{\Delta}{3}\bar{A}_3 + \frac{\Delta}{3}\bar{B}_{\bar{y},3}^\top \bar{y}_t + \frac{\Delta}{3}\bar{B}_{v,3}^\top v_t + A_\Delta^\ell + B_{\bar{y},\Delta}^{\ell\top} \bar{y}_t + B_{v,\Delta}^{\ell\top} v_t} = e^{A_\Delta^{\ell init} + (B_{\bar{y},\Delta}^{\ell init})^\top \bar{y}_t + (B_{v,\Delta}^{\ell init})^\top v_t},$$

where the constant $A_\Delta^{\ell init}$ and the elements of the column vectors $B_{\bar{y},\Delta}^{\ell init}$ for $j = 1, 2, \dots, 11$ and $B_{v,\Delta}^{\ell init}$ for $j = 1, 2$ are given by:

$$\begin{aligned} A_\Delta^{\ell init} &= \frac{\Delta}{3}\bar{A}_3 + A_\Delta^\ell \\ B_{\bar{y},\Delta}^{\ell init} &= \frac{\Delta}{3}\bar{B}_{\bar{y},3} + B_{\bar{y},\Delta}^\ell \\ B_{v,\Delta}^{\ell init} &= \frac{\Delta}{3}\bar{B}_{v,3} + B_{v,\Delta}^\ell. \end{aligned}$$

C.6. Term structure of OIS rates

To price OIS rates, we take into account the convenience yield $s_{1,t}$ and cost of collateral $s_{3,t}$, with dynamics defined in Equation (4). The formula for an n -period OIS rate is given by

$$OIS_t^n = \left(\sum_{j=1}^{n/\Delta} (\tilde{\Psi}_{j,t}^o - \Psi_{j,t}^o) \right) \left(\sum_{j=1}^{n/\Delta} \Psi_{j,t}^o \right)^{-1},$$

where the one-month OIS rate is defined as $o_t = \tilde{y}_t^1 + s_{1,t}$, Δ defines the time interval between two successive coupon periods, and where the expressions for $\tilde{\Psi}^o$ and Ψ^o are defined as

$$\tilde{\Psi}_{n,t}^o = E_t \left[e^{m_{t,t+n} + s_{3,t+n}} \exp \left(\sum_{j=1}^{\Delta} o_{t+n\Delta-j} \right) \right] \quad \text{and} \quad \Psi_{n,t}^o = E_t [e^{m_{t,t+n} + s_{3,t+n}}].$$

To derive closed-form solutions for the term structure of OIS rates, we conjecture that the expressions for $\tilde{\Psi}^o$ and Ψ^o are exponentially affine in the extended state vector $\tilde{x}_t = [y_t^\top, s^\top, v_t^\top]^\top = [\tilde{y}_t^\top, v_t^\top]^\top$:

$$\tilde{\Psi}_{n,t}^o = e^{\tilde{A}_n^o + \tilde{B}_{\bar{y},n}^o \tilde{y}_t + \tilde{B}_{v,n}^o v_t} \quad \text{and} \quad \Psi_{n,t}^o = e^{A_n^\ell + B_{\bar{y},n}^{\ell\top} \tilde{y}_t + B_{v,n}^{\ell\top} v_t}.$$

It can be shown that for all n , the scalars \tilde{A}_n^o and A_n^o , and the components of the column vectors $\tilde{B}_{\bar{y},n}^o$ and $B_{\bar{y},n}^o$ for $j = 1, 2, \dots, 11$, and $\tilde{B}_{v,n}^o$ $B_{v,j,n}^o$ for $j = 1, 2$, follow the same recursion and are given by

$$\begin{aligned} A_n^o &= A_{n-1}^o + \bar{m} - [\tilde{e}_2 - B_{\bar{y},n-1}^o - \tilde{e}_{11}]^\top \tilde{\mu}_{\bar{y}} - \sum_{j=1}^2 v_{v_j} \log \left(1 - [(\alpha - \rho) p_{v_j} + B_{v_j,n-1}^o \right. \\ &\quad \left. + B_{s_1,n-1}^o v_{s_1 v_j} + B_{s_2,n-1}^o v_{s_2 v_j} + (B_{s_3,n-1}^o + 1) v_{s_3 v_j}] c_{v_j} \right) \\ &\quad + \frac{1}{2} [(\rho - 1) \tilde{e}_1 + (\alpha - \rho) (P_{\bar{y}} + \tilde{e}_1) - [\tilde{e}_2 - B_{\bar{y},n-1}^o - \tilde{e}_{11}]]^\top \tilde{\Sigma}_{\bar{y}} [\tilde{\mathbf{I}} \odot (\tilde{\mathbf{I}}^\top \otimes \tilde{\mathbf{A}})] \\ &\quad \times \tilde{\Sigma}_{\bar{y}}^\top [(\rho - 1) \tilde{e}_1 + (\alpha - \rho) (P_{\bar{y}} + \tilde{e}_1) - [\tilde{e}_2 - B_{\bar{y},n-1}^o - \tilde{e}_{11}]] \\ &\quad - \sum_{j=1}^2 (B_{s_1,n-1}^o v_{s_1 v_j} + B_{s_2,n-1}^o v_{s_2 v_j} + (B_{s_3,n-1}^o + 1) v_{s_3 v_j}) v_{v_j} c_{v_j} \\ B_{\bar{y},n}^o &= [(\rho - 1) \tilde{e}_1 - [\tilde{e}_2 - B_{\bar{y},n-1}^o - \tilde{e}_{11}]]^\top \tilde{\Phi}_{\bar{y}} \tilde{e}_j \\ &\quad - \frac{(\alpha - \rho) p_{v_j} \phi_{v_j}}{1 - \alpha p_{v_j} c_{v_j}} - \frac{\alpha}{2} (\alpha - \rho) (P_{\bar{y}} + \tilde{e}_1)^\top \tilde{\Sigma}_{\bar{y}} [\tilde{\mathbf{I}} \odot (\tilde{\mathbf{I}}^\top \otimes \mathbf{B}_j)] \tilde{\Sigma}_{\bar{y}}^\top (P_{\bar{y}} + \tilde{e}_1) \\ &\quad + \frac{1}{2} [(\rho - 1) \tilde{e}_1 + (\alpha - \rho) (P_{\bar{y}} + \tilde{e}_1) - [\tilde{e}_2 - B_{\bar{y},n-1}^o - \tilde{e}_{11}]]^\top \tilde{\Sigma}_{\bar{y}} [\tilde{\mathbf{I}} \odot (\tilde{\mathbf{I}}^\top \otimes \mathbf{B}_j)] \\ &\quad \times \tilde{\Sigma}_{\bar{y}}^\top [(\rho - 1) \tilde{e}_1 + (\alpha - \rho) (P_{\bar{y}} + \tilde{e}_1) - [\tilde{e}_2 - B_{\bar{y},n-1}^o - \tilde{e}_{11}]] \end{aligned}$$

$$\begin{aligned}
& + \frac{\left[(\alpha - \rho) p v_j + B_{v_j, n-1}^o + B_{s_1, n-1}^o v_{s_1 v_j} + B_{s_2, n-1}^o v_{s_2 v_j} + (B_{s_3, n-1}^o + 1) v_{s_3 v_j} \right] \phi v_j}{1 - \left[(\alpha - \rho) p v_j + B_{v_j, n-1}^o + B_{s_1, n-1}^o v_{s_1 v_j} + B_{s_2, n-1}^o v_{s_2 v_j} + (B_{s_3, n-1}^o + 1) v_{s_3 v_j} \right] c v_j} \\
& - \left(B_{s_1, n-1}^o v_{s_1 v_j} + B_{s_2, n-1}^o v_{s_2 v_j} + (B_{s_3, n-1}^o + 1) v_{s_3 v_j} \right) \phi v_j
\end{aligned}$$

where \otimes defines the Kronecker product, \odot the Hadamar product, $\tilde{\mathbf{I}}$ is the identity matrix, $\tilde{\mathbf{1}}$ is a column vector of ones, \tilde{e}_i ($i = 1, 2, \dots, 11$) and e_{v_i} ($i = 1, 2$) are coordinate vectors with all elements equal to zero except element $i = 1$, \tilde{m} is defined in Equation (B.3), and the column vectors $\tilde{\mathbf{A}}$ and $\tilde{\mathbf{B}}_j$ are defined in Equation (C.3).

While the expressions $\tilde{\Psi}^o$ and Ψ^o have the same recursions, they have different starting conditions. For $\Psi_{n,t}^o$, the recursion starts at 0, with initial condition given by $A_0^o = 0$, and all elements of $B_{y,0}^o = 0$ and $B_{v,0}^o = 0$, except for $B_{s_3,0}^o = 1$. For $\tilde{\Psi}_{n,t}^o$, the recursion starts at $n = \Delta$ (i.e., $\Delta = 3$ for quarterly coupon payments), with starting condition given by:

$$\tilde{\Psi}_{\Delta,t}^o = E_t \left[e^{m_{t,t+\Delta} + s_{3,t+\Delta} + \sum_{j=1}^{\Delta} o_{t+\Delta-j}} \right] = e^{\tilde{A}_{\Delta}^o + \tilde{B}_{y,\Delta}^{o\top} \tilde{y}_t + \tilde{B}_{v,\Delta}^{o\top} v_t},$$

where the expressions for \tilde{A}_{Δ}^o , $\tilde{B}_{y,\Delta}^o$, and $\tilde{B}_{v,\Delta}^o$ are obtained recursively. Observe that

$$\tilde{\Psi}_{\Delta,t}^o = e^{o_t} E_t \left[e^{m_{t,t+1} + s_{3,t+1}} e^{o_{t+1}} E_{t+1} \left[e^{m_{t+1,t+2} + s_{3,t+2}} \dots e^{o_{t+\Delta-1}} E_{t+\Delta-1} \left[e^{m_{t+\Delta-1,t+\Delta} + s_{3,t+\Delta}} \right] \right] \right],$$

and define $\tilde{\Psi}_{n,t}^o$ to be equal to $\tilde{\Psi}_{n,t}^{o_{init}}$ characterized as

$$\tilde{\Psi}_{n,t}^{o_{init}} = E_t \left[e^{o_t + m_{t,t+1} + s_{3,t+1}} \tilde{\Psi}_{n-1,t+1}^{o_{init}} \right],$$

It can be shown that for all $n = 1, 2, 3, \dots, \Delta$

$$\tilde{\Psi}_{n,t}^{o_{init}} = e^{A_n^{o_{init}} + B_{y,n}^{o_{init}\top} \tilde{y}_t + B_{v,n}^{o_{init}\top} v_t}, \quad (\text{C.5})$$

where the scalar $A_n^{o_{init}}$ and components of the column vectors $B_{y,n}^{o_{init}}$ for $j = 1, 2, \dots, 11$ (except for $B_{s_1,n}^{o_{init}}$) and $B_{v_j,n}^{o_{init}}$ are given by:

$$\begin{aligned}
A_n^{o_{init}} &= \tilde{A}_1 + A_{n-1}^{o_{init}} + \tilde{m} - \left[\tilde{e}_2 - B_{y,n-1}^{o_{init}} - \tilde{e}_{11} \right]^\top \tilde{\mu}_{\tilde{y}} - \sum_{j=1}^2 v_{v_j} \log \left(1 - \left[(\alpha - \rho) p v_j + B_{v_j, n-1}^{o_{init}} \right. \right. \\
&\quad \left. \left. + B_{s_1, n-1}^{o_{init}} v_{s_1 v_j} + B_{s_2, n-1}^{o_{init}} v_{s_2 v_j} + (B_{s_3, n-1}^{o_{init}} + 1) v_{s_3 v_j} \right] c v_j \right) \\
&+ \frac{1}{2} \left[(\rho - 1) \tilde{e}_1 + (\alpha - \rho) (P_{\tilde{y}} + \tilde{e}_1) - \left[\tilde{e}_2 - B_{y, n-1}^{o_{init}} - \tilde{e}_{11} \right] \right]^\top \tilde{\Sigma}_{\tilde{y}} \left[\tilde{\mathbf{I}} \odot \left(\tilde{\mathbf{1}}^\top \otimes \tilde{\mathbf{A}} \right) \right] \\
&\times \tilde{\Sigma}_{\tilde{y}}^\top \left[(\rho - 1) \tilde{e}_1 + (\alpha - \rho) (P_{\tilde{y}} + \tilde{e}_1) - \left[\tilde{e}_2 - B_{y, n-1}^{o_{init}} - \tilde{e}_{11} \right] \right] \\
&- \sum_{j=1}^2 \left(B_{s_1, n-1}^{o_{init}} v_{s_1 v_j} + B_{s_2, n-1}^{o_{init}} v_{s_2 v_j} + (B_{s_3, n-1}^{o_{init}} + 1) v_{s_3 v_j} \right) v_{v_j} c v_j \\
B_{y_j, n}^{o_{init}} &= \left[(\rho - 1) \tilde{e}_1 - \left[\tilde{e}_2 - B_{y, n-1}^{o_{init}} - \tilde{e}_{11} \right] \right]^\top \tilde{\Phi}_{\tilde{y}} \tilde{e}_1 + \tilde{B}_{y_j, 1} \\
B_{s_1, n}^{o_{init}} &= \left[(\rho - 1) \tilde{e}_1 - \left[\tilde{e}_2 - B_{y, n-1}^{o_{init}} - \tilde{e}_{11} \right] \right]^\top \tilde{\Phi}_{\tilde{y}} \tilde{e}_9 + \tilde{B}_{s_1, 1} + 1 \\
B_{v_j, n}^{o_{init}} &= \left[(\rho - 1) \tilde{e}_1 - \left[\tilde{e}_2 - B_{y, n-1}^{o_{init}} - \tilde{e}_{11} \right] \right]^\top \tilde{\Phi}_{\tilde{y}v} e_{v_j} + \tilde{B}_{v_j, 1} \\
&- \frac{(\alpha - \rho) p v_j \phi v_j}{1 - \alpha p v_j c v_j} - \frac{\alpha}{2} (\alpha - \rho) (P_{\tilde{y}} + \tilde{e}_1)^\top \tilde{\Sigma}_{\tilde{y}} \left[\tilde{\mathbf{I}} \odot \left(\tilde{\mathbf{1}}^\top \otimes \mathbf{B}_j \right) \right] \tilde{\Sigma}_{\tilde{y}}^\top (P_{\tilde{y}} + \tilde{e}_1)
\end{aligned}$$

$$\begin{aligned}
& + \frac{1}{2} \left[(\rho - 1) \tilde{e}_1 + (\alpha - \rho) (P_{\tilde{y}} + \tilde{e}_1) - \left[\tilde{e}_2 - B_{\tilde{y},n-1}^{o_{init}} - \tilde{e}_{11} \right] \right]^\top \tilde{\Sigma}_{\tilde{y}} \left[\tilde{\mathbf{I}} \odot \left(\tilde{\mathbf{I}}^\top \otimes \mathbf{B}_j \right) \right] \\
& \times \tilde{\Sigma}_{\tilde{y}}^\top \left[(\rho - 1) \tilde{e}_1 + (\alpha - \rho) (P_{\tilde{y}} + \tilde{e}_1) - \left[\tilde{e}_2 - B_{\tilde{y},n-1}^{o_{init}} - \tilde{e}_{11} \right] \right] \\
& + \frac{\left[(\alpha - \rho) p_{v_j} + B_{v_j,j-1}^{o_{init}} + B_{s_1,n-1}^{o_{init}} v_{s_1 v_j} + B_{s_2,n-1}^{o_{init}} v_{s_2 v_j} + (B_{s_3,n-1}^{o_{init}} + 1) v_{s_3 v_j} \right] \phi_{v_j}}{1 - \left[(\alpha - \rho) p_{v_j} + B_{v_j,n-1}^{o_{init}} + B_{s_1,n-1}^{o_{init}} v_{s_1 v_j} + B_{s_2,n-1}^{o_{init}} v_{s_2 v_j} + (B_{s_3,n-1}^{o_{init}} + 1) v_{s_3 v_j} \right] c_{v_j}} \\
& - \left(B_{s_1,n-1}^{o_{init}} v_{s_1 v_j} + B_{s_2,n-1}^{o_{init}} v_{s_2 v_j} + (B_{s_3,n-1}^{o_{init}} + 1) v_{s_3 v_j} \right) \phi_{v_j},
\end{aligned}$$

with starting condition $\tilde{\Psi}_{1,t}^{o_{init}} = e^{o_t} E_t [e^{m_{t,t+1} + s_{3,t+1}}]$. Since $E_t [e^{m_{t,t+1} + s_{3,t+1}}] = \Psi_{1,t}^o = e^{A_1^o + B_1^o \tilde{x}_t}$, $o_t = \tilde{y}_t^1 + s_{1,t}$, with $\tilde{y}_t^1 = \tilde{A}_1 + \tilde{B}_1^\top \tilde{x}_t$, we have that:

$$\begin{aligned}
\tilde{\Psi}_{1,t}^{o_{init}} & = e^{o_t} E_t [e^{m_{t,t+1} + s_{3,t+1}}] e^{\tilde{A}_1 + A_1^o + (\tilde{B}_{\tilde{y},1} + B_{\tilde{y},1}^o + \tilde{e}_9)^\top \tilde{y}_t + (\tilde{B}_{v,1} + B_{v,1}^o)^\top v_t} \\
& = e^{A_1^{o_{init}} + (B_{\tilde{y},1}^{o_{init}})^\top \tilde{x}_t + (B_{v,1}^{o_{init}})^\top v_t},
\end{aligned}$$

where the constant $A_1^{o_{init}}$ and the elements of the column vectors $B_{\tilde{y},j,1}^{o_{init}}$ for $j = 1, 2, \dots, 11$ (except for $B_{s_1,1}^{o_{init}}$) and $B_{v,j,1}^{o_{init}}$ for $j = 1, 2$ are given by:

$$\begin{aligned}
A_1^{o_{init}} & = \tilde{A}_1 + A_1^o \\
B_{\tilde{y},j,1}^{o_{init}} & = \tilde{B}_{\tilde{y},j,1} + B_{\tilde{y},j,1}^o \\
B_{s_1,1}^{o_{init}} & = \tilde{B}_{s_1,1} + B_{s_1,1}^o + 1 \\
B_{v,j,1}^{o_{init}} & = \tilde{B}_{v,j,1} + B_{v,j,1}^o.
\end{aligned}$$

C.7. Term structure of CDS premiums

To price CDS premiums, we take into account the cost of collateral $s_{3,t}$, with dynamics defined in Equation (4), the hazard rate defined in Equation (C.1), and the corresponding survival probabilities defined in Equation (C.2). The formula for an n -period CDS premium is given by

$$CDS_t^n = L \cdot \left(\sum_{j=1}^n (\tilde{\Psi}_{j,t}^c - \Psi_{j,t}^c) \right) \left(\sum_{j=1}^{n/\Delta} \Psi_{j\Delta,t}^c + \sum_{j=1}^n \left(\frac{j}{\Delta} - \lfloor \frac{j}{\Delta} \rfloor \right) (\tilde{\Psi}_{j,t}^c - \Psi_{j,t}^c) \right)^{-1},$$

where the floor function $\lfloor \cdot \rfloor$ rounds to the nearest lower integer, Δ defines the time interval between two successive coupon periods, and where the expressions for $\tilde{\Psi}^c$ and Ψ^c are defined as

$$\tilde{\Psi}_{n,t}^c = E_t \left[e^{m_{t,t+n} + s_{3,t+n}} \frac{\mathcal{S}_{t+n-1}}{\mathcal{S}_t} \right] \quad \text{and} \quad \Psi_{n,t}^c = E_t \left[e^{m_{t,t+n} + s_{3,t+n}} \frac{\mathcal{S}_{t+n}}{\mathcal{S}_t} \right].$$

The law of iterated expectations implies that $\tilde{\Psi}_{j,t}^c$ and $\Psi_{j,t}^c$ satisfy the recursions

$$\tilde{\Psi}_{n,t}^c = E_t \left[e^{m_{t,t+1} + s_{3,t+1}} (1 - \mathcal{H}_{t+1}) \tilde{\Psi}_{n-1,t+1}^c \right], \quad \Psi_{n,t}^c = E_t \left[e^{m_{t,t+1} + s_{3,t+1}} (1 - \mathcal{H}_{t+1}) \Psi_{n-1,t+1}^c \right],$$

starting at $n = 1$ for $\tilde{\Psi}_{n,t}^c$ and at $n = 0$ for $\Psi_{n,t}^c$. To evaluate the expressions for $\tilde{\Psi}^c$ and Ψ^c , we conjecture that they are exponentially affine functions of the extended state vector \tilde{x}_t :

$$\tilde{\Psi}_{n,t}^c = e^{\tilde{A}_n^c + (\tilde{B}_{\tilde{y},n}^c)^\top \tilde{y}_t + (\tilde{B}_{v,n}^c)^\top v_t} \quad \text{and} \quad \Psi_{n,t}^c = e^{A_n^c + (B_{\tilde{y},n}^c)^\top \tilde{y}_t + (B_{v,n}^c)^\top v_t}.$$

It can be shown that for all n , the scalars \tilde{A}_n^c and A_n^c , and the components of the column vectors $\tilde{B}_{\tilde{y},n}^c$ and $B_{\tilde{y},n}^c$ for $j = 1, 2, \dots, 11$, and $\tilde{B}_{v_j,n}^c$ for $j = 1, 2$, follow the same recursion and are given by

$$\begin{aligned}
\tilde{A}_n^c &= \tilde{A}_{n-1}^c - h + \tilde{m} - \left[\tilde{e}_2 + h_{\tilde{y}} - \tilde{B}_{\tilde{y},n-1}^c - \tilde{e}_{11} \right]^\top \tilde{\mu}_{\tilde{y}} \\
&- \sum_{j=1}^2 v_{v_j} \log \left(1 - \left[(\alpha - \rho) p_{v_j} - h_{v_j} + \tilde{B}_{v_j,n-1}^c \right. \right. \\
&\quad \left. \left. + \tilde{B}_{s_1,n-1}^c v_{s_1 v_j} + \tilde{B}_{s_2,n-1}^c v_{s_2 v_j} + \left(\tilde{B}_{s_3,n-1}^c + 1 \right) v_{s_3 v_j} \right] c_{v_j} \right) \\
&+ \frac{1}{2} \left[(\rho - 1) \tilde{e}_1 + (\alpha - \rho) (P_{\tilde{y}} + \tilde{e}_1) - \left(\tilde{e}_2 + h_{\tilde{y}} - \tilde{B}_{\tilde{y},n-1}^c - \tilde{e}_{11} \right) \right]^\top \tilde{\Sigma}_{\tilde{y}} \left[\tilde{\mathbf{I}} \odot \left(\tilde{\mathbf{I}}^\top \otimes \tilde{\mathbf{A}} \right) \right] \\
&\times \tilde{\Sigma}_{\tilde{y}}^\top \left[(\rho - 1) \tilde{e}_1 + (\alpha - \rho) (P_{\tilde{y}} + \tilde{e}_1) - \left(\tilde{e}_2 + h_{\tilde{y}} - \tilde{B}_{\tilde{y},n-1}^c - \tilde{e}_{11} \right) \right] \\
&- \sum_{j=1}^2 \left(\tilde{B}_{s_1,n-1}^c v_{s_1 v_j} + \tilde{B}_{s_2,n-1}^c v_{s_2 v_j} + \left(\tilde{B}_{s_3,n-1}^c + 1 \right) v_{s_3 v_j} \right) v_{v_j} c_{v_j} \\
\tilde{B}_{\tilde{y},n}^c &= \left[(\rho - 1) \tilde{e}_1 - \left(\tilde{e}_2 + h_{\tilde{y}} - \tilde{B}_{\tilde{y},n-1}^c - \tilde{e}_{11} \right) \right]^\top \tilde{\Phi}_{\tilde{y}} \tilde{e}_j \\
&- \frac{(\alpha - \rho) p_{v_j} \phi_{v_j}}{1 - \alpha p_{v_j} c_{v_j}} - \frac{\alpha}{2} (\alpha - \rho) (P_{\tilde{y}} + \tilde{e}_1)^\top \tilde{\Sigma}_{\tilde{y}} \left[\tilde{\mathbf{I}} \odot \left(\tilde{\mathbf{I}}^\top \otimes \tilde{\mathbf{B}}_j \right) \right] \tilde{\Sigma}_{\tilde{y}}^\top (P_{\tilde{y}} + \tilde{e}_1) \\
&+ \frac{1}{2} \left[(\rho - 1) \tilde{e}_1 + (\alpha - \rho) (P_{\tilde{y}} + \tilde{e}_1) - \left(\tilde{e}_2 + h_{\tilde{y}} - \tilde{B}_{\tilde{y},n-1}^c - \tilde{e}_{11} \right) \right]^\top \tilde{\Sigma}_{\tilde{y}} \left[\tilde{\mathbf{I}} \odot \left(\tilde{\mathbf{I}}^\top \otimes \tilde{\mathbf{B}}_j \right) \right] \\
&\times \tilde{\Sigma}_{\tilde{y}}^\top \left[(\rho - 1) \tilde{e}_1 + (\alpha - \rho) (P_{\tilde{y}} + \tilde{e}_1) - \left(\tilde{e}_2 + h_{\tilde{y}} - \tilde{B}_{\tilde{y},n-1}^c - \tilde{e}_{11} \right) \right] \\
&+ \frac{\left[(\alpha - \rho) p_{v_j} - h_{v_j} + \tilde{B}_{v_j,n-1}^c + \tilde{B}_{s_1,n-1}^c v_{s_1 v_j} + \tilde{B}_{s_2,n-1}^c v_{s_2 v_j} + \left(\tilde{B}_{s_3,n-1}^c + 1 \right) v_{s_3 v_j} \right] \phi_{v_j}}{1 - \left[(\alpha - \rho) p_{v_j} - h_{v_j} + \tilde{B}_{v_j,n-1}^c + \tilde{B}_{s_1,n-1}^c v_{s_1 v_j} + \tilde{B}_{s_2,n-1}^c v_{s_2 v_j} + \left(\tilde{B}_{s_3,n-1}^c + 1 \right) v_{s_3 v_j} \right] c_{v_j}} \\
&- \left(\tilde{B}_{s_1,n-1}^c v_{s_1 v_j} + \tilde{B}_{s_2,n-1}^c v_{s_2 v_j} + \left(\tilde{B}_{s_3,n-1}^c + 1 \right) v_{s_3 v_j} \right) \phi_{v_j},
\end{aligned}$$

where \otimes defines the Kronecker product, \odot the Hadamar product, $\tilde{\mathbf{I}}$ is the identity matrix, $\tilde{\mathbf{1}}$ is a column vector of ones, \tilde{e}_i ($i = 1, 2, \dots, 11$) and e_{v_i} ($i = 1, 2$) are coordinate vectors with all elements equal to zero except element $i = 1$, \tilde{m} is defined in Equation (B.3), and the column vectors $\tilde{\mathbf{A}}$ and $\tilde{\mathbf{B}}_j$ are defined in Equation (C.3).

Even though the expressions for $\tilde{\Psi}^c$ and Ψ^c follow the same recursion, they have different initial conditions. The initial condition for Ψ^c is given by $\log \Psi_{0,t}^c = A_0^c + B_{\tilde{y},0}^{c\top} \tilde{y}_t + B_{v,0}^{c\top} v_t$, where the scalar $A_0^c = 0$ and the elements of the column vectors $B_{\tilde{y},0}^c = 0$ for $j = 1, 2, \dots, 11$, and $B_{v,0}^c = 0$ for $j = 1, 2$, except for $B_{s_3,0}^c = 1$.

The initial condition for $\tilde{\Psi}^c$ is given by:

$$\tilde{\Psi}_{1,t}^c = E_t \left[e^{m_t, t+1 + s_3, t+1} \right] = e^{\tilde{A}_1^c + \tilde{B}_{\tilde{y},1}^{c\top} \tilde{y}_t + \tilde{B}_{v,1}^{c\top} v_t},$$

where the scalar \tilde{A}_1^c and components of the column vectors $\tilde{B}_{\tilde{y},1}^c$ for $j = 1, 2, \dots, 11$ and $\tilde{B}_{v_j,1}^c$ for $j = 1, 2$ are given by:

$$\begin{aligned}
\tilde{A}_1^c &= \tilde{m} + [\tilde{e}_{11} - \tilde{e}_2]^\top \tilde{\mu}_{\tilde{y}} - \sum_{j=1}^2 v_{v_j} \log \left(1 - \left[(\alpha - \rho) p_{v_j} + v_{s_3 v_j} \right] c_{v_j} \right) - \sum_{j=1}^2 v_{s_3 v_j} v_{v_j} c_{v_j} \\
&+ \frac{1}{2} \left[(\rho - 1) \tilde{e}_1 + (\alpha - \rho) (P_{\tilde{y}} + \tilde{e}_1) + \tilde{e}_{11} - \tilde{e}_2 \right]^\top \tilde{\Sigma}_{\tilde{y}} \left[\tilde{\mathbf{I}} \odot \left(\tilde{\mathbf{I}}^\top \otimes \tilde{\mathbf{A}} \right) \right] \\
&\times \tilde{\Sigma}_{\tilde{y}}^\top \left[(\rho - 1) \tilde{e}_1 + (\alpha - \rho) (P_{\tilde{y}} + \tilde{e}_1) + \tilde{e}_{11} - \tilde{e}_2 \right] \\
\tilde{B}_{\tilde{y},1}^c &= \left[(\rho - 1) \tilde{e}_1 + \tilde{e}_{11} - \tilde{e}_2 \right]^\top \tilde{\Phi}_{\tilde{y}} \tilde{e}_j
\end{aligned}$$

$$\begin{aligned}
\tilde{B}_{v_j,1}^c &= [(\rho - 1)\tilde{e}_1 + \tilde{e}_{11} - \tilde{e}_2]^\top \tilde{\Phi}_{\tilde{y}v} e_{v_j} \\
&- \frac{(\alpha - \rho)p_{v_j}\phi_{v_j}}{1 - \alpha p_{v_j}c_{v_j}} - \frac{\alpha}{2}(\alpha - \rho)(P_{\tilde{y}} + \tilde{e}_1)^\top \tilde{\Sigma}_{\tilde{y}} \left[\tilde{\mathbf{I}} \odot \left(\tilde{\mathbf{I}}^\top \otimes \tilde{\mathbf{B}}_j \right) \right] \tilde{\Sigma}_{\tilde{y}}^\top (P_{\tilde{y}} + \tilde{e}_1) \\
&+ \frac{1}{2} [(\rho - 1)\tilde{e}_1 + (\alpha - \rho)(P_{\tilde{y}} + \tilde{e}_1) + \tilde{e}_{11} - e_2]^\top \tilde{\Sigma}_{\tilde{y}} \left[\tilde{\mathbf{I}} \odot \left(\tilde{\mathbf{I}}^\top \otimes \tilde{\mathbf{B}}_j \right) \right] \\
&\times \tilde{\Sigma}_{\tilde{y}}^\top [(\rho - 1)\tilde{e}_1 + (\alpha - \rho)(P_{\tilde{y}} + \tilde{e}_1) + \tilde{e}_{11} - \tilde{e}_2] + \frac{[(\alpha - \rho)p_{v_j} + v_{s_3v_j}]\phi_{v_j}}{1 - [(\alpha - \rho)p_{v_j} + v_{s_3v_j}]c_{v_j}} - v_{s_3v_j}\phi_{v_j}.
\end{aligned}$$

Appendix D. Estimation

We provide two different state-space representations. The first one, shown in Section D.1, is used when macroeconomic fundamentals are only used in the estimation. The second one, shown in Section D.2, is an extended state-space representation for which we can (potentially) jointly use macroeconomic fundamentals and asset data.

D.1. State-space representation

The underlying state transition dynamics run at a monthly frequency. We first provide the case in which all observables are available at the monthly frequency. The corresponding state-transition dynamics are shown in Section D.1.1 and the measurement equation is presented in Section D.1.2. In the presence of mixed-frequency observables, i.e., some observables are available at the quarterly frequency, we explain how to adjust the state space in Section D.1.3 with an illustrative example. Finally, in Section D.1.4, we explain the availability of data and provide our state-space representation that we estimate.

D.1.1. State transition dynamics

Define $x_t = [z_t^\top, w_t^\top, v_t^\top]^\top$. We describe the joint dynamics of x_t below

$$\begin{aligned}
\underbrace{\begin{bmatrix} z_{1,t+1} \\ z_{2,t+1} \\ z_{3,t+1} \\ z_{4,t+1} \\ w_{1,t+1} \\ w_{2,t+1} \\ w_{3,t+1} \\ w_{4,t+1} \\ v_{1,t+1} \\ v_{2,t+1} \end{bmatrix}}_{x_{t+1}} &= \underbrace{\begin{bmatrix} \mu_{z1} \\ \mu_{z2} \\ \mu_{z3} \\ \mu_{z4} \\ 0 \\ 0 \\ 0 \\ 0 \\ \nu_{v1}c_{v1} \\ \nu_{v2}c_{v2} \end{bmatrix}}_{\mu} + \underbrace{\begin{bmatrix} \phi_{z11} & \phi_{z12} & \phi_{z13} & \phi_{z14} & 1 & 0 & 0 & 0 & \phi_{zv11} & \phi_{zv12} \\ \phi_{z21} & \phi_{z22} & \phi_{z23} & \phi_{z24} & 0 & 1 & 0 & 0 & \phi_{zv21} & \phi_{zv22} \\ \phi_{z31} & \phi_{z32} & \phi_{z33} & \phi_{z34} & 0 & 0 & 1 & 0 & \phi_{zv31} & \phi_{zv32} \\ \phi_{z41} & \phi_{z42} & \phi_{z43} & \phi_{z44} & 0 & 0 & 0 & 1 & \phi_{zv41} & \phi_{zv42} \\ 0 & 0 & 0 & 0 & 0 & 0 & 0 & 0 & 0 & 0 \\ 0 & 0 & 0 & 0 & 0 & 0 & 0 & 0 & 0 & 0 \\ 0 & 0 & 0 & 0 & 0 & 0 & 0 & 0 & 0 & 0 \\ 0 & 0 & 0 & 0 & 0 & 0 & 0 & 0 & 0 & 0 \\ 0 & 0 & 0 & 0 & 0 & 0 & 0 & 0 & \phi_{v1} & 0 \\ 0 & 0 & 0 & 0 & 0 & 0 & 0 & 0 & 0 & \phi_{v2} \end{bmatrix}}_{\Phi} \underbrace{\begin{bmatrix} z_{1,t} \\ z_{2,t} \\ z_{3,t} \\ z_{4,t} \\ w_{1,t} \\ w_{2,t} \\ w_{3,t} \\ w_{4,t} \\ v_{1,t} \\ v_{2,t} \end{bmatrix}}_{x_t} \\
+ \underbrace{\begin{bmatrix} 1 & 0 & 0 & 0 & 0 & 0 & 0 & 0 & 0 & 0 \\ 0 & 1 & 0 & 0 & 0 & 0 & 0 & 0 & 0 & 0 \\ 0 & 0 & 1 & 0 & 0 & 0 & 0 & 0 & 0 & 0 \\ 0 & 0 & 0 & 1 & 0 & 0 & 0 & 0 & 0 & 0 \\ \theta_{w11} & \theta_{w12} & \theta_{w13} & \theta_{w14} & 0 & 0 & 0 & 0 & 0 & 0 \\ \theta_{w21} & \theta_{w22} & \theta_{w23} & \theta_{w24} & 0 & 0 & 0 & 0 & 0 & 0 \\ \theta_{w31} & \theta_{w32} & \theta_{w33} & \theta_{w34} & 0 & 0 & 0 & 0 & 0 & 0 \\ \theta_{w41} & \theta_{w42} & \theta_{w43} & \theta_{w44} & 0 & 0 & 0 & 0 & 0 & 0 \\ 0 & 0 & 0 & 0 & 0 & 0 & 0 & 0 & 1 & 0 \\ 0 & 0 & 0 & 0 & 0 & 0 & 0 & 0 & 0 & 1 \end{bmatrix}}_{\Sigma_A} \times \underbrace{\begin{bmatrix} \nu_{11} & 0 & 0 & 0 & 0 & 0 & 0 & 0 & 0 & 0 \\ \nu_{21} & \nu_{22} & 0 & 0 & 0 & 0 & 0 & 0 & 0 & 0 \\ \nu_{31} & \nu_{32} & \nu_{33} & 0 & 0 & 0 & 0 & 0 & 0 & 0 \\ \nu_{41} & \nu_{42} & \nu_{43} & \nu_{44} & 0 & 0 & 0 & 0 & 0 & 0 \\ 0 & 0 & 0 & 0 & 0 & 0 & 0 & 0 & 0 & 0 \\ 0 & 0 & 0 & 0 & 0 & 0 & 0 & 0 & 0 & 0 \\ 0 & 0 & 0 & 0 & 0 & 0 & 0 & 0 & 0 & 0 \\ 0 & 0 & 0 & 0 & 0 & 0 & 0 & 0 & 0 & 0 \\ 0 & 0 & 0 & 0 & 0 & 0 & 0 & 0 & 0 & 1 \\ 0 & 0 & 0 & 0 & 0 & 0 & 0 & 0 & 0 & 1 \end{bmatrix}}_{\Sigma_B}
\end{aligned}$$

$$\times \left(\underbrace{\begin{bmatrix} V_{1,t} & 0 & 0 & 0 & 0 & 0 & 0 & 0 & 0 & 0 \\ 0 & V_{2,t} & 0 & 0 & 0 & 0 & 0 & 0 & 0 & 0 \\ 0 & 0 & V_{3,t} & 0 & 0 & 0 & 0 & 0 & 0 & 0 \\ 0 & 0 & 0 & V_{4,t} & 0 & 0 & 0 & 0 & 0 & 0 \\ 0 & 0 & 0 & 0 & 0 & 0 & 0 & 0 & 0 & 0 \\ 0 & 0 & 0 & 0 & 0 & 0 & 0 & 0 & 0 & 0 \\ 0 & 0 & 0 & 0 & 0 & 0 & 0 & 0 & 0 & 0 \\ 0 & 0 & 0 & 0 & 0 & 0 & 0 & 0 & \omega_{v_1,t} & 0 \\ 0 & 0 & 0 & 0 & 0 & 0 & 0 & 0 & 0 & \omega_{v_2,t} \end{bmatrix}}_{V_t} \right)^{1/2} \underbrace{\begin{bmatrix} \varepsilon_{z_1,t+1} \\ \varepsilon_{z_2,t+1} \\ \varepsilon_{z_3,t+1} \\ \varepsilon_{z_4,t+1} \\ 0 \\ 0 \\ 0 \\ 0 \\ \eta_{v_1,t+1} \\ \eta_{v_2,t+1} \end{bmatrix}}_{\eta_{t+1}},$$

for $i \in \{1, 2, 3, 4\}$ and $j \in \{1, 2\}$,

$$V_{i,t} = a_i + b_{i1}v_{1,t} + b_{i2}v_{2,t}, \quad \omega_{v_j,t} = \nu_{v_j}c_{v_j}^2 + 2c_{v_j}\phi_{v_j}v_{j,t}$$

with $\varepsilon_{z_i,t+1} \sim \mathcal{N}(0, 1)$ and $\eta_{v_j,t+1}$ being a zero mean unit variance shock. In vector notations, we express the state space by

$$\underbrace{\begin{bmatrix} z_{t+1} \\ w_{t+1} \\ v_{t+1} \end{bmatrix}}_{x_{t+1}} = \underbrace{\begin{bmatrix} \mu_z \\ \mathbf{0} \\ \nu_v \odot c_v \end{bmatrix}}_{\mu} + \underbrace{\begin{bmatrix} \Phi_{z4 \times 4} & \mathbf{I}_{4 \times 4} & \Phi_{zv4 \times 2} \\ \mathbf{0}_{4 \times 4} & \mathbf{0}_{4 \times 4} & \mathbf{0}_{4 \times 2} \\ \mathbf{0}_{2 \times 4} & \mathbf{0}_{2 \times 4} & \Phi_{v2 \times 2} \end{bmatrix}}_{\Phi} \underbrace{\begin{bmatrix} z_t \\ w_t \\ v_t \end{bmatrix}}_{x_t} + \underbrace{\begin{bmatrix} \mathbf{I}_{4 \times 4} & \mathbf{0}_{4 \times 4} & \mathbf{0}_{4 \times 2} \\ \Theta_{w4 \times 4} & \mathbf{0}_{4 \times 4} & \mathbf{0}_{4 \times 2} \\ \mathbf{0}_{2 \times 4} & \mathbf{0}_{2 \times 4} & \mathbf{I}_{2 \times 2} \end{bmatrix}}_{\Sigma_A} \quad (\text{D.1})$$

$$\times \underbrace{\begin{bmatrix} \nu_{z4 \times 4} & \mathbf{0}_{4 \times 4} & \mathbf{0}_{4 \times 2} \\ \mathbf{0}_{4 \times 4} & \mathbf{0}_{4 \times 4} & \mathbf{0}_{4 \times 2} \\ \mathbf{0}_{2 \times 4} & \mathbf{0}_{2 \times 4} & \mathbf{I}_{2 \times 2} \end{bmatrix}}_{\Sigma_B} \times \left(\underbrace{\begin{bmatrix} V_{z,t4 \times 4} & \mathbf{0}_{4 \times 4} & \mathbf{0}_{4 \times 2} \\ \mathbf{0}_{4 \times 4} & \mathbf{0}_{4 \times 4} & \mathbf{0}_{4 \times 2} \\ \mathbf{0}_{2 \times 4} & \mathbf{0}_{2 \times 4} & \omega_{v,t2 \times 2} \end{bmatrix}}_{V_t} \right)^{1/2} \times \underbrace{\begin{bmatrix} \varepsilon_{z,t+1} \\ \mathbf{0} \\ \eta_{v,t+1} \end{bmatrix}}_{\eta_{t+1}}.$$

D.1.2. Measurement equation

For ease of illustration, assume that the observables are available at a monthly frequency. Define $o_t = [\Delta c_t, d_t, g_t, \pi_t]^\top$. Then, the measurement equation becomes

$$o_t = \beta^\top x_t + u_t, \quad u_t \sim N(0, \Sigma_u) \quad (\text{D.2})$$

where $\beta = [1, 1, 1, 1, 0, 0, 0, 0, 0, 0]^\top$ and Σ_u is a measurement error (diagonal) variance-covariance matrix.

D.1.3. Dealing with the mixed-frequency issue

When some observables are available at a quarterly frequency, we need to adjust both measurement and transition equations to deal with the mixed-frequency issue. We provide an example whereby the dimension of z_t , w_t , and v_t are reduced to half for ease of illustration. We assume that the first observable is available at a quarterly while the second observable is available at a monthly frequency. We introduce the superscript q to indicate if the observable is available at the quarterly frequency. Thus, $o_t = [z_{1,t}^q, z_{2,t}]'$. Also for simplicity, we do not allow for measurement errors. There are two cases to consider.

1. If $z_{1,t}^q$ is expressed in growth rates, adjust the measurement loading β and state vector to

$$\beta = \begin{bmatrix} \frac{1}{3} & \frac{2}{3} & 1 & \frac{2}{3} & \frac{1}{3} & 0 & 0 & 0 & 0 & 0 & 0 \\ 0 & 0 & 0 & 0 & 0 & 1 & 0 & 0 & 0 & 0 & 0 \end{bmatrix}, \quad x_t = \begin{bmatrix} z_{1,t} \\ z_{1,t-1} \\ z_{1,t-2} \\ z_{1,t-3} \\ z_{1,t-4} \\ z_{2,t} \\ z_{2,t-1} \\ z_{2,t-2} \\ z_{2,t-3} \\ z_{2,t-4} \\ w_{1,t} \\ w_{2,t} \\ v_{1,t} \end{bmatrix}. \quad (\text{D.3})$$

We can relate the mixed-frequency observables to the state vector by

$$o_t = \begin{bmatrix} z_{1,t}^q \\ z_{2,t} \end{bmatrix} = \begin{bmatrix} \frac{z_{1,t} + 2z_{1,t-1} + 3z_{1,t-2} + 2z_{1,t-3} + z_{1,t-4}}{3} \\ z_{2,t} \end{bmatrix} = \beta^\top x_t. \quad (\text{D.4})$$

2. If $z_{1,t}^q$ is expressed in levels, adjust the measurement loading β and state vector to

$$\beta = \begin{bmatrix} \frac{1}{3} & \frac{1}{3} & \frac{1}{3} & 0 & 0 & 0 & 0 & 0 & 0 & 0 & 0 \\ 0 & 0 & 0 & 0 & 0 & 1 & 0 & 0 & 0 & 0 & 0 \end{bmatrix}, \quad x_t = \begin{bmatrix} z_{1,t} \\ z_{1,t-1} \\ z_{1,t-2} \\ z_{1,t-3} \\ z_{1,t-4} \\ z_{2,t} \\ z_{2,t-1} \\ z_{2,t-2} \\ z_{2,t-3} \\ z_{2,t-4} \\ w_{1,t} \\ w_{2,t} \\ v_{1,t} \end{bmatrix}. \quad (\text{D.5})$$

We can relate the mixed-frequency observables to the state vector by

$$o_t = \begin{bmatrix} z_{1,t}^q \\ z_{2,t} \end{bmatrix} = \begin{bmatrix} \frac{z_{1,t} + z_{1,t-1} + z_{1,t-2}}{3} \\ z_{2,t} \end{bmatrix} = \beta^\top x_t. \quad (\text{D.6})$$

D.1.4. Implementation

We use quarterly consumption growth (Δc_t^q), output growth (d_t^q), and log government expenditure-to-output ratio (g_t^q), and monthly inflation (π_t) in the estimation. Except for consumption growth data, we are using the highest available frequency. Our choice of using quarterly consumption growth avoids modeling measurement errors in monthly consumption growth (see [Schorfheide et al. \(2018\)](#) for a detailed discussion), which significantly reduces the dimension of the state vector leading to a much more tractable estimation problem. Note that Δc_t^q and d_t^q are expressed in growth rates, but π_t and g_t^q are expressed in levels. Following the idea described in Section [D.1.3](#), we modify the measurement equation loading β and state vector X_t to

equate the observables to our state variables

$$o_t = \begin{bmatrix} \Delta c_t^q \\ d_t^q \\ g_t^q \\ \pi_t \end{bmatrix} = \begin{bmatrix} \frac{z_{1,t} + 2z_{1,t-1} + 3z_{1,t-2} + 2z_{1,t-3} + z_{1,t-4}}{3} \\ \frac{z_{2,t} + 2z_{2,t-1} + 3z_{2,t-2} + 2z_{2,t-3} + z_{2,t-4}}{3} \\ \frac{z_{3,t} + z_{3,t-1} + z_{3,t-2}}{3} \\ z_{4,t} \end{bmatrix}. \quad (\text{D.7})$$

The most efficient characterization of the state vector is

$$x_t = \begin{bmatrix} z_{1,t}, z_{1,t-1}, z_{1,t-2}, z_{1,t-3}, z_{1,t-4}, z_{2,t}, z_{2,t-1}, z_{2,t-2}, z_{2,t-3}, z_{2,t-4}, \\ z_{3,t}, z_{3,t-1}, z_{3,t-2}, z_{4,t}, w_{1,t}, w_{2,t}, w_{3,t}, w_{4,t}, v_{1,t}, v_{2,t} \end{bmatrix}^\top. \quad (\text{D.8})$$

The coefficient matrices in (D.1) are adjusted accordingly to match the dimension of (D.8). It is easy to deduce the form of β from (D.7) and (D.8).

Because of the conditionally linear structure of our state-space form, we can directly apply the Rao-Blackwellization particle filter as in Schorfheide et al. (2018). The details are omitted for brevity.

D.2. State-space representation: Extended form

We now introduce an extended state-space representation in which we additionally introduce s factors which are crucial elements for asset prices. We allow the s factors to depend on the lagged values of z and ν factors to model inter-dependence.

D.2.1. State transition dynamics

$$\begin{bmatrix} z_{1,t+1} \\ z_{2,t+1} \\ z_{3,t+1} \\ z_{4,t+1} \\ w_{1,t+1} \\ w_{2,t+1} \\ w_{3,t+1} \\ w_{4,t+1} \\ s_{1,t+1} \\ s_{2,t+1} \\ s_{3,t+1} \\ v_{1,t+1} \\ v_{2,t+1} \end{bmatrix} = \begin{bmatrix} \mu_1 \\ \mu_2 \\ \mu_3 \\ \mu_4 \\ 0 \\ 0 \\ 0 \\ 0 \\ \mu_{s1} \\ \mu_{s2} \\ \mu_{s3} \\ \nu_{v1} c_{v1} \\ \nu_{v2} c_{v2} \end{bmatrix} + \begin{bmatrix} \phi_{z11} & \phi_{z12} & \phi_{z13} & \phi_{z14} & 1 & 0 & 0 & 0 & 0 & 0 & 0 & 0 & \phi_{zv11} & \phi_{zv12} \\ \phi_{z21} & \phi_{z22} & \phi_{z23} & \phi_{z24} & 0 & 1 & 0 & 0 & 0 & 0 & 0 & 0 & \phi_{zv21} & \phi_{zv22} \\ \phi_{z31} & \phi_{z32} & \phi_{z33} & \phi_{z34} & 0 & 0 & 1 & 0 & 0 & 0 & 0 & 0 & \phi_{zv31} & \phi_{zv32} \\ \phi_{z41} & \phi_{z42} & \phi_{z43} & \phi_{z44} & 0 & 0 & 0 & 1 & 0 & 0 & 0 & 0 & \phi_{zv41} & \phi_{zv42} \\ 0 & 0 & 0 & 0 & 0 & 0 & 0 & 0 & 0 & 0 & 0 & 0 & 0 & 0 \\ 0 & 0 & 0 & 0 & 0 & 0 & 0 & 0 & 0 & 0 & 0 & 0 & 0 & 0 \\ 0 & 0 & 0 & 0 & 0 & 0 & 0 & 0 & 0 & 0 & 0 & 0 & 0 & 0 \\ 0 & 0 & 0 & 0 & 0 & 0 & 0 & 0 & 0 & 0 & 0 & 0 & 0 & 0 \\ \phi_{sz11} & \phi_{sz12} & \phi_{sz13} & \phi_{sz14} & 0 & 0 & 0 & 0 & \phi_{s11} & \phi_{s12} & \phi_{s13} & \phi_{sv11} & \phi_{sv12} \\ \phi_{sz21} & \phi_{sz22} & \phi_{sz23} & \phi_{sz24} & 0 & 0 & 0 & 0 & \phi_{s21} & \phi_{s22} & \phi_{s23} & \phi_{sv21} & \phi_{sv22} \\ \phi_{sz31} & \phi_{sz32} & \phi_{sz33} & \phi_{sz34} & 0 & 0 & 0 & 0 & \phi_{s31} & \phi_{s32} & \phi_{s33} & \phi_{sv31} & \phi_{sv32} \\ 0 & 0 & 0 & 0 & 0 & 0 & 0 & 0 & 0 & 0 & 0 & 0 & 0 \\ 0 & 0 & 0 & 0 & 0 & 0 & 0 & 0 & 0 & 0 & 0 & 0 & \phi_{v2} \end{bmatrix} \begin{bmatrix} z_{1,t} \\ z_{2,t} \\ z_{3,t} \\ z_{4,t} \\ w_{1,t} \\ w_{2,t} \\ w_{3,t} \\ w_{4,t} \\ s_{1,t} \\ s_{2,t} \\ s_{3,t} \\ v_{1,t} \\ v_{2,t} \end{bmatrix} + \begin{bmatrix} 1 & 0 & 0 & 0 & 0 & 0 & 0 & 0 & 0 & 0 & 0 & 0 & 0 & 0 \\ 0 & 1 & 0 & 0 & 0 & 0 & 0 & 0 & 0 & 0 & 0 & 0 & 0 & 0 \\ 0 & 0 & 1 & 0 & 0 & 0 & 0 & 0 & 0 & 0 & 0 & 0 & 0 & 0 \\ 0 & 0 & 0 & 1 & 0 & 0 & 0 & 0 & 0 & 0 & 0 & 0 & 0 & 0 \\ \theta_{w11} & \theta_{w12} & \theta_{w13} & \theta_{w14} & 0 & 0 & 0 & 0 & 0 & 0 & 0 & 0 & 0 & 0 \\ \theta_{w21} & \theta_{w22} & \theta_{w23} & \theta_{w24} & 0 & 0 & 0 & 0 & 0 & 0 & 0 & 0 & 0 & 0 \\ \theta_{w31} & \theta_{w32} & \theta_{w33} & \theta_{w34} & 0 & 0 & 0 & 0 & 0 & 0 & 0 & 0 & 0 & 0 \\ \theta_{w41} & \theta_{w42} & \theta_{w43} & \theta_{w44} & 0 & 0 & 0 & 0 & 0 & 0 & 0 & 0 & 0 & 0 \\ 1 & 1 & 1 & 1 & 1 & 1 & 1 & 1 & 1 & 0 & 0 & 1 & 1 & 1 \\ 1 & 1 & 1 & 1 & 1 & 1 & 1 & 1 & 1 & 0 & 1 & 0 & 1 & 1 \\ 1 & 1 & 1 & 1 & 1 & 1 & 1 & 1 & 0 & 0 & 1 & 1 & 1 & 1 \\ 0 & 0 & 0 & 0 & 0 & 0 & 0 & 0 & 0 & 0 & 0 & 0 & 1 & 0 \\ 0 & 0 & 0 & 0 & 0 & 0 & 0 & 0 & 0 & 0 & 0 & 0 & 0 & 1 \end{bmatrix}$$

$$\times \begin{bmatrix} \nu_{11} & 0 & 0 & 0 & 0 & \mathbf{0}_{1 \times 4} & \mathbf{0}_{1 \times 3} & 0 & 0 \\ \nu_{21} & \nu_{22} & 0 & 0 & 0 & \mathbf{0}_{1 \times 4} & \mathbf{0}_{1 \times 3} & 0 & 0 \\ \nu_{31} & \nu_{32} & \nu_{33} & 0 & 0 & \mathbf{0}_{1 \times 4} & \mathbf{0}_{1 \times 3} & 0 & 0 \\ \nu_{41} & \nu_{42} & \nu_{43} & \nu_{44} & 0 & \mathbf{0}_{1 \times 4} & \mathbf{0}_{1 \times 3} & 0 & 0 \\ 0 & 0 & 0 & 0 & 0 & \mathbf{0}_{1 \times 4} & \mathbf{0}_{1 \times 3} & 0 & 0 \\ 0 & 0 & 0 & 0 & 0 & \mathbf{0}_{1 \times 4} & \mathbf{0}_{1 \times 3} & 0 & 0 \\ 0 & 0 & 0 & 0 & 0 & \mathbf{0}_{1 \times 4} & \mathbf{0}_{1 \times 3} & 0 & 0 \\ 0 & 0 & 0 & 0 & 0 & \mathbf{0}_{1 \times 4} & \mathbf{0}_{1 \times 3} & 0 & 0 \\ -(\nu_{11} + \nu_{21} + \nu_{31} + \nu_{41}) + \nu_{s11} & -(\nu_{22} + \nu_{32} + \nu_{42}) + \nu_{s12} & -(\nu_{33} + \nu_{43}) + \nu_{s13} & -\nu_{44} + \nu_{s14} & \mathbf{0}_{1 \times 4} & [\nu_{s1}, 0, 0] & -1 + \nu_{sv11} & -1 + \nu_{sv12} \\ -(\nu_{11} + \nu_{21} + \nu_{31} + \nu_{41}) + \nu_{s21} & -(\nu_{22} + \nu_{32} + \nu_{42}) + \nu_{s22} & -(\nu_{33} + \nu_{43}) + \nu_{s23} & -\nu_{44} + \nu_{s24} & \mathbf{0}_{1 \times 4} & [0, \nu_{s2}, 0] & -1 + \nu_{sv21} & -1 + \nu_{sv22} \\ -(\nu_{11} + \nu_{21} + \nu_{31} + \nu_{41}) + \nu_{s31} & -(\nu_{22} + \nu_{32} + \nu_{42}) + \nu_{s32} & -(\nu_{33} + \nu_{43}) + \nu_{s33} & -\nu_{44} + \nu_{s34} & \mathbf{0}_{1 \times 4} & [0, 0, \nu_{s3}] & -1 + \nu_{sv31} & -1 + \nu_{sv32} \\ 0 & 0 & 0 & 0 & \mathbf{0}_{1 \times 4} & \mathbf{0}_{1 \times 3} & 1 & 0 \\ 0 & 0 & 0 & 0 & \mathbf{0}_{1 \times 4} & \mathbf{0}_{1 \times 3} & 0 & 1 \end{bmatrix}$$

select the maturities of 1y, 3y, 5y, 7y, 10y, and 15y in the estimation, which are collected in

$$y_t^j = \begin{bmatrix} y_{1,t}^j \\ \vdots \\ y_{m,t}^j \\ \vdots \\ y_{15,t}^j \end{bmatrix} = \begin{bmatrix} \Xi^j(A_1^j, B_1^j, \tilde{A}_1^j, \tilde{B}_1^j, \tilde{x}_t) \\ \vdots \\ \Xi^j(A_m^j, B_m^j, \tilde{A}_m^j, \tilde{B}_m^j, \tilde{x}_t) \\ \vdots \\ \Xi^j(A_{15}^j, B_{15}^j, \tilde{A}_{15}^j, \tilde{B}_{15}^j, \tilde{x}_t) \end{bmatrix}. \quad (\text{D.11})$$

We consider y_t^T, y_t^C, y_t^I in the estimation and use y_t^O as out-of-sample validation. We have defined $s_{1,t}$ and $s_{2,t}$ as observables in the main body of our paper. Define vectors e_{s_1} and e_{s_2} that select $s_{1,t}$ and $s_{2,t}$ from \tilde{x}_t , respectively. Put together,

$$\begin{bmatrix} s_{1,t} \\ s_{2,t} \end{bmatrix} = \begin{bmatrix} e_{s_1}^\top \\ e_{s_2}^\top \end{bmatrix} \tilde{x}_t \quad (\text{D.12})$$

disciplines the dynamics of the s factors. In sum, our state-space representation is comprised of state transition equations (D.9) and measurement equations (D.11) for $j \in \{T, C, I\}$ and (D.12). There are two ways in which we can proceed.

1. A joint estimation of macroeconomic observables and prices:

We augment our measurement equations with (D.7) and adjust the state transition equation (D.9) to deal with mixed-frequency observations as explained in Section D.1.3. While the joint estimation approach can be appealing, it is computationally challenging since we have to increase the dimension of our state vector substantially. More importantly, because the system no longer preserves the conditionally linear structure, e.g., (D.11), we cannot apply the solution proposed by Schorfheide et al. (2018), and thus the non-linear filtering algorithm can be highly inefficient.

2. Two-stage estimation in which macroeconomic observables and prices are separated:

For this, we treat the filtered estimates of \hat{z}_t and \hat{w}_t from the first stage estimation, which only involves macroeconomic data, as observables for the second stage estimation. Among our state vector \tilde{x}_t , we are assuming that $z_t, w_t, s_{1,t}, s_{2,t}$ are observed factors and treating $s_{3,t}, v_{1,t}, v_{2,t}$ as latent factors. We can then partition the state vector into

$$\tilde{x}_t = (\tilde{x}_t^{o,\top}, \tilde{x}_t^{l,\top})^\top \quad (\text{D.13})$$

where the superscript o and l indicate ‘‘observed’’ and ‘‘latent’’ respectively. The non-linear filtering technique only deals with \tilde{x}_t^l in the state transition equation (D.9), since the other variables are observed. In this case, the measurement equations are (D.11) for $j \in \{T, C, I\}$ and (D.12).

D.2.3. Particle filter

We use a particle-filter approximation of the likelihood function and embed this approximation into a fairly standard random walk Metropolis algorithm. In the subsequent exposition, we omit the dependence of all densities on the parameter vector Θ . In slight abuse of notations, we denote all observables with

$$y_t = [y_t^{C,\top}, y_t^{T,\top}, y_t^{I,\top}, s_{1,t}, s_{2,t}]^\top \quad (\text{D.14})$$

The particle filter approximates the sequence of distributions $\{p(\tilde{x}_t^l | y_{1:t})\}_{t=1}^T$ by a set of pairs $\left\{ \tilde{x}_t^{l,(i)}, \pi_t^{(i)} \right\}_{i=1}^N$, where $\tilde{x}_t^{l,(i)}$ is the i th particle vector, $\pi_t^{(i)}$ is its weight, and N is the number of particles. As a by-product, the filter produces a sequence of likelihood approximations $\hat{p}(y_t | y_{1:t-1})$, $t = 1, \dots, T$.

- Initialization: We generate the particle values $\tilde{x}_0^{l,(i)}$ from the unconditional distribution. We set $\pi_0^{(i)} = 1/N$ for each i .

- Propagation of particles: We simulate (D.9) forward to generate $\tilde{x}_t^{l,(i)}$ conditional on $\tilde{x}_{t-1}^{l,(i)}$ and observed \tilde{x}_{t-1}^o . We use $q(\tilde{x}_t^{l,(i)}|\tilde{x}_{t-1}^{l,(i)}, \tilde{x}_{t-1}^o, y_t)$ to represent the distribution from which we draw $\tilde{x}_t^{l,(i)}$.
- Correction of particle weights: Define the unnormalized particle weights for period t as

$$\tilde{\pi}_t^{(i)} = \pi_{t-1}^{(i)} \times \frac{p(y_t|\tilde{x}_t^{l,(i)}, \tilde{x}_t^o)p(\tilde{x}_t^{l,(i)}|\tilde{x}_{t-1}^{l,(i)}, \tilde{x}_{t-1}^o)}{q(\tilde{x}_t^{l,(i)}|\tilde{x}_{t-1}^{l,(i)}, \tilde{x}_{t-1}^o, y_t)}.$$

The term $\pi_{t-1}^{(i)}$ is the initial particle weight and the ratio $\frac{p(y_t|\tilde{x}_t^{l,(i)}, \tilde{x}_t^o)p(\tilde{x}_t^{l,(i)}|\tilde{x}_{t-1}^{l,(i)}, \tilde{x}_{t-1}^o)}{q(\tilde{x}_t^{l,(i)}|\tilde{x}_{t-1}^{l,(i)}, \tilde{x}_{t-1}^o, y_t)}$ is the importance weight of the particle.

The approximation of the log likelihood function is given by

$$\log \hat{p}(y_t|y_{1:t-1}) = \log \hat{p}(y_{t-1}|y_{1:t-2}) + \log \left(\sum_{i=1}^N \tilde{\pi}_t^{(i)} \right).$$

- Resampling: Define the normalized weights

$$\pi_t^{(i)} = \frac{\tilde{\pi}_t^{(i)}}{\sum_{j=1}^N \tilde{\pi}_t^{(j)}}$$

and generate N draws from the distribution $\{\tilde{x}_t^{l,(i)}, \pi_t^{(i)}\}_{i=1}^N$ using multinomial resampling. In slight abuse of notation, we denote the resampled particles and their weights also by $\tilde{x}_t^{l,(i)}$ and $\pi_t^{(i)}$, where $\pi_t^{(i)} = 1/N$.